STRESS RESPONSES IN THE HYPERTHERMOPHILIC ARCHAEON

PYROCOCCUS FURIOSUS

by

MICHAEL VANCE WEINBERG

(Under the Direction of MICHAEL W. W. ADAMS)

ABSTRACT

The objective of this research was to understand the response of the hyperthermophilic archaeon, *Pyrococcus furiosus* to two environmental stresses, oxidative and cold stress. The first aim was to purify and determine the biochemical and kinetic properties of the protein rubrerythrin (Rr), and determine its role in the organism's response to oxidative stress. The native protein from *P. furiosus* contains three iron atoms per subunit and reduces hydrogen peroxide using Rd as the electron donor. The gene encoding Rr (PF1283) was cloned and expressed in *Escherichia coli* growing on various media. These recombinant Rr proteins had reduced iron contents and lower Rd peroxidase activities.

A second protein involved in oxidative stress, NADPH:rubredoxin (Rd) oxidoreductase (NROR) was studied to produce an active, recombinant form of the enzyme by a reconstitution protocol using FAD and heat treatment.

In addition to studying oxidative stress in *P. furiosus*, the "cold" shock response was also studied using cellular, transcriptional, translational and enzymatic approaches. Growth studies were performed to determine the cellular response to cold shock and to continuous growth at low temperature (72 ^{o}C). Whole genome DNA microarray analyses compared these transcriptional

profiles with those of cultures grown at 95 ^{o}C. The cellular response to a cold shock was a 5 hour acclimation phase, after which growth resumed at a four times lower rate than that at 95 ^{o}C.The microarray data revealed three separate types of responses, involving the up-regulation (> 2.5 fold, $P < 0.01$) of 55, 30 and 59 ORFs, respectively.

INDEX WORDS: *Pyrococcus furiosus,* hyperthermophilic archaea, cold shock response, rubrerythrin, NADPH:rubredoxin oxidoreductase.

STRESS RESPONSES IN THE HYPERTHERMOPHILIC ARCHAEON *PYROCOCCUS FURIOSUS*

by

MICHAEL VANCE WEINBERG

B.S., Binghamton University, 1997

A Dissertation Submitted to the Graduate Faculty of The University of Georgia in Partial Fulfillment of the Requirements for the Degree

DOCTOR OF PHILOSOPHY

ATHENS, GEORGIA

2004

STRESS RESPONSES IN THE HYPERTHERMOPHILIC ARCHAEON *PYROCOCCUS FURIOSUS*

by

MICHAEL VANCE WEINBERG

Major Professor: Michael W. W. Adams

Committee: Timothy Hoover
William B. Whitman
Anna Karls
Robert Maier

Electronic Version Approved:

Maureen Grasso
Dean of the Graduate School
The University of Georgia
December 2004

ACKNOWLEDGEMENTS

First and foremost I would like to thank Dr. Michael W.W. Adams for his endless guidance and support throughout my graduate school career. I would also like to thank my committee members, past (Dr. Pamela Jones and Dr. Frank Gherardhini) and present (Dr. Tim Hoover, Dr. Anna Karls, Dr. Rob Maier and Dr. Barny Whitman), for continued ideas and open discussion throughout my time at UGA. I'd also like to thank Dr. Frank Jenney, who made the oxidative stress project move along that much quicker and Dr. Gerrit Schut and Scott Brehm for hours of explanation and help during the cold shock study. The long road to my Ph.D. would have been a lot less fun without Adams' lab members, as well as friends in the Microbiology Department.

I suppose Mom and Dad, you guys deserve your own paragraph, as you constantly never let me give up and supported me with a kind word, a heated discussion of "encouragement" or simply monetary support when I needed it to see me through. Thank you for constant support throughout my graduate study. You finally get what you've always wanted, and what this Ph.D. is really all about: you can finally retire to Southern Florida and impress all the alta kakas down there by starting conversations with, "My son, the doctor…".

Finally, Kendall. Though I only knew you for the last 2 years of my time in graduate school, you probably had the biggest impact. You gave me direction and a purpose to finish off my work sooner rather than later even though you probably did not understand the majority of what I was talking about.

TABLE OF CONTENTS

Page

LIST OF TABLES

Page

LIST OF FIGURES

Page

LIST OF ABBREVIATIONS

AARE-acyl aminoacid releasing enzyme

ACS-acetyl CoA synthase

ADP-adenosine 5’-diphosphate

ATP-adenosine 5’-triphosphate

Cip-cold induced protein

CoA-coenzyme A

CsdA-cold shock dead protein A

CSP-cold Shock protein

CspA-cold shock protein A

DNA-deoxyribonucleic acid

DT-dithionite

DTPA-diethylenetriaminepentaacetic acid

DTT-dithiothreitol

FAD-flavin adenine dinucleotide

Fd-ferredoxin

FKBP-FK506 binding proteins

GAPDH- glyceraldehyde-3-phosphate dehydrogenase

GAPOR- glyceraldehyde-3-phosphate oxidoreductase

H_2O_2-hydrogen peroxide

$HO^{\cdot}$-hydroxyl radical

IOR-indolepyruvate oxidoreductase

IF-initiation factor

IPTG-isopropyl-β-D-thiogalactopyranoside

KGOR-2-ketoglutarate oxidoreductase

ORF-open reading frame

NADH-nicotinamide adenine dinucleotide, reduced form

NADPH-nicotinamide adenine dinucleotide phosphate, reduced form

NROR-NADPH:rubredoxin oxidoreductase

O_2^--superoxide anion

PCR-polymerase chain reaction

POR-pyruvate oxidoreductase

Rd-rubredoxin

RbfA-ribosomal binding factor A

RNA-ribonucleic acid

ROI-radical oxygen intermediates

Rr-rubrerythrin

SOD-superoxide dismutase

SOR-superoxide reductase

5’ UTR-5’ untranslated region

VOR-2-ketosisovalerate oxidoreductase

CHAPTER 1

INTRODUCTION AND LITERATURE REVIEW

Archaea represent the third domain of life that was first recognized in the late 1970s. Through the pioneering studies of Carl Woese, a new universal phylogenetic tree of life was proposed based on 16S rRNA sequences (137). This tree forms three main branches, or domains: the bacteria, the eukaryotes and the archaea (Figure 1.1). Although they physically resemble bacteria in that they are single-celled prokaryotes, archaea possess cell walls, cell membranes, and transcription and translation machinery that make them a distinct domain of life (33). In addition, antibiotics that are effective against bacterial growth have no effect on archaea, further highlighting the differences in the transcriptional and translational machinery between these two domains. Archaea are best known for inhabiting extreme temperatures (both hot and cold), pH and salt environments that would not be considered hospitable to traditional life forms and thus most are categorized as extremophiles. The extreme environments in which they are found contributed to their relatively recent discovery.

The domain of archaea is traditionally split into two phyla, euryarchaeaota and crenarchaeaota (Figure 1.1). A third, newly defined phylum is represented by the nanoarchaeaota. It has one member, the symbiont *Nanoarchaeum equitans*, which is a recent addition to the archaeal domain (55). In addition, a fourth phylum known as the korarchaeota has been proposed based only on environmental DNA sequences.

Euryarchaeota, from the Greek word for wide, encompass a great phenotypic and metabolic diversity. Included in this group are the halophiles, methanogens, thermoacidophiles and hyperthermophiles (33). In contrast to the euryarchaeaota, the crenarchaeaota contains only

Figure 1.1.

Universal phylogenetic tree in rooted form, showing the three domains. Branching order and branch lengths are based upon 16s rRNA sequence comparisons. The root position was determined by comparing sequences of paralagous genes that diverged from each other before the three primary lineages emerged from a common ancestor. Hyperthermophilic species in red. The genus *Pyrococcus* is shown in blue [redrawn and modified from (10)].

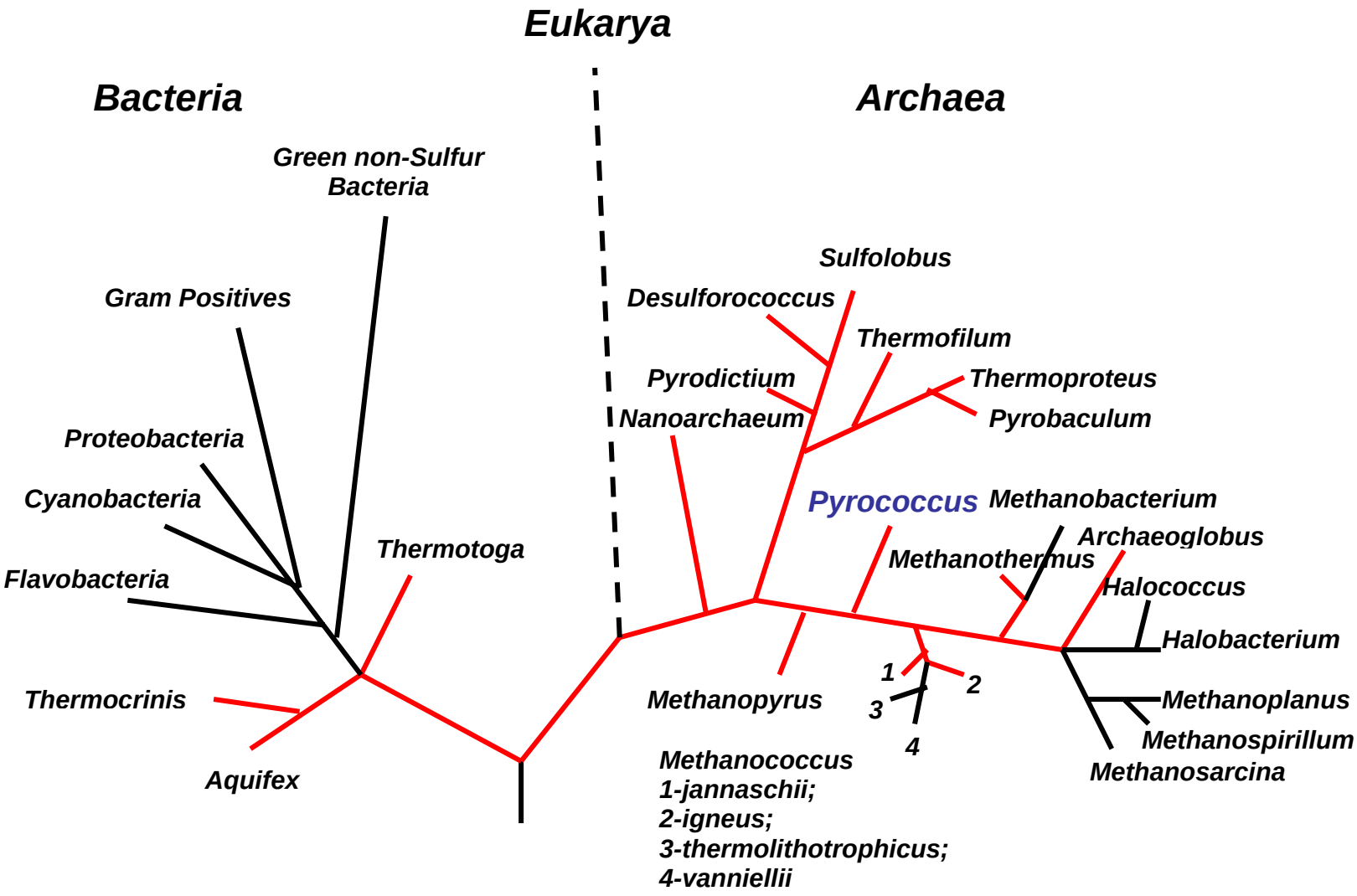
Eukarya
Bacteria
Archaea
Green non-Sulfur Bacteria
Gram Positives
Proteobacteria
Cyanobacteria
Flavobacteria
Thermotoga
Thermocrinis
Aquifex
Sulfolobus
Desulfurococcus
Thermofilum
Pyrodictium
Thermoproteus
Nanoarchaeum
Pyrobaculum
Pyrococcus
Methanobacterium
Archaeoglobus
Methanothermus
Halococcus
Halobacterium
Methanoplanus
Methanospirillum
Methanosarcina
Methanopyrus
1
2
3
4
Methanococcus
1-jannaschii;
2-igneus;
3-thermolithotrophicus;
4-vanniellii

high temperature species. This phylum is named from the Greek word spring, due to the popular hypothesis that all modern day life came from high temperature organisms. This is based on 16S rRNA analyses which indicate that such organisms are the most slowly evolving organisms of all life forms.

Hyperthermophiles are defined as microorganisms that have an optimal growth temperature above 80 ^{o}C with a maximum growth temperature above 90 ^{o}C. The most extreme of the hyperthermophiles that has been characterized is *Pyrolobus fumarii*, which is unable to grow below 90 ^{o}C and has the ability to grow in temperatures up to 113 ^{o}C (There is recent evidence of an environmental isolate that grows up to 121 ^{o}C, but this has yet to be verified). Although two hyperthermophilic genera, *Aquifex* and *Thermotoga*, belong to the domain bacteria, all others are classified as archaea. Hyperthermophiles were first isolated in the early 1980s through the revolutionary work of Stetter and coworkers (126). Since then the hyperthermophilic world has expanded greatly, and today more than 75 hyperthermophilic species are known that represent 32 genera (55).

Hyperthermophiles form complex communities in both terrestrial and marine high temperature environments. Terrestrial environments include continental hot springs, mud holes and solfataric fields (56). These characteristically are low to slightly alkaline pH (0.5-9.0) and low salt (0.1-0.5%) environments that are usually situated near active volcanoes. Marine environments are found at both shallow coastal water and deep sea hydrothermal vents where the pH values range from slightly acidic to slightly alkaline (5.0-8.5) and the salt concentration is quite high (~ 3%). The shallow coastal areas occur around the world at such spots as Vulcano Island, Italy and Ribeira Quente in the Azores. The vents at the deep sea sites can reach temperatures as high as 400 ^{o}C, heated by sub-seafloor volcanic activity. These vents are known

as ‘black smokers’ because they spew plumes of black metal sulfide precipitates into the cold deep sea water (61). Because of the extremely cold surrounding water (~ 4 ^{o}C), the smoker walls display a steep temperature gradient. It is from these vent walls as well as from the plumes of hot black water that hyperthermophilic microorganisms have been isolated.

1. Metabolism of Hyperthermophiles

Hyperthermophiles are diverse in their metabolic capabilities. As a group they include methanogens, sulfate reducers and nitrate reducers. Although most hyperthermophilic archaea are anaerobes, there are a few species which utilize and even require oxygen. Of the 5 genera that contain aerobic species, two of them are microaerophiles (*Pyrobaculum* and *Pyrolobus*) (Table 1.1). The hyperthermophilic archaea are mainly obligate anaerobes. This is not surprising due to the low availability of oxygen in many of the environments in which they are found. The majority of hyperthermophiles fall into the “sulfur–dependent” category, as they are able to reduce elemental sulfur (S^{o}) to H_2S (1)**.** Most members of this group obtain energy for growth solely by S^{o} respiration. Some exceptions to this rule are *Pyrococcus* and *Thermococcus*, both of which have the ability to grow by apparent fermentative metabolism in the absence of S^{o}. In contrast to the “S^{o}–dependent” archaea, three genera are able to grow without S^{o}, known as the “S^{o}–independent” category (Table 1.1). The fermentatively-growing *Sulfolobus* (49) and the obligate-anaerobe *Aeropyrum* (117) are two of the genera that makeup this category. The third member, *Pyrolobus*, has a respiratory metabolism where the electron donor is H_2 and nitrate, thiosulfate or low concentrations of O_2 are utilized as electron acceptors (1). The type species of *Pyrolobus*, *P. fumarii*, has an upper growth limit of 113 ^{o}C. Exponentially growing cultures of this organism have even been reported to survive autoclaving (121 ^{o}C for 1 hour) (11).

Table 1.1 The hyperthermophilic genera; organisms that grow at $\geq$ 90 ^{o}C[a]

Genus	T_{max}[b]	Metabolism[c]	Substrates[d]	Acceptors
S^o-dependent archaea				
Thermofilum (c)[e]	100^o	Hetero	Pep	S^o, H^+
Staphylothermus (d/m)	98^o	Hetero	Pep	S^o, H^+
Thermodiscus (d/c)	98^o	Hetero	Pep	S^o, H^+
Desulfurococcus (d/c)	90^o	Hetero	Pep	S^o, H^+
Thermoproteus (c)	92^o	hetero (auto)	Pep, CBH (H_2)	S^o, H^+
Pyrodicum (d/m)	110^o	hetero (auto)	Pep, CBH (H_2)	S^o, H^+
Pyrococcus (d/m)	105^o	Hetero	Pep	$\pm S^o$, H^+
Thermococcus (d/m)	97^o	Hetero	Pep, CBH	$\pm S^o$, H^+
Hyperthermus (m)	110^o	Hetero	Pep (H_2)	$\pm S^o$, H^+
Stetteria (m)	103^o	Hetero	Pep + H_2	S^o, $S_2O_3^{2-}$
Pyrobaculum (d/c)	102^o	hetero (auto)	Pep (H_2)	$\pm S^o$, mO_2, NO_3^-
Acidianus (m/c)	96^o	Auto	S^o, H_2	S^o, O_2
Palaeococcus (d)	90^o	Hetero	Pep, Fe^{2+}	S^o, H^+
Ignicoccus (d/m)	98^o	Auto	H_2	S^o
Vulcanisaeta (c)	90^o	Hetero	Pep	S^o, $S_2O_3^{2-}$
Caldivirga (c)	92^o	Hetero	Pep, CBH	S^o, $S_2O_3^{2-}$, SO_4^{2-}
S^o-independent archaea				
Sulfophobococcus (c)	95^o	Hetero	Pep	-
Pyrolobus (d)	113^o	Auto	H_2	$S_2O_3^{2-}$, mO_2, NO_3^-
Aeropyrum (m)	100^o	Hetero	Pep	O_2
Thermosphaera (c)	90^o	Hetero	Pep	-
Sulfate-reducing archaea				
Archaeoglobus (d/m)	95^o	hetero (auto)	CBH, H_2	$S_2O_3^{2-}$, SO_4^{2-}
Iron-oxidizing archaea				
Ferroglobus (m)	95^o	Auto	Fe^{2+}, H_2, S_2^-	$S_2O_3^{2-}$, NO_3^-
Iron-reducing archaea				
Geoglobus (d)	90^o	hetero (auto)	Fe^{3+} + H_2, long-chain FAs	Fe_2O_3

Methanogenic archaea				
Methanococcus (d/c)	91^{o}	Auto	H_2	CO_2
Methanothermus (c)	97^{o}	Auto	H_2	CO_2
Methanopyrus (d/m)	110^{o}	Auto	H_2	CO_2
Bacteria				
Thermotoga (d/m)	90^{o}	Hetero	Pep, CBH	S^{o}, H^{+}
Aquifex (m)	95^{o}	Auto	S^{o} (H_2)	mO_2, NO_3^{-}
Thermocrinis (c)	90^{o}	Auto		$\pm$ S^{o}, H^{+}

[a]Table adapted from Adams, 1999. Data taken from Kelly and Adams, 1994, Blochl et al., 1997, Sako et al., 1996, Jochimsen et al., 1997, Kashefi et al., 2002, Itoh, 2002, Huber et al., 2000, Takai et al., 2000, Itoh et al., 1999, and Hensel et al., 1997.
[b]Maximum growth temperature.
[c]Denotes heterotrophic (hetero) or autotrophic (auto) growth mode.
[d]Growth substrates include peptides (Pep), carbohydrates (CBH), hydrogen (H_2), elemental sulfur (S^{o}), and fatty acids (FA) as electron donors.
[e]Species have been found in continental hot springs (c), shallow marine (m), and/or deep (d) sea environments

A third group of hyperthermophiles are made up of three genera of methanogens. As their name implies, these archaea produce methane from H_2 and CO_2. Two other closely-related genera, the sulphate-reducing *Archaeoglobus* and the iron-oxidizing *Ferroglobus*, also are able to grow in the absence of S^o. There are also two genera of hyperthermophiles that belong to the bacterial domain rather than the archaeal domain. One of these, *Thermotoga*, is a fermentative organism that reduces S^o to H_2S, although growth does occur without S^o present. The other, *Aquifex*, is a microaerophilic denitrifier that does not use S^o (1).

With few exceptions, the majority of hyperthermophiles are obligate heterotrophs, with their carbon sources mainly derived from the breakdown of peptides rather than carbohydrates (Table 1.1). Complex proteinaceous substrates, such as yeast, bacterial or meat extracts, peptone and tryptone, are required for significant growth. Therefore, the true growth substrates for many hyperthermophiles are not known. A few species of hyperthermophiles, such as *Pyrococcus*, *Thermococcus*, and *Desulphurococcus* have also been reported to grow on mixtures of amino acids (114). The highest yields and fastest doubling times, however, are seen when growth occurs on complex media. As shown in Table 1.1, hyperthermophilic species are proteolytic, but a few have the ability to grow by saccharolytic methods. Most of these species are only able to use either complex carbohydrates such as starch or glycogen, or disaccharides such as maltose or cellobiose. With the exception of *Thermoproteus*, which utilizes glucose as its primary carbon source, none of the hyperthermophilic archaea are able to grow on monosaccharides. In stark contrast, the utilization of monosaccharides for growth is characteristic of species of the hyperthermophilic bacterium *Thermotoga*. The reason for this difference between hyperthermophilic archaea and bacteria is not clear.

Pyruvate is the only other carbon source shown to support growth of hyperthermophilic archaea, including some species of *Pyrococcus*. However, cell yields are much lower when pyruvate is used as a carbon source as opposed to complex peptides or carbohydrates (1). A novel hyperthermophilic archaeon has recently been isolated that is capable of growth not only on pyruvate, but also acetate, palmitate and stearate. All of these growth substrates are coupled to the reduction of Fe (III) (72). Thus, most of the hyperthermophiles so far isolated are strict anaerobic heterotrophs that are either obligately or facultatatively dependent on S^o for optimal growth.

Pyrococcus furiosus (Figure 1.2) has been a model organism for the study of hyperthermophilic archaeal physiology and metabolism. It was first isolated from geothermally-heated marine sediments off the coast of Vulcano, Italy by Stetter and coworkers (31). This hyperthermophilic archaeon ranges from 0.8 to 2.5 μm in diameter, is coccoid in shape and possesses monopolar peritrichous flagella. It has an optimal growth temperature of 100 ^oC, with a doubling time of ~ 40 minutes. *P. furiosus* is a strictly anaerobic heterotroph that has the ability to grow both proteolytically on peptides (in the presence of S^o) and saccharolytically utilizing starch, glycogen and cellobiose as its primary carbon source. Acetate, H_2 and CO_2 are produced as metabolic end products (74). As mentioned previously, complex media including yeast extract or tryptone are required for high cell yields and obtaining optimal doubling times (2, 52, 76, 112).

Figure 1.2.

Electron micrograph of *P. furiosus.* The image shows monopolar, peritrichous flagellation. It is platinum shadowed. Taken from (31).

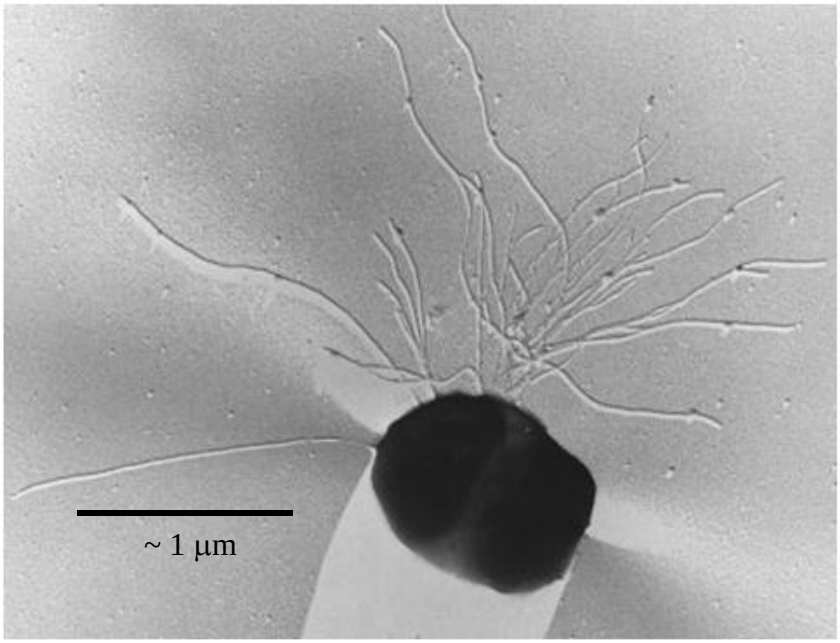
~ 1 μm

2. **Major metabolic pathways of *Pyrococcus furiosus***

2.A. Saccharolytic pathway

As stated previously, most hyperthermophilic archaea can only utilize protein-based substrates as their sole carbon source. However, *P. furiosus* is able to utilize various disaccharides and complex carbohydrates (but not monosaccharides) such as maltose, starch and glycogen as a growth substrate. Various enzymes involved in the breakdown of these compounds have been characterized (128) and it has been determined via ^{13}C NMR spectroscopy that *P. furiosus* makes use of a modified Embden-Meyerhof (EM) pathway (Figure 1.3) to catabolize sugars (73). Although *P. furiosus* cell-free extracts possess significant amounts of glyceraldehye-3-phosphate dehydrogenase (GAPDH), this enzyme is replaced in the EM pathway with the enzyme glyceraldehyde-3-phosphate ferredoxin oxidoreductase (GAPOR) (103). This enzyme is distinct from GAPDH as it utilizes ferredoxin (Fd) as its electron carrier rather than NAD and yields 3-phosphoglycerate instead of 1, 3-bisphosphoglycerate as a product of the reaction. It has also been shown that sugar metabolism in *P. furiosus* differs from the usual EM pathway in a number of other ways. Namely, the hexokinase and phosphofructokinase (73) in this pathway are ADP- rather than ATP-dependent. Additionally, the pathway contains two acetate-producing acetyl CoA synthetases, ACS I and II (98). Finally, the second oxidation step in which Fd is the electron acceptor is carried out by the enzyme pyruvate Fd oxidoreductase (POR) to produce acetyl CoA (3). This reduced Fd is oxidized ultimately by the reduction of protons to yield H_2 or of S^o (if present) to produce hydrogen sulfide (H_2S). The pathway for H_2 production was recently elucidated (118). Fd donates electrons to a membrane-bound hydrogenase which both evolves H_2 and generates a proton-gradient, which is used to

Figure 1.3.

Schematic representation of the modified Embden-Meyerhof pathway for Glycolysis and acetate production by *P. furiosus*. Metabolism of glucose to acetate in *P. furiosus*. Fd represents ferredoxin and enzymes germane to *P. furiosus* are highlighted in red. Modified from (103).

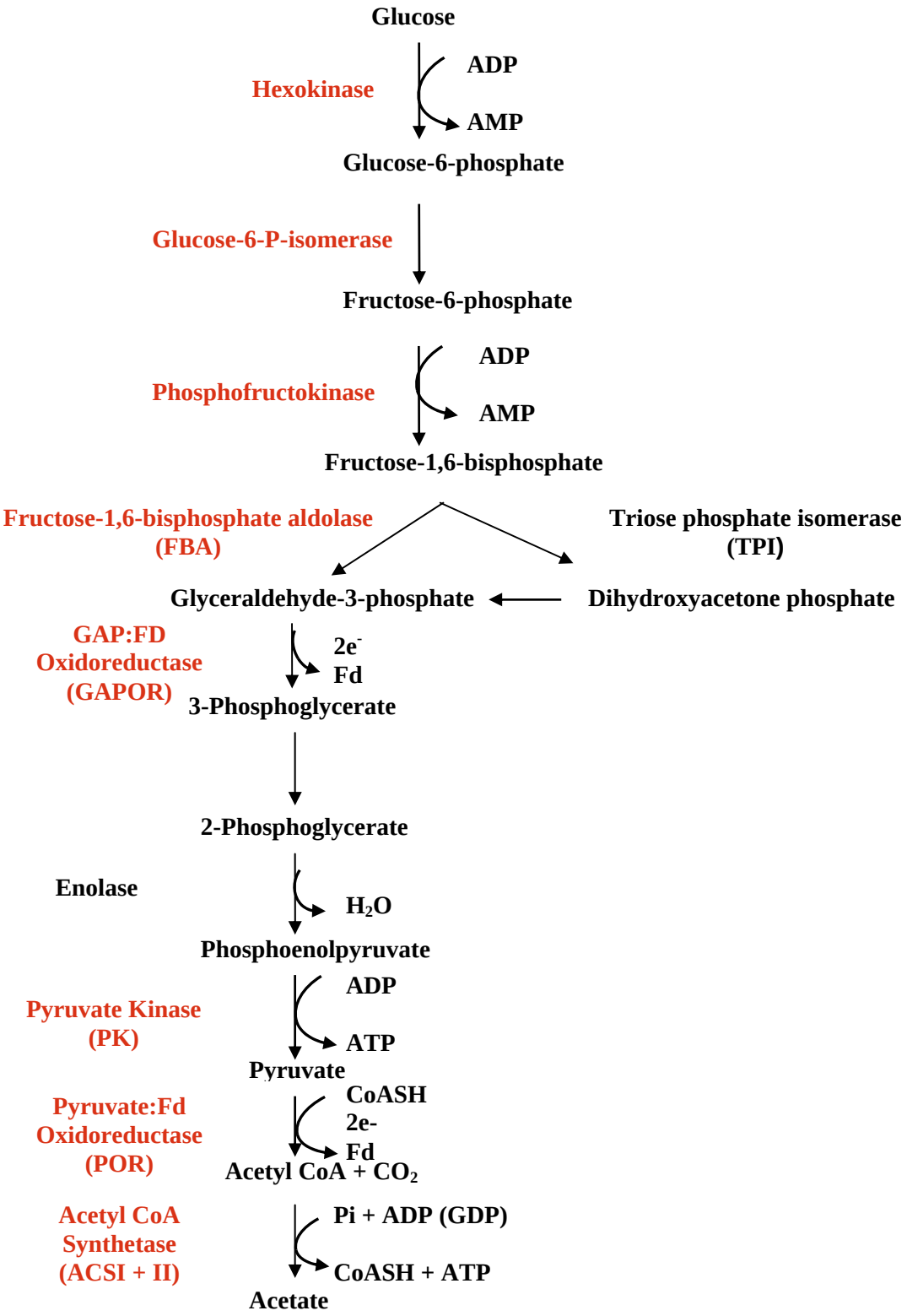
Glucose
Hexokinase
ADP
AMP
Glucose-6-phosphate
Glucose-6-P-isomerase
Fructose-6-phosphate
Phosphofructokinase
ADP
AMP
Fructose-1,6-bisphosphate
Fructose-1,6-bisphosphate aldolase (FBA)
Triose phosphate isomerase (TPI)
Glyceraldehyde-3-phosphate
Dihydroxyacetone phosphate
GAP:FD Oxidoreductase (GAPOR)
2e-
Fd
3-Phosphoglycerate
2-Phosphoglycerate
Enolase
H2O
Phosphoenolpyruvate
Pyruvate Kinase (PK)
ADP
ATP
Pyruvate
Pyruvate:Fd Oxidoreductase (POR)
CoASH
2e-
Fd
Acetyl CoA + CO2
Acetyl CoA Synthetase (ACSI + II)
Pi + ADP (GDP)
CoASH + ATP
Acetate

generate ATP. On the other hand, the pathway by which S^o is reduced has yet to be elucidated.

2.B. Proteolytic pathway

Like the majority of hyperthermophilic archaea, *P. furiosus* can utilize protein-based substrates as their carbon source. This process, however, is dependent on the presence of elemental sulfur. This proteolytic pathway begins with peptide breakdown via numerous proteases and peptidases. High intracellular and extracellular protease activity has been determined for *P. furiosus* (8). Amino acids derived from the peptides are further metabolized by specific aliphatic and aromatic aminotransferases to convert them to 2-keto acids (Figure 1.4). Four different 2-keto acid oxidoreductases in *P. furiosus* convert these transaminated amino acids to their corresponding acyl CoA derivatives. Branched chain 2-keto acids are converted by 2-ketoisovalerate oxidoreductase (VOR), aromatic 2-keto acids by indolepyruvate oxidoreducatse (IOR), pyruvate by pyruvate oxidoreducatse (POR) and 2-ketoglutarate by 2-ketoglutarate oxidoreductase (KGOR) (Figure 1.4). All of these reactions are coupled to Fd reduction, all of these enzymes share significant sequence similarity. What sets them apart from each other is their individual substrate specificities. VOR shows the highest affinity for 2-ketoacids from valine, leucine and isoleucine, and IOR for phenylalanine, tyrosine and tryptophan derived 2-ketoacids. KGOR and POR show much more specificity for their particular substrates, 2-ketoglutarate and pyruvate, respectively (1). Acyl CoA intermediates generated from these reactions are further converted to acids by two separate acyl CoA synthetases, ACS I and II, with the coupled production of ATP (97). ACS I utilizes products from the POR and VOR reactions (ie, acetyl CoA and isobutyryl CoA) as substrates but cannot use aryl CoAs (from IOR). ACS II can utilize products from all three reactions, acetyl CoA,

Figure 1.4.

Proposed pathway of peptide fermentation in *P. furiosus*. Schematic representation of the proposed involvement of 2-keto acid:ferredoxin oxidoreductases and acetyl-CoA synthetases in the fermentation of amino acids by *P. furiosus* [redrawn and modified from (98)]. IOR, POR, KGOR and VOR represent Fd-dependent oxidoreductases that utilize indolepyruvate, pyruvate, 2-ketoglutarate and 2-ketoisovalerate, respectively. ACS is acyl CoA synthetase, Fd_{red} and Fd_{ox} indicates the reduced and oxidized forms of ferredoxin, respectively.

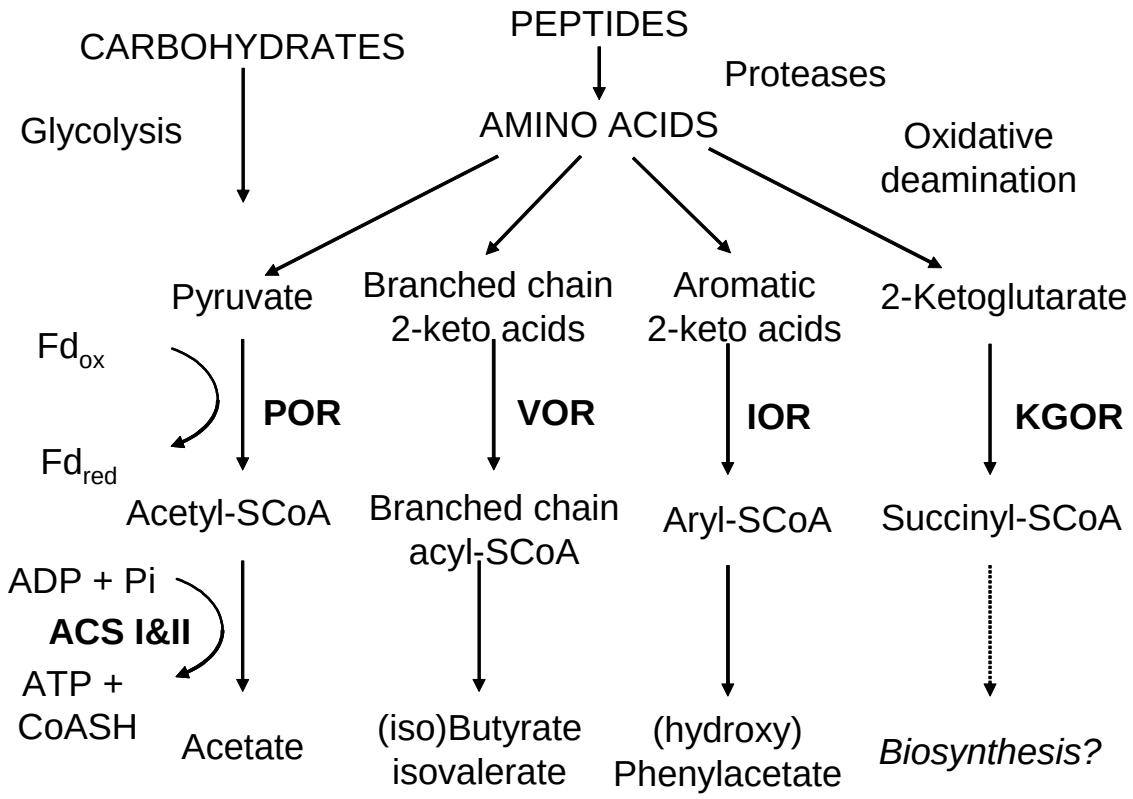
CARBOHYDRATES
PEPTIDES
Proteases
Glycolysis
AMINO ACIDS
Oxidative deamination
Pyruvate
Branched chain 2-keto acids
Aromatic 2-keto acids
2-Ketoglutarate
Fdox
Fdred
POR
VOR
IOR
KGOR
Acetyl-SCoA
Branched chain acyl-SCoA
Aryl-SCoA
Succinyl-SCoA
ADP + Pi
ACS I&II
ATP + CoASH
Acetate
(iso)Butyrate isovalerate
(hydroxy) Phenylacetate
Biosynthesis?

isobutyryl CoA and aryl CoAs. Neither ACS I nor ACS II can utilize succinyl CoA as a substrate, which is generated from the KGOR reaction, and it is thought that succinyl CoA is used for biosynthesis rather than energy conservation (1).

3. **The cold shock response**

3.A. Bacterial cold shock response and cold shock proteins

The response of bacteria to a decrease in growth temperature has been studied for the better part of two decades. This response is characterized by a temporary stoppage in growth, called the acclimation phase, during which the majority of protein synthesis stops. After this acclimation phase, growth resumes at a much slower pace than prior to the shock and the cells are considered “cold adapted”. Bacteria encountering a sudden drop in growth temperature have three issues to deal with in order to overcome this stress (Figure 1.5). First, they must maintain the fluidity of their membrane. This is essential for proper transport and exchange of solutes with their environment. Second, it is evident during this time that translation of most cellular protein stops and ribosome functioning is compromised. In order for translation, and in turn growth, to resume, the ribosome must be made “cold competent”. Finally, upon cold shock, certain secondary structures in the mRNA are stabilized, which adds to the difficulty in translation at low temperatures. These secondary structures must be inhibited in order for proper translation to occur at low temperatures.

The cell membrane plays a significant role in how a cell interacts with its environment. It is responsible for the acquisition of nutrients and solutes as well as the excretion of waste products. Lowering the growth temperature in the environment of a bacterial cell changes the membrane from a liquid, crystalline form to a gel phase state (131). Organisms compensate for

Figure 1.5.

Schematic representation of the mesophilic bacterial cold shock response. All possible sensors (ribosome, cell membrane, DNA), a proposed cellular signal [(p)ppGpp] and all types of possible regulation are indicated. Adapted from (106).

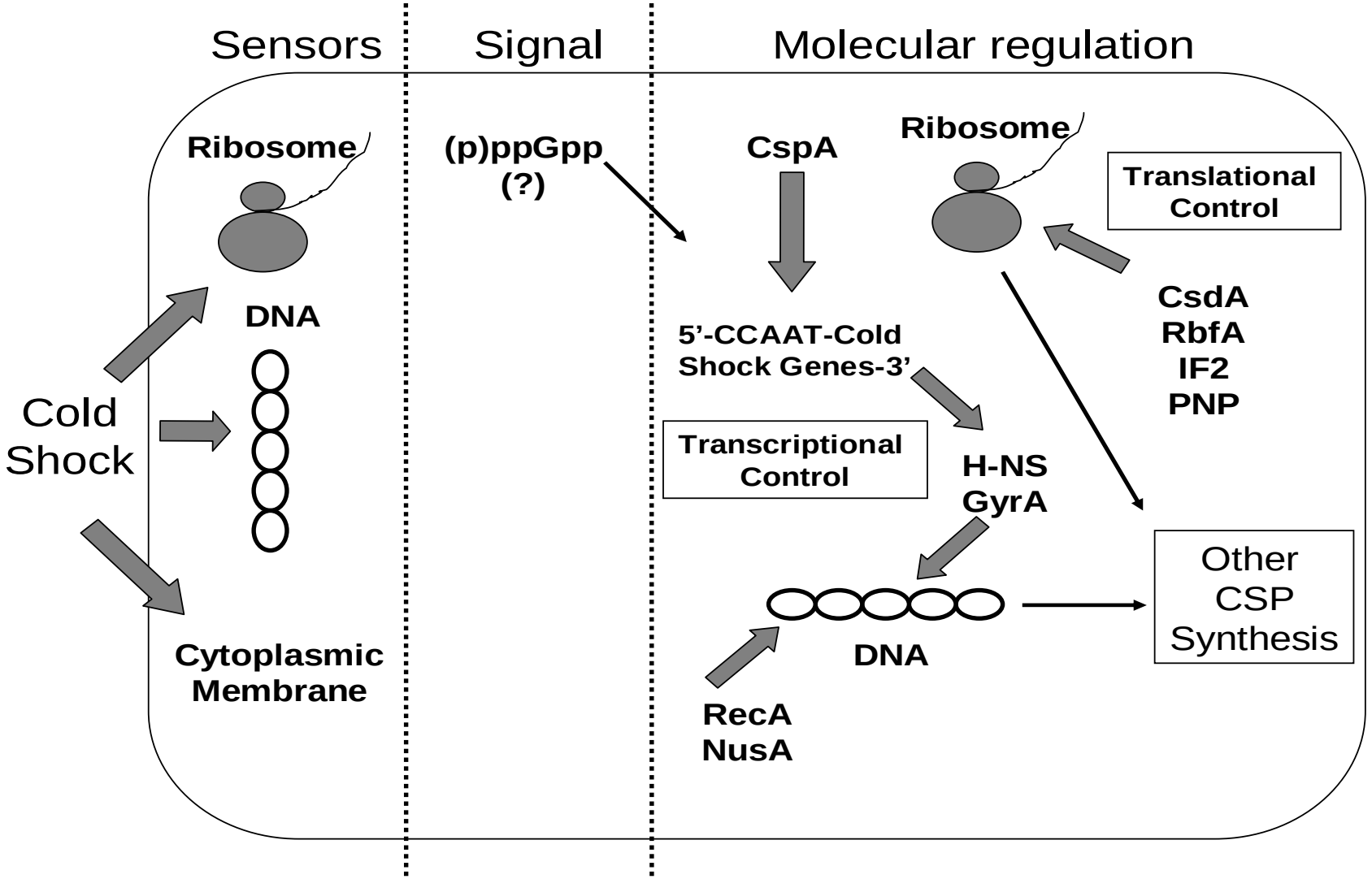
Sensors
Signal
Molecular regulation
Ribosome
DNA
Cold
Shock
Cytoplasmic
Membrane
(p)ppGpp
(?)
CspA
5'-CCAAT-Cold
Shock Genes-3'
Transcriptional
Control
H-NS
GyrA
RecA
NusA
DNA
Ribosome
Translational
Control
CsdA
RbfA
IF2
PNP
Other
CSP
Synthesis

this transition in response to cold shock via desaturating their membrane fatty acids. This increases the level of inherent fluidity and flexibility of the membrane and allows for membrane functioning at these lower temperatures. A variety of mechanisms exist to achieve this alteration in membrane lipid composition, but the first and best studied model is in *E. coli* (35, 36, 125). It was in this organism that cold inducible proteins were first discovered (68). While most protein synthesis in the cell stops during acclimation phase, there is a group of about 25 proteins identified whose expression is actually induced at this time, termed cold shock proteins (CSPs) (Table 1.2). These proteins function primarily as either DNA or RNA chaperones or have some role in translation. CSPs exist as two classes, class I and class II. Class I CSPs are expressed at a very low level at optimal temperatures (in *E. coli* this would be 37 ^{o}C) and are dramatically induced to extremely high levels after a drop in temperature. Class II CSPs are expressed at optimal temperatures and their induction upon cold shock is not dramatic (< 10 fold induction) (107).

Perhaps the best studied cold shock proteins are the CspA family of *E. coli*. CspA was the first protein described as a major protein induced upon cold shock (43) and can account for as much as 10% of cellular protein synthesis during the aforementioned acclimation phase. The CspA family is comprised of nine homologous proteins (CspA-CspI) that are all small in size (~ 7 kDa). However, only CspA, CspB, CspG and CspI have been shown to be cold inducible (83, 104, 136). CspC is expressed both at optimal and low temperatures (142), and CspD has been shown to be induced upon stationary phase and during nutrient starvation conditions (140). During acclimation phase, the expression of CspA, CspB, CspG and CspI are all dramatically, transiently and tightly regulated at the levels of transcription, translation and mRNA stability. The regulation of cold shock proteins will be discussed in more detail in section 3.B. While

Table 1.2 Cold shock proteins identified in *E. coli*[a]

Protein	(Proposed) Function/Properties	CSP class[a]
AceE	Pyruvate dehydrogenase (decarboxylase)	II
AceF	Pyruvate dehydrogenase (dihydrolipoyltransacetylase)	II
CspA	RNA and DNA binding ; RNA chaperone	I
CspB	RNA binding	I
CspE	RNA binding; RNA chaperone; transcriptional antiterminator; PNPase and RNAse inhibitor	I
CspG	Unknown	I
CspI	Unknown	I
DeaD	RNA helicase	I
DnaA	DNA binding and replication; transcriptional regulator	I
GyrA	DNA binding, cleaving and rejoining	II
H-NS	Transcriptional repressor;DNA supercoiling	II
Hsc66	DnaK homolog	II
HscB	DnaJ homolog	II
HUβ	DNA supercoiling	II
IF1	Translation initiation; RNA binding	II
IF2	Translation initiation; protein chaperone	II
IF3	Translation initiation; RNA binding	II
NusA	Transcription elongation/termination/antitermination	I
OtsA	Trehalose phosphate synthase	II
OtsB	Trehalose phosphatase	II
PNPase	3’-5’ exonuclease	I
RbfA	Ribosome assembly/maturation	I
RecA	Homologous recombination	II
Trigger factor	Multiple stress responsive; protein chaperone	II
Ves	Unknown	I
PY	Translational inhibitor	I

[a]Table adapted from Gualerzi, et al, 2003.

the exact functions of these proteins are difficult to elucidate due to their overlap in mutation studies (139), as a group the CspA family are thought to function as mRNA chaperones inhibiting the stabilization of secondary structures stabilized at low temperatures and allowing for proteins synthesis to occur (7).

There is a growing library of cold inducible proteins in *E. coli*, most of which have been identified using two-dimensional gel electrophoresis (Table 1.2). In addition to the CspA family, other cold shock proteins include: CsdA, a ribosomally-associated RNA helicase (67); RecA, which is involved in DNA recombination (64); H-NS, a transcriptional repressor involved in DNA supercoiling (81); HUβ, also involved in DNA supercoiling (39); DnaA, a transcriptional regulator (6); GyrA, the DNA binding, cleaving and rejoining portion of the topoisomerase DNA gyrase (66); NusA, involved in transcription termination and antitermination (64); PNPase, an exoribonuclease (9, 141, 144); Hsc66, a heat shock protein chaperone homolog (86); the translation initiation factors IF1, IF2 and IF3 (46, 64); RbfA, a ribosomal binding factor believed to be involved in ribosome assembly and maturation (65); Trigger factor, a general stress protein that is a ribosome associated protein chaperone (71); OtsA and OtsB, involved in trehalose biosynthesis (70). As evidenced by the functions of these cold induced proteins of *E. coli*, it is apparent that cold stress affects many cellular functions, including transcription, translation, ribosome assembly and function and protein folding.

3.B. Regulation of bacterial cold shock proteins

Although there have been many studies to identify cold inducible proteins, the mechanism of regulation of these proteins has yet to be fully worked out. Unlike the heat shock response, where regulation is governed by increased synthesis and stability of a specific sigma

factor that recognizes an alternative promoter sequence in response to an increase in temperature (102, 143), regulation of the cold shock response is much more complex. Depending on the protein, cold shock regulation involves varying degrees of transcriptional, posttranscriptional, and translational regulation (46).

Initial studies of cold shock regulation centered on the discovery of a cold responsive regulatory element. Indeed, the first studies showed CspA interacting with the promoter sequences of two genes encoding CSPs, *hns* and *gyrA*, resulting in their increased transcription (66, 81). This led researchers to initially dub CspA a transcriptional regulator of the cold shock response. Later studies, however, revealed these interactions were serendipitous, more a result of CspA's ability to bind ssDNA and RNA (15), and did not significantly enhance transcription of these genes (40, 42). In addition, several genes encoding CSPs have been identified that lack the region thought to be responsible for the CspA-DNA interaction (called the Y-box) (15, 86). Indeed, exactly what role and to what degree transcriptional regulation plays in the cold shock response is yet to be fully understood.

Fortunately, information on the posttranscriptional control of the cold shock response is more convincing. Interestingly, the *cspA* promoter is not needed for cold shock induction (14, 28), indicating that posttranscriptional events are more responsible for its cold regulation than initially thought. Studies on the *cspA* transcript indicate that enhanced mRNA stability following a cold shock is primarily responsible for its cold shock induction (41). The transcript for HUβ and IF2 also are stabilized in response to cold shock (46), indicating this type of regulation mechanism exists for CSPs other than just CspA. The most recent theory that has been advanced is that there is some type of alteration in the RNA degrading machinery during acclimation phase, which increases the stability of the mRNA of CSPs (41). However, it has also been

demonstrated that this stability is temporary and towards the end of acclimation phase returns to what is seen pre-shock (41). This is explained by there being a new or altered RNA degradosome that is in effect at the end of acclimation phase, ready to degrade accumulating amounts of mRNA encoding CSPs (46). Much has been postulated about this difference in mRNA stability, and it appears to be related to the 5'untranslated region (5'UTR) that precedes the initiation codon of many cold shock genes such as *cspA, cspB, cspG, cspI* and *dead* (which encodes for CsdA) (46). Adjustments in this 5' UTR of *cspA* can stabilize its transcript at optimal temperatures (37 ^{o}C), which indicates it having some role in the stabilization effect seen at low temperatures (14, 28).

The overlying dogma of cold shock induction for many years has been that there is some step in translation initiation that is compromised upon a decrease in temperature, thus preventing protein synthesis from occurring (29). However, with the exception of the mRNA-ribosome interaction, none of these initiation steps has ever been shown to be cold-sensitive (25). The fact that *E. coli* can translate CSPs during the acclimation phase of cold shock, and that low levels of antibiotics that affect translation can lead to the induction of CSPs in the absence of a decrease in temperature (68) lead to the hypothesis that the ribosome is some type of "microbial thermostat" (133).

Thus, it is not surprising that cold shock induces a modification in the translation machinery in *E. coli*. This modification enables the translation of CSP mRNA during acclimation phase, while non-CSP mRNA are not efficiently translated until the end of acclimation phase (14, 42). It is thought that there was an interaction between the 5'UTR and an as yet identified "cold shock factor" (46). This interaction supposedly enables CSP mRNA to preferentially occupy the ribosome.

The most recent studies center on this CSP mRNA translation bias by the translational apparatus of cold shocked cells. These studies show that this bias for CSP mRNA translation occurs only at low temperatures (46). At 37 ^{o}C, however, translation of both CSP and non-CSP mRNA using cold shock translation machinery improves. The presence of certain *trans*-acting "cold induced factors" in the cold shocked extracts, as well as the potential *cis*-acting elements of the CSP mRNA are thought to be responsible for this CSP translation bias. Recent studies also have revealed new evidence about these *trans*-acting elements. In addition to an increase in translation initiation factor 2 (IF2), long known to be cold induced (68, 144), IF1 and IF3 also appear to increase in response to cold shock (46). In addition to increasing over time, the IF/ribosome ratio temporarily increases in response to cold shock, shown to result from an increase in transcription as well as an increase in mRNA stability.

3.C. The overlap of archaeal and bacterial cold shock response

The most recent review on archaeal cold stress highlights the overall lack of knowledge regarding the effects of cold shock in any archaea (18). In fact, the majority of this review discusses how certain species of archaea thrive at low temperatures (and how they have become adapted to this environment) simply due to the fact that there was so little information regarding cold shock in this domain of life. Using these clues the authors hypothesize about a possible cold shock response in archaea, particularly hyperthermophilic archaea.

There exists a single study where a mesophilic bacterial class I cold shock protein is identified in an archaeon and was shown to be cold inducible. The CSP CsdA, a cold inducible RNA helicase, was shown to be low temperature regulated in the psychrotolerant archaeon *Methanococcoides burtonii* (88). Like other class I CSPs, this protein was not expressed at

optimal (23 ^{o}C) growth temperatures and its gene contained the 5'UTR characteristic of CSPs identified in mesophilic bacteria that is thought to play a role in their regulation.

3.D. Hyperthermophilic cold shock response

As stated in the previous section, there is an overall paucity of data involving cold stress in hyperthermophilic archaea. Not surprisingly, what studies have been done show an altogether different response to cold stress than seen in bacteria. The subjects of these studies are a protein chaperone known as FKBP that is expressed at low but not optimal temperature and changes in DNA topology in response to cold stress.

FK506 binding proteins (FKBPs) have peptidyl-prolyl *cis-trans* isomerase activity (PPIase), catalyzing the *cis-trans* isomerization of the proline imide bond in polypeptides (82). Two types of FKBPs have been identified in archaea. The short form (~ 17 kDa) possesses PPIase activity similar to that seen in bacteria in addition to the ability to refold unfolded proteins. The second, long form (~ 28 kDa) has low PPIase as well as low level chaperone-like activity (99). Interestingly, a new protein identified in the *E. coli* cold shock response (called trigger factor) is a ribosome-associated FKBP that possesses chaperone-like activity (71). It has been demonstrated that this short type FKBP is expressed at higher concentrations in the hyperthermophilic archaeon *Thermococcus* sp. KS-1 when grown at 60 ^{o}C compared to 75 ^{o}C (58). Further analysis showed that the FKBP transcript was induced 1 hour after cold shock, however, the transcript subsequently returned to normal levels. Similar results were seen in *Methanococcus jannaschii* when grown at 60 ^{o}C compared to 85 ^{o}C. This study also pointed out that other hyperthermophilic archaea such as *Pyrococcus horikoshii* and *Aeropyrum pernix* only contain the gene for the long type FKBP in their genomes (57). The *P. horikoshii* FKBP was

investigated and was found to not be cold regulated. There was also no evidence for cold-regulation of the FKBP homolog (PF1401) in the cold shock studies of *P. furiosus* (see chapter 5).

How cold stress can influence plasmid DNA topology has been studied in the hyperthermophilic archaeon *Sulfolobus islandicus*. Plasmid DNA isolated from cells grown at low temperatures (60-65 ^{o}C) were considerably more negatively supercoiled than cells grown at the optimal temperature (80 ^{o}C) (91). Similar results were seen with plasmid DNA isolated from other *Sulfolobus* species as well as from *Thermococcus* sp. GE31 and *Pyrobaculum abyssi* (93). Furthermore, plasmid DNA from *S. islandicus* cells subjected to a cold shock (growing cells at 80 ^{o}C shifted to 65 ^{o}C) showed a transient (~ 4 hour) increase in negative supercoiling (91). After 4 hours, supercoiling slowly recovered, returning to the normal state ~ 22 hours after the stress was induced. However, none of the known topoisomerases of this organism (such as reverse gyrase, Topo VI, or Sis7) were induced upon cold shock (91). This would indicate that either this change in DNA topology does not require any enzyme activity and is due to the intrinsic nature of the temperature change, or that the protein(s) responsible for such reactions are unknown at present and are annotated as conserved/hypothetical.

It is interesting to note that not only does DNA topology change in *E. coli* during cold shock, DNA gyrase and HU are two topoisomerases that are induced during this stress (92). This provides some connection between the mesophilic bacterial and hyperthermophilic archaeal cold shock responses, although the fact that none of the topoisomerases from *S. islandicus* are induced upon cold shock calls into question the exact similarities of these responses.

4. **The oxidative stress response**

4.A. Aerobic oxidative stress response

Molecular oxygen is a powerful oxidant (O_2/H_2O, $E_o' = + 818$ mV) that possesses some unusual chemistry. Its orbital structure will only allow univalent electron transfer reactions despite it being a triplet species (having two spin aligned, unpaired electrons) (138):

$$O_2 \xrightarrow{-0.16\ V} O_2^{\cdot -} \xrightarrow{+0.94} H_2O_2 \xrightarrow{+0.38\ V} HO^{\cdot} + H_2O \xrightarrow{+2.33\ V} H_2O$$

As the above reaction indicates, one electron can be donated to molecular oxygen by a electron donor to form superoxide. It is this property that makes molecular oxygen so stable in a biological environment; most biomolecules are not amenable to single electron oxidations. For example, the redox potential for $NADH^{\cdot +}/NADH$ is high enough, + 0.93 V (17), that the reaction rate of NADH with oxygen is practically nonexistent (59). This is true for many other biomolecules that are the cellular building blocks. Oxygen does not directly oxidize carbohydrates, nucleic acids, lipids or amino acids at high enough rates to warrant the amount of damage it causes (59).

In fact, this inertness of biomaterials to molecular oxygen led to much confusion in the early attempts to define the deleterious effects of oxygen on biological systems (59)**.** It was only after the serendipitous discovery of superoxide dismutase (SOD) as an enzyme functioning to suppress intracellular levels of superoxide that some advances in this line of research began to take place (100). Along with the discovery that SOD is, with few exceptions, present in aerotolerant organisms, this lead to the theory that anaerobic organisms cannot tolerate oxygen because they lacked the enzymes needed to scavenge excess superoxide (101). A similar

distribution was demonstrated for catalase, a hydrogen peroxide scavenger, further fueling researchers to study these two enzymes and how they related to oxygen and oxidative stress.

Oxidative stress is a major issue in organisms that respire aerobically. As alluded to above, it is caused by extensive exposure to reactive oxygen intermediates (ROI) such as the superoxide anion ($O_2^{\cdot-}$), hydrogen peroxide (H_2O_2), and the hydroxyl radical ($HO^{\cdot}$). These are natural by-products of aerobic respiration, making this lifestyle a potentially suicidal one. Steady state intracellular levels of $O_2^{\cdot-}$ and H_2O_2 in aerobically growing *E. coli* have been measured at 10^{-10} M (45) and 10^{-7} M (44), respectively, both just below the toxicity level (5^{-10} M and 10^{-5} M, respectively). This would indicate *E. coli* carefully regulates its metabolism to avoid oxidative damage from naturally occurring ROI.

The reactivity for each ROI differs, which leads to distinct types of intracellular damage (Figure 1.6). $O_2^{\cdot-}$ tends to attack iron sulfur clusters [4Fe-4S], oxidatively inactivating them (32). A side effect of [4Fe-4S] damage is the huge amount of iron released into the cytosol (75). Here it can react with H_2O_2 to form $HO^{\cdot}$, which is an extremely powerful oxidant that can react with most biomolecules (DNA, protein, membrane lipids) (60). H_2O_2 can also directly oxidize enzyme thiols which results in a loss of activity for those enzymes relying upon active site localized cysteine residues (127).

In order for aerobic organisms to survive the inherent danger of their lifestyle, they must have some way of defending themselves against these ROIs. As expected, aerobes contain one or more enzymes that possess antioxidant activity (such as superoxide dismutase, catalase and alkyl hydroperoxide reducatse) and repair systems (such as Endonuclease IV, Exonuclease III and RecA) to act when damage actually occurs (Table 1.3). The two major systems responsible for regulation of these systems in *E. coli* are the SoxRS transcription factors (in response to $O_2^{\cdot-}$)

Figure 1.6.

Mechanisms of oxidative cell damage. Molecular oxygen (O_2) passively diffuses through the cell membrane. It can be converted in the cell to $O_2^{\cdot -}$ or H_2O_2 by the direct oxidation of flavoproteins. $O_2^{\cdot -}$ generated here can oxidatively destroy protein iron sulfur clusters, which results in the release of iron. This released iron can react with H_2O_2 to form $HO^{\cdot}$, which can damage DNA directly. H_2O_2 can also directly oxidize protein cysteinyl residues, which would also inactivate the protein. Modified from (127).

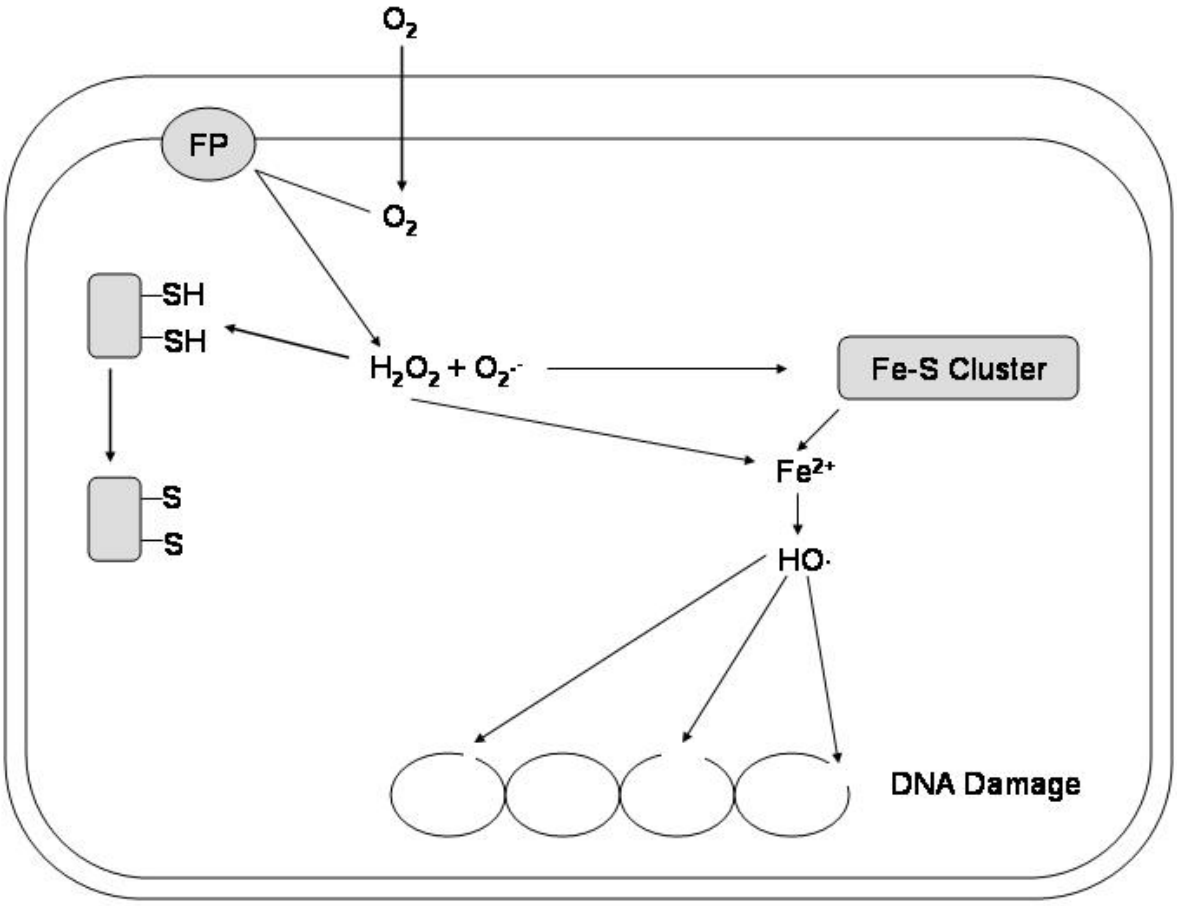
O_2
FP
O_2
SH
SH
$H_2O_2 + O_2^{\cdot-}$
Fe-S Cluster
Fe^{2+}
S
S
HO·
DNA Damage

and the OxyR transcription factors (in response to H_2O_2) (Figure 1.7). Like SOD and catalase, OxyR and SoxR are typically not present in anaerobic organisms. Regulation of SoxRS is a two step process, beginning with the activation of the constitutively expressed SoxR by the oxidation of its two [2Fe-2S] centers (27, 37, 50). This active form of SoxR enhances the transcription of SoxS, finally resulting in the increased transcription of those genes under its control (51) (Table 1.3). OxyR, much like SoxR, exists in 2 forms, a reduced (inactive) and an oxidized (active) form (145), although in this case the redox sensitive domain is composed of disulfide bonds rather than [2Fe-2S] clusters as in SoxR.

4.B. Anaerobic oxidative stress response

Although it would seem that by nature anaerobic organisms would not be able to defend themselves against ROIs, it has recently been shown that they possess a primitive scavenger system. This defense system revolves around the recently discovered enzyme superoxide reductase (SOR), which plays a role analogous to that of SOD in aerobes (62). The major difference between the two are that SOD produces molecular oxygen in addition to hydrogen peroxide, whereas SOR only produces hydrogen peroxide (79):

SOD: $2O_2^{\bullet -} + 2H^+ \rightarrow H_2O_2 + O_2$

SOR: $O_2^{\bullet -} + 2H^+ + e^- \rightarrow H_2O_2$

It is this property that makes SOR much more suitable than SOD for anaerobic organisms. Both reactions, however, produce hydrogen peroxide, which, as mentioned previously, can cause either direct or indirect cellular damage. Aerobes employ the enzyme catalase to reduce the potentially toxic hydrogen peroxide to water (62):

Catalase Reaction: $2H_2O_2 \rightarrow 2H_2O + O_2$

Table 1.3 Antioxidant activities in *E. coli*

Gene	Activity	Regulator(s)
sodA	Manganese superoxide dismutase	SoxRS, ArcAB, FNR, Fur, IHF
fumC	Fumarase C	SoxRS, ArcAB, σ^s
acnA	Aconitase A	SoxRS, ArcAB, FNR, Fur, σ^s
zwf	Glucose-6-phosphate dehydrogenase	SoxRS
fur	Ferric uptake repressor	SoxRS, OxyR
micF	RNA regulator of *ompF*	SoxRS, OmpR, LRP
acrAB	Multidrug efflux pump	SoxRS
tolC	Outer membrane protein	SoxRS
fpr	Ferredoxin reductase	SoxRS
fldA	Flavodoxin	SoxRS
nfo	Endonuclease IV	SoxRS
sodB	Iron superoxide dismutase	σ^s, FNR
sodC	Copper-zinc superoxide dismutase	σ^s, FNR
katG	Hydroperoxidase I	OxyR, σ^s
ahpCF	Alkyl hydroperoxide reductase	OxyR
gorA	Glutathione reductase	OxyR, σ^s
grxA	Glutaredoxin I	OxyR
dps	Non-specific DNA binding protein	OxyR, σ^s, IHF
oxyS	Regulatory RNA	OxyR
katE	Hydroperoxidase II	σ^s
xthA	Exonuclease III	σ^s
polA	DNA polymerase I	??
recA	RecA	RecA, LexA
msrA	Methionine sulfoxide reducatse	??
hsfO	Molecular chaperone	??
mutM (fpg)	8-hydroxyguanine endonulease	FNR
hmp	Flavohemoglobin	MetR

Adapted from (127). The list of regulators is merely what is known at this time and not doubt will be expanding with time. It is simply meant as a guide.

Figure 1.7.

Mechanisms of SoxR and OxyR activation and inactivation. The redox-active center of SoxR is directly or indirectly activated by $O_2^{\cdot-}$, which damages iron-sulfur clusters upon oxidation. What is interesting about SoxR in this scenario is that its redox active center itself is an iron sulfur cluster. The redox active center of OxyR is directly activated by H_2O_2, which oxidizes protein cysteinyl residues. The active center here is a redox-sensitive disulfide bond. Adapted from (127).

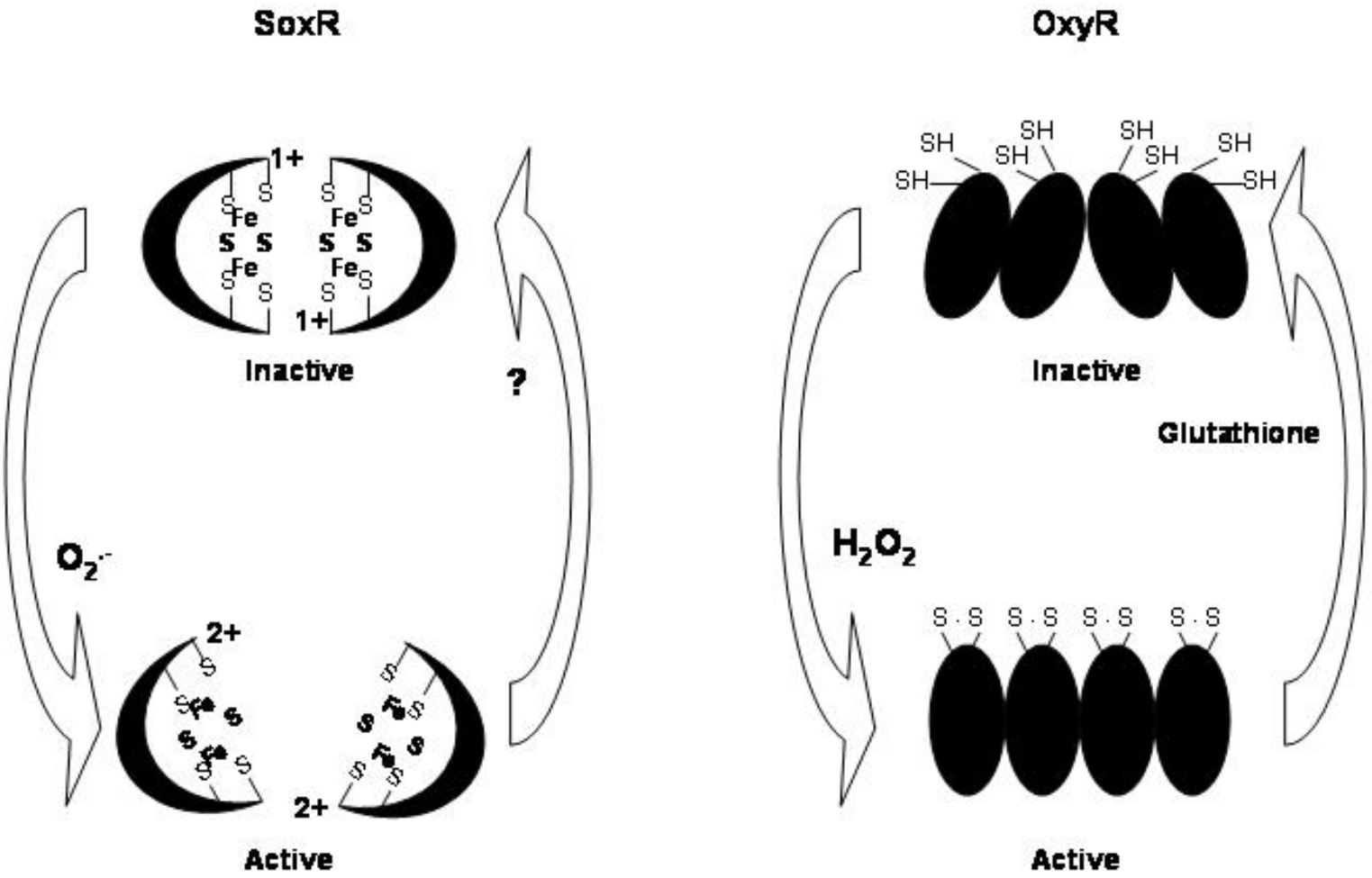
SoxR
1+
Fe
S
Fe
S
S
S
Fe
S
Fe
S
1+
Inactive
?
$O_2^{\cdot-}$
2+
2+
Active
OxyR
SH
SH
SH
SH
SH
SH
SH
Inactive
Glutathione
H_2O_2
S·S
S·S
S·S
S·S
Active

Thus, much like SOR takes the place of SOD in anaerobes, there must be some enzyme that anaerobes substitute for catalase. Most sequenced anaerobic genomes do not possess a classical catalase gene (62), further highlighting the need for a new enzyme to reduce hydrogen peroxide. What is seen in anaerobic genomes are genes coding for other enzymes involved in peroxide detoxification, such as putative NADH dependent peroxidases, peroxiredoxins and alkyl hydroperoxidases, indicating there are other, non-classical systems in place in anaerobes for peroxide detoxification.

There has been some evidence that rubrerythrin (Rr) is involved in ROI detoxification in anaerobes. The genomes of both *T. maritima* (105) and *P. furiosus* (53, 115) have their Rr encoding gene adjacent to the rubredoxin (Rd, believed to be the physiological electron donor to SOR) and SOR genes, indicating a possible common or related function. Although no definitive function has been attributed to Rr, it has been shown to possess SOD, ferroxidase and peroxidase activity (5, 12, 85), depending on the organism. However, the true function for this protein remains unclear.

The best studied Rr is from the obligate anaerobe *Desulfovibrio vulgaris*, the organism from which it was first isolated (84). Rr is a homodimer with a subunit molecular weight of 21.9 kDa. Two separate metal binding domains have been described for Rr. One resembles the protein Rd, while the second resembles hemerythrin and contains a dinuclear site. In fact, Rr derives its name from these two words: RUBREdoxin and hemeRYTHRIN. Since its first isolation, a vast amount of physical, spectroscopic and magnetic data has been accumulated, much of which is related to these metal-binding domains (24, 47, 80, 108, 113, 132)

The metal content of these sites has been the subject of controversy throughout the study of Rr, as both iron and zinc seems to be employed by the protein depending on the isolation

method. The current structural studies highlight these preparation-dependent metal discrepancies. Three structures have been solved for *D. vulgaris* Rr. The first structure is a recombinant form prepared under aerobic conditions where the hemerythin-like site is composed of two irons (26). Structure two is a native protein also prepared under aerobic conditions. In this form, however, the binuclear site is composed of a mixture of iron and zinc (123). The third structure is also a native form, although this one was prepared anaerobically and also contains Fe-Zn in its binuclear site (87). Upon exposure to air, the Zn moves to allow for the entrance of a water molecule into the binuclear center location. The authors propose that this Zn movement is somehow related to the enzymatic activity of Rr (87).

The search for an activity and function for Rr has lead to it being defined first as a pyrophosphatase (89, 132), then a ferroxidase (12), and finally a NADH peroxidase (19, 20, 22). While most of the physical, spectroscopic and magnetic data on Rr exists from the *D. vulgaris* system, much of the physiological evidence attributing a role in peroxide detoxification stems from research on other organisms. Rr was isolated from the obligate anaerobe *Clostridium perfringens* by following SOD activity from cell extracts, an activity not previously seen for Rr (85). Further study showed an *E. coli* mutant strain lacking SOD activity could be complemented by the *C. perfringens rbr* gene. A study profiling the transcriptional regulation of the *C. perfringens rbr* gene showed it was not responsive to oxidative stress, however (38). Another study showed that a hydrogen peroxide-resistant mutant strain of the microaerophile *Spirillum volutans* (which does not possess the catalase gene) overexpressed Rr and that in the wild type strain it was undetectable and noninducible (5). Cell extracts of the peroxide-resistant mutant strain possessed significant NADH peroxidase activity, whereas the wild type strain lacked such activity (4). Yet another study performed on the obligate anaerobe *Porphyromonas*

gingivalis showed that *rbr*$^{-}$ mutants were more oxygen- and hydrogen peroxide-sensitive than wild type strains (129). In stark contrast to the *C. perfringens* transcriptional analysis study, Rr in wild type strains of *P. gingivalis* was shown to be inducible by oxidative stress.

Hence, while the exact role of Rr has yet to be firmly defined, it seems clear from most of the recent studies that it is an oxidative stress protein in many obligate anaerobes and microaerophiles (16, 59, 95). Thus, there is a serious need to define a specific function for Rr before any further presumptions are put forth.

5. Proposed Research

The overall goal of this research was to advance the knowledge of the stress response in hyperthermophilic archaea, specifically in *P. furiosus*. Prior to this project there were no known cold inducible elements identified in any hyperthermophilic archaeon, nor was it known that anaerobes and microaerophiles were able to enzymatically reduce ROIs in order to protect themselves from their deleterious effects. In the following, chapters 2 and 3 will address the issue of how hydrogen peroxide produced from the recently-identified superoxide reductase (SOR) reaction is reduced further to water, as well as describe a protocol in which a recombinantly-produced NROR is reconstituted to the native form. Chapter 4 describes the first extensive and genome-wide study of the cold shock response of hyperthermophilic archaea at the cellular, transcriptional, translational and enzymatic levels.

CHAPTER 2

RECONSTITUTION OF INACTIVE, RECOMBINANT NADPH:RUBREDOXIN OXIDOREDUCTASE FROM THE HYPERTHERMOPHILIC ARCHAEON *PYROCOCCUS FURIOSUS*[1]

[1] Weinberg, M.V. and M.W.W. Adams. 2004. To be submitted to *Journal of.Bacteriology*.

ABSTRACT

An inactive form of NAD(P)H:rubredoxin oxidoreductase (NROR) from the hypothermophilic archaeon *Pyrococcus furiosus* has been recombinantly expressed and purified from *Escherichia coli* cells. The as-purified recombinant protein was approximately 40-fold less active than the form purified from *P. furiosus* (23 vs. 490 U/mg). It was shown that the low activity was due to a lack of FAD in the recombinant protein. After a heat treatment in the presence of FAD, the protein contained 1 FAD moiety per protein and activity increased to a value similar to that measured in the native enzyme (475 U/mg). The apparent K_m values for rubredoxin, NADH and NADPH measured at 80 ^oC in the reconstituted recombinant protein (100, 7 and 45 μM, respectively) compared favorably with the values measured for the native enzyme (50, 5 and 34 μM, respectively). This is the first report of an active form of recombinant NROR from *P. furiosus*.

INTRODUCTION

Pyroccoccus furiosus is an obligately anaerobic hyperthermophilic archaea, growing optimally at 100 ^{o}C (5, 15). *P. furiosus* inhabits shallow and deep-sea volcanic environments, growing by fermentation of carbohydrates or peptides and producing organic acids, CO_2 and H_2 as waste products. When elemental sulfur (S^o) is added to the medium, H_2S is formed as a waste product in the place of H_2.

A small, iron-containing redox protein termed rubredoxin (Rd, ~ 5.9 kDa) has been purified from *P. furiosus* and studied extensively (2, 9). In addition, Rd from a number of other organisms have been purified and characterized to varying degrees (11). Despite almost forty years of extensive study, the physiological role of Rd had been undefined until recently.

The discovery of superoxide reductase (SOR) activity carried out by the non-heme iron proteins previously denoted as neelaredoxin and desulfoferrodoxin (9, 13), led to the proposal of a reactive oxygen species (ROS) detoxification pathway in anaerobic and microaerophilic microbes separate from the superoxide dismutase (SOD) based pathway seen in aerobes (16). It was shown that SOR has the ability to reduce superoxide using reduced Rd as the electron donor to produce hydrogen peroxide and water. Rd is reduced by the enzyme NADPH:Rd oxidoreductase (NROR) which has also been purified from *P. furiosus* (12). NROR is thought to provide a constant pool of reduced Rd for SOR using NADPH as the electron donor. While the vast majority of enzymes from hyperthermophilic organisms have no significant activity at mesophilic temperatures (~ 23 ^{o}C), both SOR and NROR are very active. This factor is consistent with the hypothesis that both of these enzymes play a role in the ROS detoxification pathway, since the only time *P. furiosus* would presumably encounter such species is when it is expelled into the cold water surrounding the hot smokers in which they normally thrive.

Attempts to clone and recombinantly produce active NROR in *Escherichia coli* have been unsuccessful (Grunden, A., unpublished data). This was believed to be due to its interference with normal intracellular redox chemistry, a consequence of the unusual ability of NROR to function at the low temperatures at which *E. coli* grows. In this report, it is shown that an inactive, recombinant form of *P. furiosus* NROR can be produced and that reconstitution with FAD yields an enzyme with an activity at or near that which is described previously for the native protein (12).

MATERIALS AND METHODS

Cloning, expression and purification of recombinant *P. furiosus* NROR. All standard molecular biology techniques were performed essentially as described previously (14). A pET-24 plasmid containing a modified NROR gene (PF1197) with a His-6 tag at the N terminus (MAHHHHHHGS-) was provided by the Southeastern Collaboratory for Structural Genomics (6) at the University of Georgia. This was transformed into *E. coli* strain BL21(DE3) Star/pRIL which was grown in Luria Bertani media (LB**)** at 37 ^{o}C. Kanamycin (50 μg/ml) and chloramphenicol (34 μg/ml) were added as needed for plasmid maintenance. The expression of the NROR gene was induced with isopropyl-β-thiogalactopyranoside (IPTG) (0.4 mM) when the growth medium reached an optical density at 600 nm of 0.6. The culture was induced for 3.5 hours at 25 ^{o}C prior to harvesting of the cells by centrifugation at 10,000 x *g* for 20 minutes at 4 ^{o}C.

All purification steps were performed under anaerobic conditions using degassed buffers and when necessary were carried out in an anaerobic chamber as described previously (3). IPTG-induced BL21(DE3) Star/pRIL cells that had been harvested from 2 separate 1L cultures

were each suspended in 20 ml of 10 mM imidazole buffer (pH 8.2) containing 20 mM sodium phosphate and 0.5 mM NaCl (Buffer A). The samples were frozen at -80 ^{o}C until needed. Cells were thawed under argon flow and lysed by sonication for 5 minutes, under a flow of argon. The extracts were centrifuged at 16,000 x *g* for 20 min at 4 ^{o}C to remove cell debris. The supernatants were applied to two separate columns (1.5 x 3 cm) of Ni-NTA affinity (Novagen, Madison, WI) that were equilibrated with Buffer A. After washing the column with 5 column volumes of buffer A, protein was eluted with 300 mM imidazole buffer (pH 8.2) containing 20 mM sodium phosphate and 0.5 mM NaCl (Buffer B). Sodium dithionite (DT) was immediately added to the fractions containing the eluted protein to a final concentration of 2 mM. These fractions were mixed and concentrated by ultrafiltration (YM-30 membrane) to 5 ml. The buffer was replaced with 50 mM Tris, pH 8.0 containing 200 mM NaCl and 2 mM DT (Buffer C). The protein was then concentrated to a final volume of 4 ml and applied to a Superdex 200 (Amersham Biosciences, Piscataway, NJ) column (26 x 60 cm) equilibrated with Buffer C. Those fractions deemed pure on the basis of sodium dodecyl (SDS)-polyacrylamide gel electrophoresis (10) were combined, concentrated by ultrafiltration (YM-30 membrane) and stored as pellets in liquid N_2. A typical purification of the recombinant NROR is outlined in Table 2.1. The protein was unstable in the absence of 200 mM NaCl, as attempts to buffer exchange or dilute the protein resulted in precipitation.

The activity of rNROR was measured as described previously at 80 ^{o}C (12). Briefly, the reaction mixture (2.0 ml) contained 50 mM CAPS [3-(cyclohexylamino)-1-propanesulfonic acid] buffer (pH 10.2). NADH (0.3 mM) was used as the electron donor and benzyl viologen (BV, 1 mM) as the electron acceptor. The assay was initiated by the addition of NROR and a molar

absorptivity of 7.8 $mM^{-1}cm^{-1}$ at 598 nm was used for reduced BV. One unit (U) of activity is equivalent to 1 μmol of BV reduced/min/mg.

RESULTS AND DISCUSSION

Purification of NROR from *P. furiosus*. The gene (PF1197) encoding NROR of *P. furiosus* was cloned and expressed in *E. coli* and the recombinant protein (rNROR) containing an N-terminal polyhistidine tag was purified. The specific activity of pure rNROR using NADH as the electron donor and benzyl viologen as an artificial electron acceptor was 23 U/mg. This is approximately 40-fold lower than the activity reported for the pure native form of enzyme (nNROR, 490 U/mg) purified from *P. furiosus* (12). This low activity, much like the protein instability, was attributed to a lack of FAD cofactor in the recombinant protein, discussed further below.

Reconstitution of recombinant NROR. Since nNROR is known to contain 1 FAD per protein (12), an attempt was made to reconstitute rNROR by incubating it with a 10-fold molar excess of FAD for 15 min at 85 ^{o}C. rNROR was also subjected to this heat treatment with and without a 10-fold molar excess of FMN. Following the heat treatments, the proteins were loaded onto a 5 ml Hitrap desalting column (Amersham Biosciences) equilibrated with Buffer C to remove excess flavin cofactor.

After reconstitution, rNROR was assayed as above using NADH as the electron donor and BV as the electron acceptor. The heat treatment without any cofactor or with FMN did not significantly increase the activity of the recombinant protein. However, the heat treatment with FAD resulted in a protein with a dramatic increase in activity (475 U/mg), comparative to that

Table 2.1. Purification table for recombinant NROR

Step	Protein (mg)
Cell-free extract	388
Ni-NTA Affinity	145
Gel Filtration	81

reported for nNROR (12). The results of the reconstitution experiment are summarized in Table 2.2. In addition, samples reconstituted with FAD remained soluble during the heat treatment, whereas samples incubated without FAD had some precipitation. Moreover, the FAD-reconstituted protein no longer precipitated when diluted (to ~ 1 mg/ml) in buffer. These data suggest a lack of FAD was the cause of this instability and precipitation.

Biophysical properties of rNROR. As seen in figure 2.1, SDS-PAGE of purified rNROR showed a single protein band corresponding to a M_r of 40,000 Da. LC-MS analysis performed at the Mass Spectrometry Facility (University of Georgia Department of Chemistry) revealed a mass of 40,882 Da, which is close to the calculated value of 40,848 Da for rNROR (with a polyhistidine tag).

The UV-visible absorption spectra of nNROR exhibits peaks at 375 and 450 nm, indicative of a flavin-containing cofactor. Further analysis by HPLC revealed its identity as a flavin adenine dinucleotide (FAD) via mass spectroscopy. Using a molar absorptivity of 11.3 $mM^{-1}cm^{-1}$ (1), it was determined to contain 1 mole of FAD per mole of protein. The UV-visible spectra of as-purified rNROR revealed very minor absorption maxima at 375 and 450 nm (data not shown), and using the same molar absorptivity constant, it was determined to contain a negligible amount of FAD (less than 0.05 FAD/protein). Following reconstitution with FAD, however, the maxima at 375 and 450 nm became much more pronounced (data not shown), and it contained 1.0± 0.1 FAD molecule/mole of protein. Reconstituted rNROR was thermostable, with times required for a 50% loss in catalytic activity at 80 and 95 ^oC of about 24 and 1 h, respectively. This compares favorably to the half life of the native protein at the same temperatures (12 and 2 h, respectively) and similar protein concentrations (~ 0.5 mg/ml).

Table 2.2. Reconstitution of recombinant NROR

Sample	Specific Activity (U/mg)
No Heat Treatment[a]	11.8
Heat Treatment – Cofactor	17.5
Heat Treatment + FMN	16.3
Heat Treatment + FAD	475.5

[a]Heat treatment was performed anaerobically in 50 mM CAPS buffer (pH 10.2) at 85 ^{o}C for 15 minutes.

Catalytic properties of reconstituted NROR. Kinetic parameters for the native form of NROR have been reported (12). Apparent K_m and V_{max} for a number of these substrates were determined over the same concentration ranges for reconstituted rNROR. Unless otherwise indicated, the assay temperature was 80 ^oC. In addition to the NADH:BV oxidoreductase assay, NADPH:Rd oxidoreductase activity was also measured (12). Briefly, activity was determined anaerobically by following Rd reduction at 494 nm [molar absorptivity 9.22 $mM^{-1}cm^{-1}$ (2)]. The reaction mixture (2.0 ml) contained 100 mM EPPS [*N*-(2-hydroxyethyl)-piperazine-*N'*-(S-propanesulfonic acid)] buffer (pH 8.0), NADPH (0.3 mM) and Rd (0.0013-0.0075 mM). Rd was obtained as described previously (8).

The kinetic parameters for nNROR and reconstituted rNROR were strikingly similar (table 2.3). These data further establish Rd as the physiological electron acceptor and NADPH, as opposed to NADH, as the electron donor. Using the Rd:NADPH assay, native NROR had an apparent V_{max} at 80 ^oC of approximately 20,000 U/mg, which compares very favorably to the 21,000 U/mg for the reconstituted rNROR. In addition, the K_m of 0.1 mM for reconstituted rNROR was close to the native K_m of 0.05 mM over the same concentration range for Rd. The K_m of the native compared to reconstituted NROR for NADPH (5 vs.7 μM) and NADH (34 vs. 45 μM) shows NADPH as the preferred electron donor in each case (Table 2.3). An interesting and unique characteristic of nNROR was its high catalytic activity at low temperatures, exhibiting a V_{max} value at 25 ^oC of ~ 300 umol/min/mg. Reconstituted rNROR showed the same ability, with a V_{max} at the same temperature of 310 μmol/min/mg. Both forms of the protein also showed an increase in the apparent K_m value for Rd upon an increase in assay temperature from 25 to 80 ^oC. For undetermined reasons, the increase was much more significant for the native protein.

Figure 2.1.

SDS-PAGE (12.5%) of recombinant NROR. Lane 1: standard molecular weight markers; Lane 2: recombinant NROR purified from *E. coli* cells (4 μg of protein loaded)

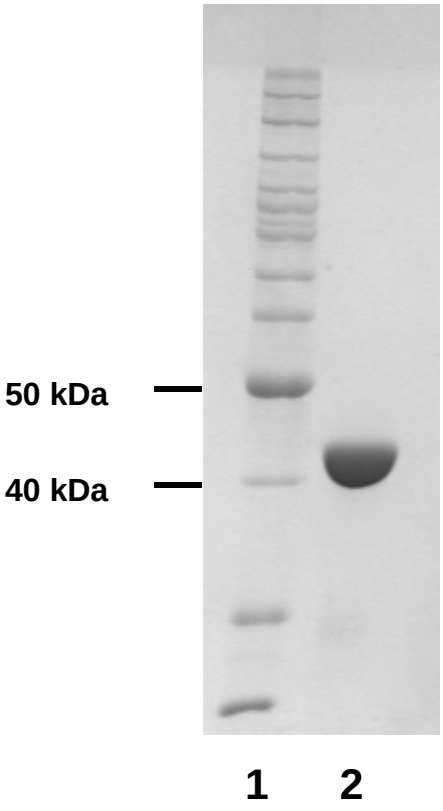
50 kDa
40 kDa
1
2

Implications for the physiological role of NROR. NROR is proposed to function in the oxidative stress response of *Pyrococcus furiosus*, providing reduced Rd as an electron donor for SOR to reduce superoxide in times of oxidative stress (9). Recent studies have brought to light Rd's ability to serve as an electron donor for rubrerythrin (Rr), a peroxidase enzyme thought to be involved in the oxidative stress response of *P. furiosus* (17) as well as in anaerobic bacteria (4). Consistent with a physiological relationship between SOR, Rd and Rr is the fact that the genes encoding these three proteins are clustered together in the *P. furiosus* genome (7). Since both NROR and SOR have been shown to be catalytically-active at temperatures where the vast majority of hyperthermophilic enzymes are not is also consistent with their role in oxidative stress at sub- optimal growth temperatures. The only proposed time *P. furiosus* and other hyperthermophilic microbes will encounter oxidative stress is when they are expelled from the hot smokers on the sea floor where they thrive in into the very cold (4 ^{o}C), oxygenated surrounding water (15).

Current studies are under way to determine the nature of how NROR, SOR, Rd and Rr interact with one another to serve in concert for oxygen detoxification when *P. furiosus* is under oxidative stress. The native and recombinant (reconstituted) forms of NROR appear to be essentially identical with respect to catalytic activity, kinetic parameters, size and cofactor composition, meaning the reconstituted form can substitute for the previously necessary (not to mention time consuming to purify) native form in this study. A typical yield of native protein is ~ 0.03 mg per gram of wet cell weight (12), as opposed to a typical yield of ~ 11 mg per gram of wet cell weight purified recombinantly from *E. coli*. An active recombinant form of NROR eases the strain on those experiments requiring large quantities of the protein.

Table 2.3. Kinetic parameters of recombinant NROR after reconstitution in comparison to native NROR

		nNROR[a]		rNROR	
Substrate (mM)[b]	**Cosubstrate (mM)**	**Apparent K_m (mM)**	**Apparent V_{max} (U/mg)**	**Apparent K_m (mM)**	**Apparent V_{max} (U/mg)**
NADH (0.03-0.2)	BV (1.0)	0.034	472	0.045	527
NADPH (0.01-0.2)	BV (1.0)	0.005	455	0.007	539
BV (0.4-2.0)	NADH (0.3)	1.25	1,000	2.52	715
Rd (0.0013-0.0075)	NADPH (0.3)	0.05	20,000	0.10	20990
Rd[c] (0.0013-0.0075)	NADPH (0.3)	0.01	294	0.004	310

[a] As reported previously (12).
[b] Concentration range used to determine the kinetic values.
[c] The activity was determined at 25 ^{o}C. All other assays were performed at 80 ^{o}C.

REFERENCES

1. **Beaucamp, K., H. U. Bergmeyer, and H.-O. Beutler.** 1974. Coenzymes, metabolites, and other biochemical reagents, p. 532. *In* H.U. Bergmeyer (ed.), Methods of enzymatic analysis, vol. I. Verlag Chemie, Academic Press, Inc., New York, N.Y.

2. **Blake, P., J.-B. Park, F. Bryant, S. Aono, J. Magnuson, E. Eccleston, J. Howard, M. Summers, and M. Adams.** 1991. Determinants of protein hyperthermostability: Purification and amino acid sequence of rubredoxin from the hyperthermophilic archaebacterium *Pyrococcus furiosus* and secondary structure of the zinc adduct by NMR. Biochemistry **30**:10885-10895.

3. **Bryant, F. O., and M. W. W. Adams.** 1989. Characterization of hydrogenase from the hyperthermophilic archaebacterium, *Pyrococcus furiosus*. J. Biol. Chem. **264**:5070-5079.

4. **Coulter, E. D., and D. M. Kurtz. 2001.** A role for rubredoxin in oxidative stress protection in *Desulfovibrio vulgaris*: Catalytic electron transfer to rubrerythrin and two-iron superoxide reductase. Arch. Biochem. Biophys. **394**:76-86.

5. **Fiala, G., and K. O. Stetter.** 1986. *Pyrococcus furiosus* sp-nov represents a novel genus of marine heterotrophic archaebacteria growing optimally at 100 ^{o}C. Arch. Microbiol. **145**:56-61.

6. http://www.secsg.org.

7. http://www.tigr.org.

8. **Jenney, F. E., and M. W. W. Adams.** 2001. Rubredoxin from *Pyrococcus furiosus*. Method Enzymol. **334**:45-55.

9. **Jenney, F. E., M. F. J. M. Verhagen, X. Y. Cui, and M. W. W. Adams.** 1999. Anaerobic microbes: Oxygen detoxification without superoxide dismutase. Science **286**:306-309.

10. **Laemmli, U. K.** 1970. Cleavage of structural proteins during assembly of head of bacteriophage-T4. Nature **227**:680-&.

11. **LeGall, J., J. Moura, H. J. Peck, and A. Xavier.** 1982. Hydrogenase and other iron-sulfur proteins from sulfate-reducing and methane-forming bacteria, p. 207-214. *In* T.G. Spiro (ed.), Iron-sulfur proteins. John Wiley & Sons, New York, NY.

12. **Ma, K., and M. W. W. Adams.** 1999. A hyperactive NAD(P)H : rubredoxin oxidoreductase from the hyperthermophilic archaeon *Pyrococcus furiosus*. J. Bacteriol. **181**:5530-5533.

13. **Niviere, V., and M. Fontecave.** 2004. Discovery of superoxide reductase: An historical perspective. J. Biol. Inorg. Chem. Epub.

14. **Sambrook, J., and D. Russell.** 2001. Molecular Cloning: A Laboratory Manual, 3rd ed. Cold Spring Harbor Laboratory Press, Cold Spring Harbor, NY.

15. **Stetter, K.** 1996. Hyperthermophilic prokaryotes. FEMS Microbiol. Rev. **18**:149-158.

16. **Storz, G., and J. A. Imlay.** 1999. Oxidative stress. Curr. Opin. Microbiol. **2**:188-194.

17. **Weinberg, M. V., F. E. Jenney, Jr., X. Y. Cui, and M. W. W. Adams.** 2004. Rubrerythrin from the hyperthermophilic archaeon *Pyrococcus furiosus* is a rubredoxin-dependent, iron-containing peroxidase. J. Bacteriol. **In Press.**

CHAPTER 3

RUBRERYTHRIN FROM THE HYPERTHERMOPHILIC ARCHAEON *PYROCOCCUS FURIOSUS* IS A RUBREDOXIN-DEPENDENT, IRON-CONTAINING PEROXIDASE[1]

[1] Weinberg, M.V., F.E. Jenney, Jr., X. Cui and M.W.W. Adams**.** Accepted by *Journal of Bacteriology*. Reprinted here with the permission from the publisher, 09/20/04.

ABSTRACT

Rubrerythrin was purified by multi-step chromatography under anaerobic, reducing conditions from the hyperthermophilic archaeon, *Pyrococcus furiosus*. It is a homodimer with a molecular mass of 39.2 kDa and contains 2.9 ± 0.2 iron atoms per subunit. The purified protein had peroxidase activity at 85 °C using hydrogen peroxide with reduced *P. furiosus* rubredoxin as the electron donor. The specific activity was 36 μmol rubredoxin oxidized/min/mg with apparent K_m values of 35 and 70 μM for hydrogen peroxide and rubredoxin, respectively. When rubrerythrin was combined with rubredoxin and *P. furiosus* NADH:rubredoxin oxidoreductase, the complete system used NADH as the electron donor to reduce hydrogen peroxide with a specific activity of 7.0 μmol H_2O_2 reduced/min/mg of rubrerythrin at 85°C. Strangely, as-purified (reduced) rubrerythrin precipitated when oxidized by either hydrogen peroxide, air or ferricyanide. The gene encoding rubrerythrin (PF1283) was expressed in *Escherichia coli* grown in media with various metal contents. The purified recombinant proteins each contained approximately three metal atoms/subunit ranging from 0.4 Fe plus 2.2 Zn to 1.9 Fe plus 1.2 Zn, where the metal content of the protein depended on metal content of the *E. coli* growth medium. The peroxidase activities of the recombinant forms were proportional to the iron content. *P. furiosus* rubrerythrin is the first to be characterized from a hyperthermophile or from an archaeon, and the results are the first demonstration that this protein functions in an NADH-dependent, hydrogen peroxide:rubredoxin oxidoreductase system. Rubrerythrin is proposed to play a role in the recently defined anaerobic detoxification pathway for reactive oxygen species.

INTRODUCTION

Rubrerythrin (Rr) is a non-heme iron protein that was originally isolated from the cytoplasm of the anaerobic bacterium *Desulfovibrio vulgaris* (26). The native protein is purified as a dimer with a subunit molecular weight of 21.9 kDa (40). Although *D. vulgaris* Rr (4, 7-9, 12, 26, 29, 34, 41) and the Rrs from a variety of other microorganisms (2, 3, 10, 15, 27, 46) have been extensively studied, its cellular function is still not understood. A number of enzyme activities have been reported for Rr, including pyrophosphatase (29), ferroxidase (4), and NADH peroxidase (7-9), but which are of physiological significance and the nature of its redox partner proteins have not been established. Even the true metal content of Rr is still a matter of controversy. The *D. vulgaris* protein was originally reported to contain two iron atoms per monomer. However, this was subsequently increased to three iron atoms per monomer (17, 33, 34) and more recently the protein was proposed to contain one zinc atom and two iron atoms per monomer (40).

What is not in doubt is that each monomer of Rr contains two separate structural domains. One is similar to the protein rubredoxin (Rd) and contains a single iron atom coordinated by four Cys residues (26). This domain appears to contain an iron atom even in the 1Zn/2Fe form of the protein (40). The other domain is comprised of four helices and contains a binuclear center that is coordinated by one His and five Glu residues, and one atom of molecular oxygen (34). In the 3Fe-form of the protein, the binuclear site in the four-helix domain has similar spectroscopic and magnetic properties to other di-iron containing proteins such as hemerythrin. In the 1Zn/2Fe form of the protein, this site is thought to contain one Zn and one Fe atom (40). Crystal structures are available for both the 3Fe- and the 1Zn/2Fe-forms (40), the overall structures of which are very similar.

The metal content and redox state of the purified forms of Rr from *D. vulgaris* affect its catalytic activity *in vitro*. The oxidized form of the 1Zn/2Fe-protein has inorganic pyrophosphatase activity (29) although the reduced protein is inactive (28). On the other hand, the oxidized form of 3Fe-Rr exhibits ferroxidase activity, the O_2-dependent oxidation of Fe^{2+} to Fe^{3+} (4). A recombinant form of Rr containing the diiron, but not the Rd-like domain, did not have ferroxidase activity (4, 17), indicating both metal sites are required for activity. That Rr may have a peroxidase-type activity was first demonstrated using the *D. vulgaris* protein with an artificial electron donor but this had relatively low activity (9). Subsequently, the peroxidase activity of reduced Rr was demonstrated utilizing reduced Rd as the electron donor. Rd was reduced either chemically with stoichiometric amounts of dithionite or enzymatically via spinach ferredoxin-$NADP^+$ oxidoreductase (FNR) using NADH as the electron donor (7), so a physiologically relevant electron donor was not established.

In contrast to the results with the *D. vulgaris* proteins, Rr was purified from the cell-free extract of the obligate anaerobe, *Clostridium perfringens*, by measuring its superoxide dismutase (SOD) activity (27). Although the metal content of the purified protein was not reported, the amino acid sequence (deduced from the cloned gene) was 52% identical to that of *D. vulgaris* Rr and it contained the putative metal-binding sites for both the Rd-like and di-iron sites. Furthermore, the *sod*$^-$ mutant of *Escherichia coli* expressing the gene encoding Rr (*rbr)* from *C. perfringens* exhibited SOD activity. This mutant also had a higher resistance to oxidative stress than a mutant lacking *rbr*, implying a role for Rr in scavenging reactive oxygen species (ROS) (27). Rr appears to be unregulated by ROS in *C. perfringens*, however, as the transcription levels of the genes encoding Rr and SOD were unaffected by oxidative stress (15). Despite all of

this evidence for the *C. perfringens* Rr, the *D. vulgaris* protein did not show detectable SOD activity (33).

Evidence for a relationship between Rr and ROS also comes from studies of other microorganisms. For example, a peroxide-resistant mutant of *Spirillium volutans* contained a high level of Rr but no expression could be detected in the wild type strain, even in the presence of peroxide (3). Cell-free extracts of the mutant strain also had measurable NADH peroxidase activity (0.07 U/mg) but this was not detected in extracts of the wild type (2). Unfortunately, the protein(s) responsible for the activity was not purified. Similarly, an *rbr*$^-$ mutant of the anaerobic pathogen *Porphyromonas gingivalis* was more sensitive than the wild type strain to oxygen and peroxide (42). In this case, the transcription of *rbr* was up-regulated in response to exposure of cells to either oxygen or hydrogen peroxide. It therefore appears that Rr does play some role in the response of anaerobes to ROS exposure. In fact, with few exceptions, a gene encoding a homolog of the protein is found in all complete genome sequences currently available for anaerobic and microaerophilic prokaryotes (20). It is therefore essential that the precise function and metal content of Rr be defined.

Herein we focus on the anaerobic archaeon *Pyrococcus furiosus* (14). This organism grows optimally near 100°C utilizing either carbohydrates or peptides as a carbon source. Interestingly, in its genome sequence (35), the gene (PF1283) encoding the homolog of *D. vulgaris* Rr is adjacent to those encoding Rd and the enzyme superoxide reductase (SOR). SOR was recently postulated to be a key enzyme in a novel detoxification pathway in anaerobes wherein it reduces superoxide to peroxide using Rd as the electron donor (23). An intriguing possibility was that in *P. furiosus,* Rd also supplied reductant to Rr, as proposed in *D. vulgaris* (7), so that it could reduce the peroxide generated by SOR to water. The goal of this study was

therefore to purify Rr from *P. furiosus*, to determine its metal content and its catalytic activity, and to examine these and other properties of the recombinant protein. The results show that native Rr is an iron-dependent peroxidase that does not contain zinc and probably functions to remove the peroxide produced by SOR using Rd, ultimately reduced by NADH, as the electron donor.

MATERIAL AND METHODS

Growth of Microorganisms. *Pyrococcus furiosus* (DSM 3638) was routinely grown at 95 °C in a 600-L fermentor with maltose as the carbon source as described previously (6). The cells were harvested by centrifugation and stored at –80 °C until needed.

Purification of Rr from *P. furiosus*. All procedures were carried out under anaerobic conditions at 23 ^{o}C. All buffers were degassed and flushed with Ar and contained 2 mM sodium dithionite (DT) unless otherwise stated. Rr was identified throughout the purification procedure by its migration after SDS-PAGE analysis to a position corresponding to a molecular weight of 19 kDa. Frozen cells (250 g, wet weight) were thawed in 750 ml of 50 mM Tris-HCl, pH 8.0 (buffer A) containing 2 µg/ml DNAse I. Cells were lysed by incubation at 37 °C for 2 h. A cell-free extract was obtained by ultracentrifugation at 100,000 x *g* for 1.5 h at 4 °C. The resulting supernatant (12,045 mg of protein) was applied onto a DEAE Fast Flow column (5 x 30 cm) (Pharmacia, Piscataway, NJ) equilibrated with buffer A. The solution was diluted 50% with buffer A during loading. Protein was eluted at a flow rate of 12 ml/min with a 10 column volume (5 L) linear gradient of 0 to 1 M NaCl in buffer A. Fractions of 100 ml were collected. Rr eluted as 100 to 175 mM NaCl was applied. These fractions were combined (2,510 mg),

concentrated to 200 ml using a PM-10 Amicon membrane, and loaded onto a hydroxyapatite (HAP) (BioRad, Hercules, CA) column (2.6 x 20 cm) equilibrated with buffer A. The protein solution was diluted 50% with buffer A during loading. The adsorbed protein was eluted at 4 ml/min using a 1.2 liter linear gradient of 0 to 1 M potassium phosphate buffer and 50 ml fractions collected. Rr eluted from the column as 100 to 230 mM potassium phosphate was applied. These fractions containing Rr (1,906 mg) were combined, solid ammonium sulfate was added to a final concentration of 1.5 M, and the solution was loaded onto a column (2.6 x 11 cm) of Phenyl Sepharose (Pharmacia) equilibrated with buffer A containing 1.5 M ammonium sulfate. Protein was diluted 50% with the equilibration buffer during loading. The adsorbed protein was eluted using a linear gradient (720 ml) of 1.5 to 0 M ammonium sulfate in buffer A at 4 ml/min, and fractions of 25 ml were collected. Rr eluted as 560 to 300 mM ammonium sulfate was applied. Rr-containing fractions were combined (307 mg), concentrated through a PM-10 Amicon membrane to ~ 10 ml, diluted to ~ 100 ml with buffer A, and then concentrated to 6 ml. This was applied to a column (2.6 x 60 cm) of Superdex 75 equilibrated with buffer A containing 200 mM NaCl. The column was run at a flow rate of 0.5 ml/min and 10 ml fractions were collected. Rr eluted after 190 ml had been applied to the column. Rr-containing fractions (123 mg) were loaded onto a column (2.6 x 13 cm) of Q-Sepharose High Performance (Pharmacia) equilibrated with buffer A. The protein solution was diluted by 60% during loading with buffer A. The column was eluted with a 550 ml linear gradient from 0 to 1 M NaCl in buffer A and 25 ml fractions were collected. Rr eluted as 150 to 270 mM NaCl was being applied. Rr-containing fractions (65 mg) were combined and loaded onto an HAP column (2.6 x 1 cm) equilibrated with 50 mM BisTris pH 6.0. The protein solution was diluted 90% with equilibration buffer during loading. The column was run at a flow rate of 1 ml/min and a linear

gradient (40 ml) of 0 to 50% of 1 M potassium phosphate buffer, pH 6.0, was applied and 2 ml fractions were collected. Rr began to elute as 240 mM potassium phosphate buffer was being applied. Rr-containing fractions were combined (56 mg) and loaded onto a Q-Sepharose High Performance column (1.6 x 2.5 cm, Amersham Pharmacia, Uppsala, Sweden) equilibrated with 50 mM BisTris, pH 7.0 (buffer B). The protein solution was diluted 85% with buffer B during loading. Protein was eluted using a 75 ml linear gradient from 0 to 1 M NaCl in buffer B at a flow rate of 1 ml/min and 1.5 ml fractions were collected. Rr eluted as 210 to 270 mM NaCl was being applied to the column. Rr-containing fractions judged pure by SDS-PAGE analysis were combined (26 mg) and stored frozen as pellets in liquid nitrogen until needed.

Cloning and heterologous expression of the *P. furiosus* Rr gene. A pET 21 plasmid containing a modified Rr gene (PF1283) with a His-6 tag at the N terminus (MAHHHHHHGS-) was provided by the Southeastern Collaboratory for Structural Genomics at the University of Georgia (19). This was transformed into *E. coli* strain BL21(D23) Star/pRIL which was grown at 37 °C in three variations of M9 minimal media (38) containing 100 µg/ml ampicillin and 34 µg/ml chloramphenicol. Medium M-Zn was unmodified and contained Fe and Zn at concentrations of 10 and 20 µM, respectively. Medium M-Fe lacked added Zn but contained 10-times the normal Fe concentration (100 µM $FeSO_4$), while medium M-FeZn contained Zn (20 µM) and additional Fe (110 µM in total). The recombinant cells were grown in 1 liter cultures until an OD_{600} of 0.6, isopropyl-β-D-thiogalactopyranoside (IPTG, 0.4 mM) was added and the temperature was reduced to 25 °C. After 3.5 hr, cells were harvested by centrifugation at 10,000 x *g* for 15 min at 4 °C, transferred to an anaerobic chamber containing Ar and resuspended in

anaerobic lysis buffer (10 mM imidazole, 20 mM sodium phosphate and 0.5 M NaCl, pH 7.4). They were stored in sealed serum bottles under Ar at –80 °C until required.

Purification of recombinant Rr from *E. coli*. All steps were carried out under anaerobic conditions at 23 °C. *E. coli* cells (3-4 g, wet weight, from 1 L growth) were thawed at room temperature under a constant flow of Ar in lysis buffer. Phenylmethylsulfonylfluoride (PMSF) was added to a final concentration of 100 µM and cells were lysed by sonication under flow of Ar. Cell-free extracts were centrifuged at 10,000 x *g* for 20 min at 4 °C and the supernatants were applied to 4 ml Ni-NTA His-bind affinity columns (Novagen, Madison, WI) equilibrated with lysis buffer. Recombinant Rr (rRr) was eluted with 20 mM sodium phosphate, 0.5 M NaCl and 300 mM imidazole, pH 7.0. Those fractions containing rRr as determined by SDS-gel electrophoresis were then loaded on to a column (1.6 x 2.5 cm) of Q-Sepharose High Performance (Amersham Pharmacia) equilibrated with 50 mM Tris-HCl, pH 8.0 containing 2 mM DT. Protein was diluted 80% with equilibration buffer during loading and was eluted in 2 ml fractions at a flow rate of 1 ml/min using a linear gradient (100 ml) from 0 to 1.0 M NaCl in the equilibration buffer. rRr eluted as 0.3 to 0.4 M NaCl was applied. Fractions containing pure rRr as judged by electrophoresis were combined, concentrated through a PM-10 Amicon membrane and stored frozen as pellets on liquid nitrogen until needed.

Enzyme assays. Peroxidase assays were routinely carried out anaerobically at 85 °C in 3 ml glass cuvettes containing 2 ml of 50 mM MOPS, pH 7.5. Rd (21) and NADH:Rd oxidoreductase (NROR) (31) were purified as previously described. Rd (150 µM) reduced by sodium dithionite (200 µM) was used as an electron donor and hydrogen peroxide (250 µM) was the electron

acceptor. The reaction was initiated by the addition of between 2 and 5 µM Rr or rRr. Activity was measured by the rate of Rd oxidation at 490 nm using an extinction coefficient of 9.2 $cm^{-1}mM^{-1}$ (21) . One unit of peroxidase activity is defined as the amount of enzyme that oxidizes 1 µmol Rd/min. The same assay conditions were used when NADH was the electron donor except that NROR, Rd and Rr were added in catalytic amounts (~ 0.5 µM) and NADH was used at a final concentration of 150 µM. Its oxidation was measured at 340 nm using an extinction coefficient for NADH of 6.2 $cm^{-1}mM^{-1}$ (11). SOD activity was measure at 50 °C by cytochrome c reduction (32) and pyrophosphatase activity was determined at 80 °C by the release of inorganic phosphate from sodium pyrophosphate (29). Inorganic phosphate was estimated as described previously (18). Alkaline phosphatase and bovine SOD (Sigma Chemical Co.) were used as the positive controls for both assay systems. NADH peroxidase activity was measured anaerobically at 85 °C following the oxidation of NADH at 340 nm. The reaction mixture (2.0 ml) included 50 mM EPPS buffer (pH 8.0) with 1 mM DTPA using NADH (0.3 mM) as the electron donor and hydrogen peroxide (0.25 mM) as the electron acceptor. Ferroxidase activity was measured at 25, 50 and 80 °C at 315 nm following the conversion of $[Fe^{2+}]$ to $[Fe^{3+}]$ by the addition of Rr (0.45 - 3.6 µmol/ml) to air-saturated buffer containing 0.12 mM ferrous ammonium sulfate added from a freshly-prepared anaerobic solution (4).

Other methods. Iron and zinc were determined by inductively coupled plasma emission spectroscopy at the Chemical Analysis Laboratory of the University of Georgia. The iron content was also determined using a colorimetric iron assay (30). UV-visible spectra were recorded on a Shimadzu UV-2501PC spectrophotometer and all samples were in 50 mM Tris-HCl, pH 8.0. Liquid Chromatography-Mass Spectroscopy (LC-MS) analysis was performed at

the Mass Spectrometry Laboratory at the University of Georgia. Protein was measured using the Bradford protein assay kit (BioRad, Hercules, CA). Amino acid sequences were aligned using Vector NTI AlignX software (Suite 9.0.0, Invitrogen, Carlsbad, CA). Phylogenetic trees were constructed using the Neighbor Joining (NJ) method (37) and the Minimum Evolution (ME) method (36), both from MEGA software version 3.0 (25). The p-distance and poisson-correction substitution models were used in both tree building methods. Bootstrap values were calculated based on 1000 replicates of the data (14).

RESULTS

Purification of rubrerythrin from *P. furiosus*. Rubrerythrin was purified to homogeneity from cell-free extracts of maltose-grown *P. furiosus* by multistep chromatography. The protein is present in cells in sufficiently high amounts such that it can be identified on a 1D SDS-PAGE gel after just one column chromatography step. Rr is the only major protein band near 19 kDa in fractions eluting near 150 mM NaCl from the first ion-exchange column (data not shown). The purification procedure was carried out using buffers containing sodium dithionite under anaerobic conditions because, as described below, Rr was found to be soluble only in its reduced state. The procedure yielded approximately 25 mg of Rr from 250 g of *P. furiosus* cells (wet weight). This migrated as a single band on a denaturing electrophoresis gel corresponding to a molecular mass of approximately 19 kDa (Figure 3.1). Its N-terminal amino acid sequence (VVKRTMT-) indicated that the N-terminal methionine residue is cleaved *in vivo*. According to the gene sequence (PF1283), this should result in a protein of 170 amino acids with a predicted mass of 19,349 Da. This is consistent with the analysis of the purified protein by mass spectrometry, which indicated a mass of 19,377 Da. Analytical gel filtration data showed that

Fig. 3.1.

SDS-PAGE (12.5%) of native and recombinant rubrerythrin. Lane 1: standard molecular weight markers; Lane 2: native rubrerythrin purified from *P. furiosus*; Lanes 3-5: recombinant rubrerythrin purified from *E. coli* cells grown on M9-Zn, M9-Fe and M9-FeZn, respectively. Each lane contained 2 μg of protein.

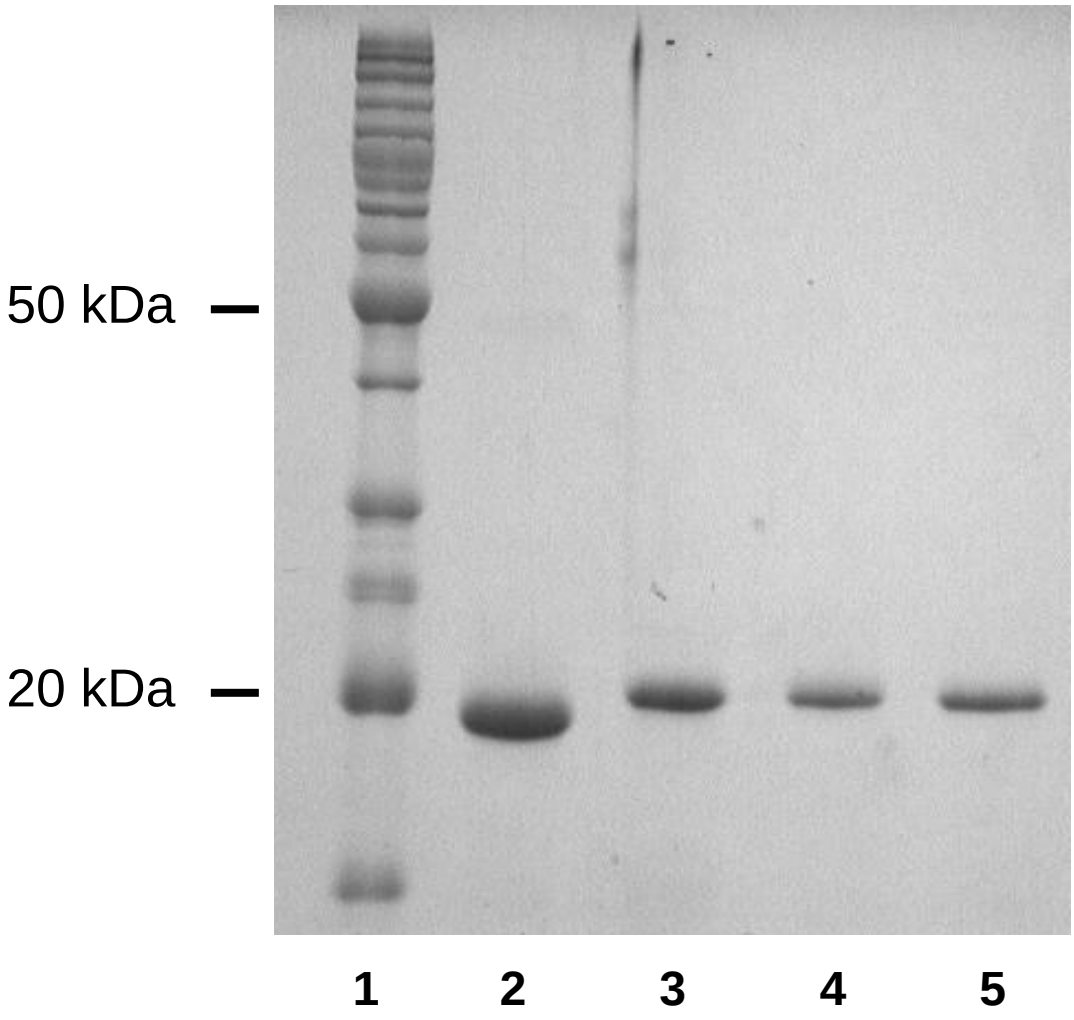
50 kDa
20 kDa
1
2
3
4
5

native Rr has a molecular weight of 36 ± 0.3 kDa and therefore appears to be a homodimeric protein. The amino acid sequence of *P. furiosus* Rr was 29 and 27% identical to those of the Rrs of *D. vulgaris* and *C. perfringens*, respectively.

Purification of recombinant *P. furiosus* rubrerythrin. The gene encoding Rr was successfully expressed in *E. coli* grown on a minimal medium after induction with IPTG for 3.5 h at 25 °C. The presence of recombinant Rr (rRr) in cell-free extracts of *E. coli* was evident by a protein band corresponding to a molecular mass of 19 kDa after SDS-PAGE analysis. rRr was purified in two steps by affinity and ion exchange chromatography with yields of 42, 32 and 13 mgs using cells (4 g, wet weight) grown on the M-Zn, MFe and M-FeZn media, respectively. The three preparations of rRr were indistinguishable from each other by SDS-gel electrophoresis although they migrated more slowly than the native protein presumably because of the additional N-terminal residues that incorporate the His-tag (Figure 3.1). LC-MS analyses gave respective subunit molecular weights of 20,615, 20,530 and 20,640 Da for the three types of rRr, compared with a calculated value of 20407 Da**.** Analytical gel filtration data were consistent with a molecular mass of ~ 37 kDa for all three forms, indicating that all three are homodimers, like the native protein.

Physical properties of the native and recombinant forms of rubrerythrin. The metal contents of native Rr and the three forms of rRr are summarized in Table 3.1. While the native protein contained three Fe atoms/subunit, the values for the rRrs were much lower, with zinc apparently replacing the iron. Thus, rRr purified from *E. coli* grown on the M-Zn medium contained approximately 1 Fe and 2 Zn atoms/subunit, but cells grown in the same medium

Table 3.1. Metal contents and peroxidase activities of the native and recombinant forms of rubrerythrin.

Rubrerythrin[a]	ICP-MS [Fe]	ICP-MS [Zn]	Colorimetric [Fe]	Spec. Act.[b] (U/mg)
P. furiosus	2.8±0.2	0.3± 0.1	2.9± 0.2	36.1
M-Fe	1.9± 0.2	1.2± 0.1	1.8± 0.1	3.1
M-FeZn	1.0± 0.2	1.7± 0.2	0.8± 0.1	0.7
M-Zn	0.4± 0.1	2.2± 0.2	0.9± 0.2	0.3

[a]This refers to either the native form purified from *P. furiosus* or the recombinant form purified from *E. coli* cells grown on the indicated medium (see Methods for details of the media).

[b]Specific activity refers to peroxidase activity using dithionite-reduced rubredoxin as the electron donor and hydrogen peroxide as the electron acceptor.

lacking added zinc and supplemented with iron (M-Fe) yielded rRr containing approximately 2 Fe and 1 Zn per subunit. In spite of no added zinc, the M-Fe medium was found to contain 2.0 μM Zn as determined by ICP-MS, presumably due to the contamination by zinc in other mediumcomponents. Accordingly, rRr obtained from cells grown on the M-Zn medium contained approximately 0.5 Fe and 2.5 Zn/subunit (Table 3.1).

A characteristic of *D. vulgaris* Rr is that it is colorless in its reduced state and becomes red upon oxidation due to the redox properties of the Rd-like, monomeric Fe site (26). Similarly, native *P. furiosus* Rr in its dithionite-reduced form was colorless as purified but, strangely, the protein precipitated when exposed to either oxygen (air) or by the addition of 10 molar equivalents of either potassium ferricyanide or hydrogen peroxide, e.g., when hydrogen peroxide was added to a 0.1 mM Rr solution at a final concentration of 1.0 mM**.** The precipitated protein was red in color, indicating that the monomeric Fe site was oxidized. This was also evident by an absorbance peak at 490 nm that appeared as the protein changed from colorless to red immediately prior to precipitation (see Figure 3.2). In contrast, the rRr proteins containing one or less iron atom per subunit (from cells grown in the M-Zn or M-FeZn media) did not show any features in the visible region upon oxidation (data not shown) and did not precipitate**.** Thus, the monomeric site in these proteins should contain predominantly zinc. On the other hand, the rRr that contained two Fe atoms/subunit, obtained from cells grown in the M-Fe medium, did change from colorless to red upon oxidation (see Figure 3.2). The extinction coefficient at 490 nm was 1.6 $mM^{-1}cm^{-1}$. This compares with the value 10.6 $mM^{-1}cm^{-1}$reported for *D. vulgaris* Rr (34). This suggests that the monomeric Fe site in the *P. furiosus* recombinant protein is approximately 15% occupied, while the binuclear site should be almost fully occupied (for an aggregate of two Fe atoms/subunit), but this state did not precipitate. Thus, it appears that

Figure 3.2.

UV-visible absorption spectra for A) native Rr and B) rRr from *E. coli* cells grown on medium M-Fe. The reduced samples contained a 3-fold molar excess of sodium dithionite and were oxidized with a 5-fold molar excess of hydrogen peroxide. The final protein concentration in each case was approximately 1 mg/ml (the higher absorbance of the native protein is due to protein precipitation).

A.

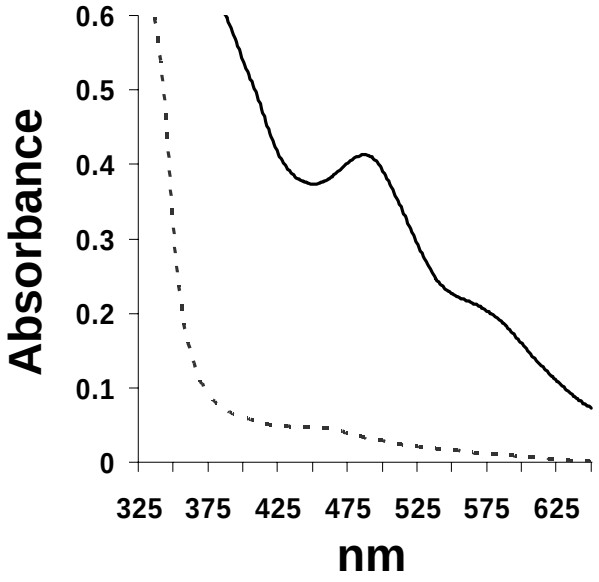
Absorbance
0.6
0.5
0.4
0.3
0.2
0.1
0
325 375 425 475 525 575 625
nm

B.

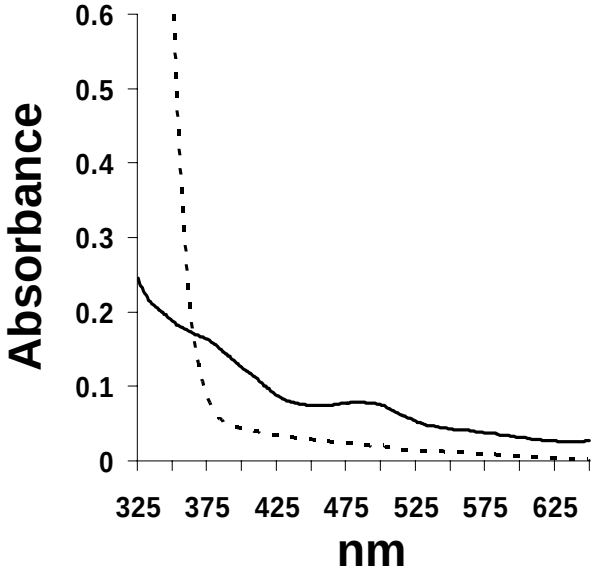
Absorbance
0.6
0.5
0.4
0.3
0.2
0.1
0
325 375 425 475 525 575 625
nm

the binuclear site is more readily occupied by iron and that the protein precipitates only as the 3Fe-form.

Catalytic properties of native and recombinant forms of rubrerythrin. *P. furiosus* Rr was assayed for pyrophosphatase, SOD, ferroxidase and NADH peroxidase activities, all of which have been previously attributed to the Rrs of *D. vulgaris* and/or *C. perfringens* (4, 7, 9, 27-29). However, there was no detectable activity using any of the assays for the *P. furiosus* protein. On the other hand, it did exhibit Rd-dependent peroxidase activity using hydrogen peroxide (250 μM) as the electron acceptor and *P. furiosus* Rd (150 μM, chemically-reduced with sodium dithionite) as the electron donor. The specific activity was 36 U/mg of Rr at 85 °C and pH 7.5, which is comparable to that previously reported with the *D. vulgaris* protein (measured at 22 ^{o}C) (7). As shown in Fig. 3.3, the activity showed a bimodal response to pH with an optimum near 7.8 (at 85 °C) and a temperature optimum of $\geq$ 90 ^{o}C (at pH 7.5). Using standard assay conditions, the apparent K_m values, calculated from linear reciprocal plots, were 35 μM for hydrogen peroxide (using a concentration range of 15-300 μM with 150 μM Rd), and 70 μM for Rd (over a concentration range of 15-270 μM, using 250 μM hydrogen peroxide).

When the recombinant forms of Rr were assayed under the same conditions, the specific activities were significantly lower, by at least an order of magnitude (Table 3.1). The 2Fe/1Zn-form obtained from cells grown in the M-Fe medium was the most active with approximately 10% of the activity of the native protein. This roughly corresponds to the amount of iron in the mononuclear site (15% occupancy), rather than the binuclear site (approximately 60% occupancy). One would therefore expect the 1Fe/2Zn-form (obtained from M-FeZn-grown cells, Table 3.1) to be virtually inactive, and this form of the protein exhibited only 2% of the activity

Figure 3.3.

Effect of A) temperature and B) pH on the peroxidase activity of native rubrerythrin. For the temperature measurements, all assays were carried out in 50 mM MOPS (pH 7.5), 0.1 mM EDTA buffer, while the pH-dependent assays were performed at 85 ^{o}C using the following buffers (each 50 mM): Bis-Tris, pH 5.8, 6.4, 6.8, 7.2; MOPS, pH 7.4, 7.8; HEPES, pH 8.0, 8.2; EPPS, pH 8.4, 8.7; CHES, pH 9.4, 10.0; CAPS, pH 10.2, 10.4, 11.

A.

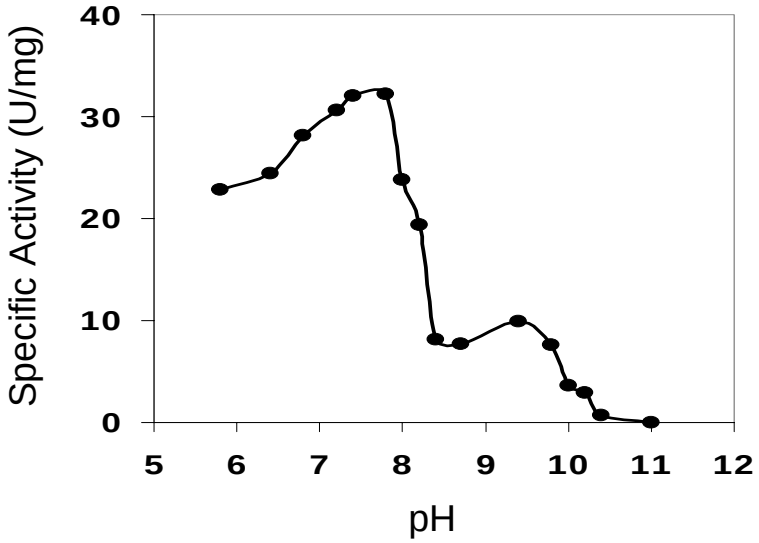
Specific Activity (U/mg)
40
30
20
10
0
5
6
7
8
9
10
11
12
pH

B.

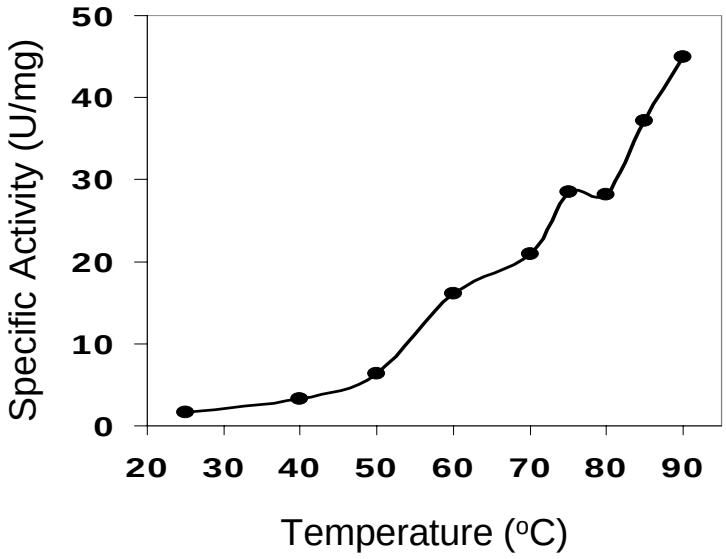
Specific Activity (U/mg)
50
40
30
20
10
0
20
30
40
50
60
70
80
90
Temperature (°C)

of the native protein. This is about twice that of the rRr form obtained from M-Zn-grown cells, which has an even lower iron content (Table 3.1).

In the proposed SOR-dependent pathway of ROS detoxification of *P. furiosus* (23), the ultimate source of reductant for superoxide reduction is NADH, wherein NROR reduces Rd, and this in turn supplies reductant to SOR. To investigate whether NADH via NROR and Rd could also supply reductant to Rr, a system was reconstituted containing all three purified proteins. At 85 °C the reconstituted pathway containing NADH (150 μM), Rd (0.5 μM), NROR (0.5 μM), Rr (0.5 μM) and hydrogen peroxide (250 μM) had a specific activity of 7.0 U/mg of Rr. However, little or no NADH oxidation activity (< 0.5 U/mg) could be measured if any of the components (NADPH, NROR, Rd, Rr or H_2O_2) were omitted from the reaction mixture.

DISCUSSION

Representatives of Rr are present in the majority (23 of 29) of anaerobic and microaerophilic microorganisms for which genome sequences are available. These include organisms from both the bacterial and archaeal domains. There are also three aerobic organisms that contain homologs of Rr, and these include both bacteria (*Magnetococcus*, *Nostoc*) and archaea (*Sulfolobus*). The crystal structure of *D. vulgaris* Rr (12, 28, 40) shows that there are five glutamyl and one histidinyl residues that bind the binuclear metal site, as well as two CXXC motifs that coordinate the Rd-like mononuclear Fe center. However, of the 42 Rr-like sequences currently available, several of them (7/42) do not contain the two Cys motifs and most of these (5/7) also lack one or more of the Glu residues that bind the binuclear site, leaving only 35 that appear to be homologs of the *D.vulgaris* protein in that they contain all of the predicted metal-binding sites. A phylogenetic tree was constructed using all 42 Rr-like sequences by the

Figure 3.4.

Rooted phylogenetic tree of Rr homologs. Archaeal genes are indicated in bold. Bootstrap values are indicated at the branch points. The bar indicates a branch length equivalent of 0.1 changes per amino acid. The *Wolinella* (WS1374) and *Campylobacter* (Cj0112c) cluster was used as the outgroup. (C) indicates those sequences that do not contain Cys motifs that coordinate the rubredoxin-like mononuclear site. (CG) indicates those sequences that do not contain Cys motifs as well as the fourth Glu residue conserved in all Rr homologs. All sequences were obtained from the TIGR website (20) except for the *D. vulgaris* sequence (45). The position of *P. furiosus* Rr (PF1283) is underlined. The abbreviations are as follows: AF, *Archaeoglobus fulgidus*, BT is *Bacteroides thetaiotaomicron*, Cj is *Campylobacter jejuni*, CT, *Chlorobium tepidum*; CAC, *Clostridium acetobutylicum*; CPE, *Clostridium perfringens*; CTC, *Clostridium tetani*; DV, *Desulfovibrio vulgaris*; FN, *Fusobacterium nucleatum*; GSU, *Geobacter sulfurreducens*; NT01MC, *Magnetococcus sp.*; MTH, *Methanobacterium thermoautotrophicum*; MJ, *Methanococcus jannaschii*; MA, *Methanosarcina acetivorans*; MM, *Methanosarcina mazei*; Nostoc, *Nostoc sp.*; PG, *Porphyromonas gingivalis*; PIN, *Prevatella intermedia*; PAB, *Pyrococcus abyssi*; PF, *Pyrococcus furiosus*; SSO, *Sulfolobus solfataricus*; ST, *Sulfolobus tokadaii*; TTE, *Thermoanaerobacter tengcongensis*; TM, *Thermotoga maritima;* TDE, *Treponema denticola*; WS, *Wolinella succinogenes*.

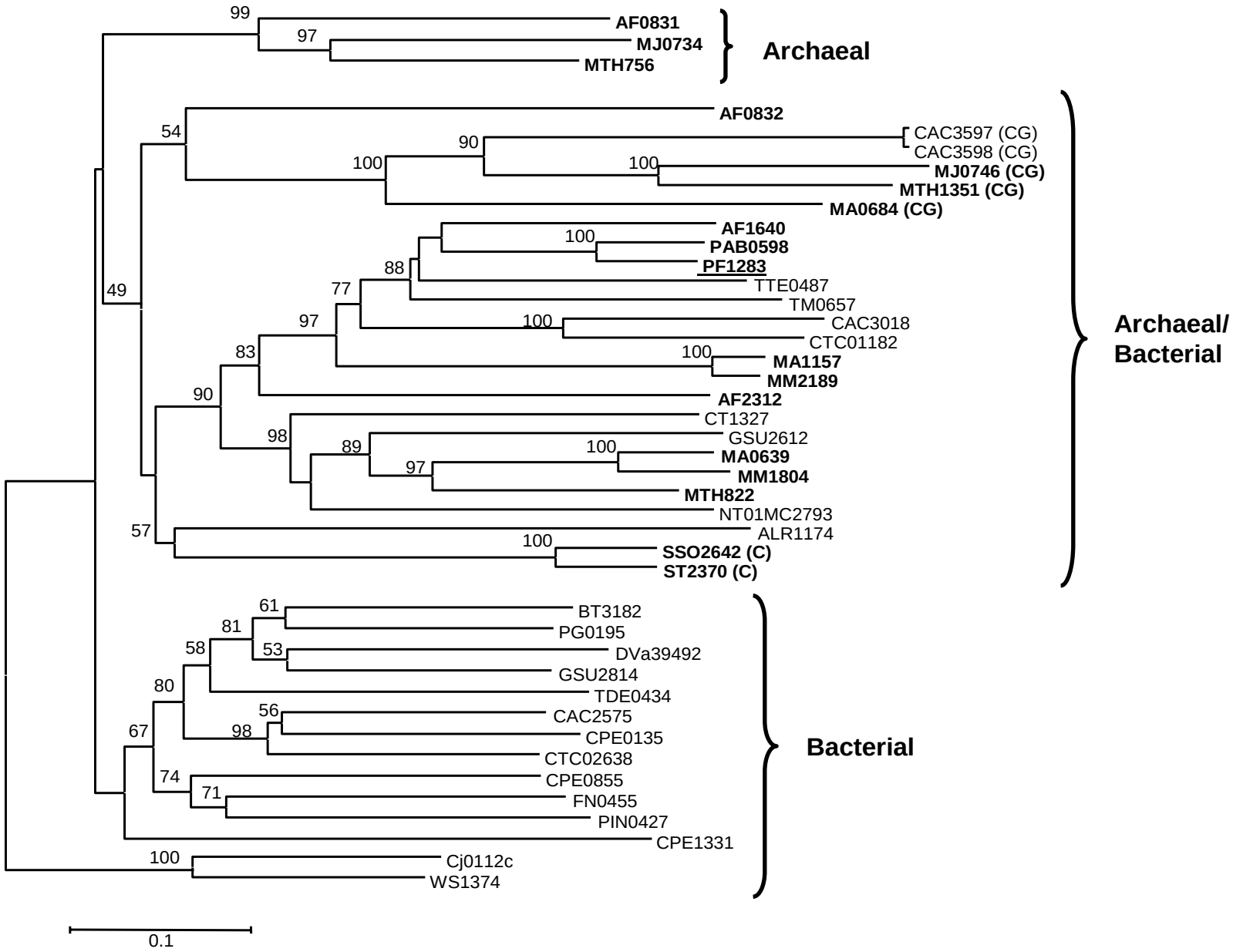
99
97
AF0831
MJ0734
MTH756
Archaeal
AF0832
54
90
CAC3597 (CG)
CAC3598 (CG)
100
100
MJ0746 (CG)
MTH1351 (CG)
MA0684 (CG)
AF1640
100
PAB0598
88
PF1283
49
77
TTE0487
TM0657
97
100
CAC3018
CTC01182
83
100
MA1157
MM2189
90
AF2312
CT1327
98
GSU2612
89
100
MA0639
97
MM1804
MTH822
NT01MC2793
57
ALR1174
100
SSO2642 (C)
ST2370 (C)
Archaeal/
Bacterial
61
BT3182
81
PG0195
58
53
DVa39492
GSU2814
80
TDE0434
56
CAC2575
67
98
CPE0135
CTC02638
74
CPE0855
71
FN0455
PIN0427
CPE1331
100
Cj0112c
WS1374
Bacterial
0.1

Neighbor-Joining method using the p-distance method (Fig. 3.4). Similar topologies resulted from different tree building methods (Neighbor-Joining vs. Minimum Evolution) and distance estimations (p-distance vs. poisson-correction), showing the tree's robustness. It contains two major branches, one with both archaeal and bacterial representatives (which includes the *P. furiosus* protein) and one with only bacterial proteins (including that from *D. vulgaris*). There is also a third smaller branch containing only archaeal proteins. Bootstrap values indicate that the archaeal branch is very well conserved (99%), although both the bacterial and mixed (archaeal/bacterial) branches have much lower bootstrap values (47% and 49%, respectively).

As shown in Fig. 3.4, the five Rr homologs that lack both the Cys motifs (which coordinate the Rd-site) and one or more of the Glu residues that typically coordinate the binuclear site (from *M. acetivorans* [MA0684], *M. thermoautotrophicum* [MTH1351], *M. jannaschii* [MJ0746], and *C. acetobutylicum* [CAC3597 and CAC3598]) cluster together in the major bacterial/archaeal branch. These are well separated from the two Rrs that lack just the Cys motifs (from *Sulfolobus tokodaii* and *S. sulfolobus*). Interestingly, the expression of CAC3597 and CAC3598 in *C. acetobutylicum* is induced by oxygen (25) although their functions are not known. Herein we demonstrate that both metal sites (containing only Fe) are needed for the peroxidase activity of *P. furiosus* Rr (see below) and so these seven Rr homologs (including CAC3597 and CAC3598) lacking at least one metal site are unlikely to possess this activity. One might predict that the other members of the archaeal/bacterial branch (Fig. 3.4) that contain the metal-binding motifs are peroxidases like that of *P. furiosus*, although additional biochemical analyses are required to define the physiological activities of the proteins in the bacterial-only branch.

P. furiosus Rr is a homodimeric protein, and this is also true for the only Rr homolog (containing both metal sites) for which a crystal structure is available, that of *D. vulgaris* (12, 28, 40). A structure was recently reported for the Rr sequence-homolog from the archaeon *Sulfolobus tokodaii*, which was given the name sulerythrin (this lacks the Rd-binding domain). Interestingly, a comparison of the two structures showed a rare case of domain swapping to constitute the binuclear site of the *S. tokodaii* protein. The crystal structure for the *P. furiosus* Rr has recently been determined (43) and there is also strong evidence for domain swapping in this metal-site homolog of the *D. vulgaris* protein. Thus, the two domain-swapped Rrs (relative to *D. vulgaris* Rr) include a sequence homolog (lacking one metal site/domain, in *S. tokodaii* Rr) and a metal-site homolog (with Fe in both metal sites, in *P. furiosus* Rr), and both are from archaea. Clearly, this domain-swapping phenomenon with Rr is independent of metal sites, but whether it is a property of archaeal Rrs remains to be seen. At present one cannot predict from an amino acid sequence just which domain structure ("bacterial" or "archaeal") a particular Rr adopts.

The true physiological function of Rr has been the subject of much debate, as a multitude of activities have been attributed to this protein. In this study we have shown that the *P. furiosus* protein has Rd-dependent peroxidase activity which is comparable to that reported for one bacterial Rr protein (7), and archaeal and bacterial (non-Rr) peroxidases, such as from *Archaeoglobus fulgidus* (24), *Thermus brockianus* (44), *Bacillus stearothermophilus* (16) and *Halobacterium halobium* (5). The gene encoding Rr is adjacent to those encoding Rd and SOR in the *P. furiosus* genome, consistent with a functional relationship between them (23). SOR reduces superoxide to hydrogen peroxide and thereby plays a major role in the detoxification of reactive oxygen species in anaerobes such as *P. furiosus* (23).

Figure 3.5.

Proposed role of rubrerythrin in the SOR-dependent pathway of ROS detoxification in anaerobic microorganisms. Modified from (23).

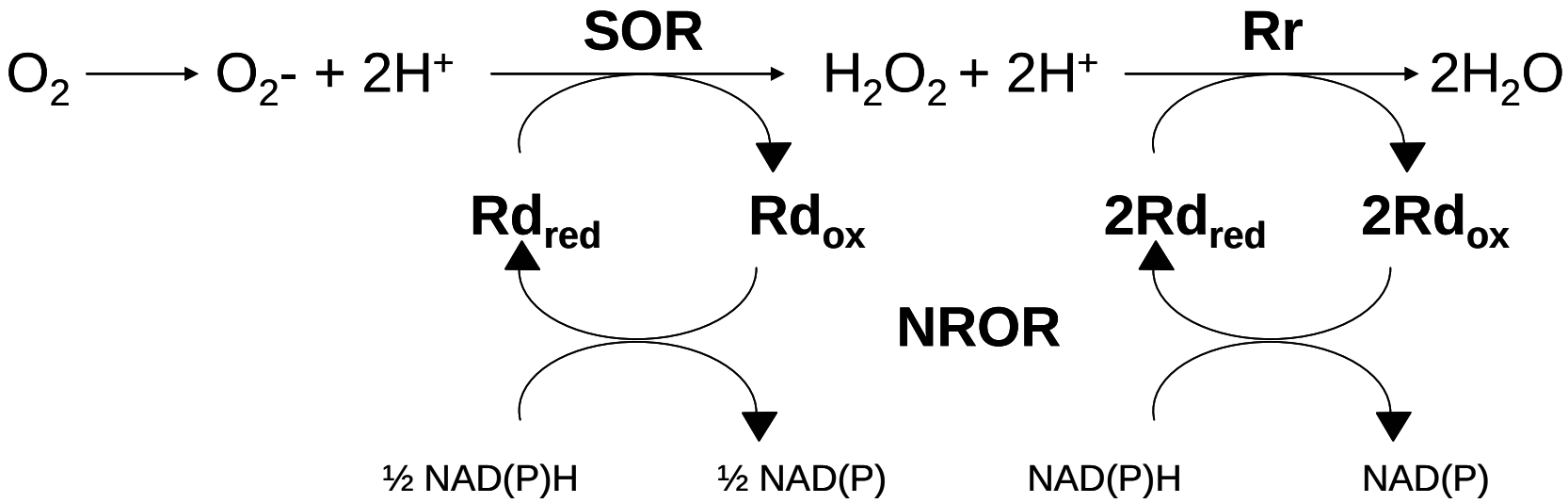
O2 → O2- + 2H+
SOR
H2O2 + 2H+
Rr
2H2O
Rdred
Rdox
2Rdred
2Rdox
NROR
½ NAD(P)H
½ NAD(P)
NAD(P)H
NAD(P)

In a recent assessment of the SOR-dependent pathway (1), the most fundamental unanswered question was what happens to peroxide produced by SOR? The answer appears to be, at least in part, that it is reduced to water by Rr, which functions as a Rd:hydrogen peroxide oxidoreductase. The reductant for this reaction ultimately comes from NADH, using the same mechanism (NROR and Rd) that provides electrons for the reduction of superoxide by SOR. This is illustrated in Fig. 3.5. It is also shown herein that this pathway can be reconstituted in vitro where electrons from NADH serve to reduce hydrogen peroxide to water using NROR, Rr and Rd as the intermediate electron carriers. Rr is present at a relatively high concentration in cell-free extracts of maltose-grown *P. furiosus* cells, as shown by the fact that it is readily seen on an SDS-PAGE gel after only one purification step. SOR and Rd are also present at high concentrations (21, 22). Further, microarray studies indicate that the genes encoding Rr, SOR and Rd, are among the highest expressed genes in the *P. furiosus* genome when grown under anaerobic (non-oxidative stress) conditions (39). This makes it very unlikely these genes will be up-regulated even further in response to oxidative stress. Indeed, preliminary analyses indicate that the addition of hydrogen peroxide to a culture of *P. furiosus* does not have a significant affect on the expression of these three genes (Sun, C.-J. and Adams, M. W. W., unpublished results). These data suggest that anaerobically-grown *P. furiosus* is 'armed' and readily responds via the SOR pathway to an oxidative challenge.

The three recombinant forms of *P. furiosus* Rr all contained much less than the 3 Fe atoms/subunit found in the native protein purified from *P. furiosus* biomass, although the overall metal contents were approximately 3 ions/subunit where the balance was zinc. Unfortunately, little is known about how simple (mono- and binuclear) metal centers are assembled in any organism. Consequently, there is no information as to why *P. furiosus* only inserts iron into its

Rr, while *E. coli* inserts predominantly zinc. In fact, *E. coli* mainly inserts zinc rather than iron into the recombinant form of clostridial rubredoxin (13). The lower iron contents of the recombinant forms appeared to be directly related to the lower peroxidase activity of the proteins (relative to native Rr from *P. furiosus*), with an approximate 10-fold reduction in peroxidase activity with each equivalent of an iron atom that was replaced by zinc (Table 3.1). The binuclear site in the native rubrerythrin-like protein from the aerobic hyperthermophilic archaeon *S. tokodaii*, appears to contain both iron (0.9 mol Fe/Rr monomer) and zinc (0.5 mol Zn/Rr monomer). This could be the reason why no activity was detected when it was assayed for SOD and inorganic pyrophosphatase (46). In the case of *P. furiosus* rRr, the presence of the N-terminal His-tag might interfere with metal ion insertion, protein folding and/or peroxidase activity. However, the crystal structure (44) of the recombinant protein shows that is fully folded, the metal sites are fully occupied and coordinated by the expected residues, and that the His tag is not in close proximity to the proposed active site or the metal centers. It is therefore extremely unlikely that the variable metal contents and variable peroxidase activities of the recombinant proteins are in any way related to the His-tag.

The observation that *P. furiosus* Rr in its purified reduced state precipitates when oxidized by air, ferricyanide or peroxide is a puzzling phenomenon. None of the recombinant forms exhibited this property, even the 2Fe/1Zn form which had significant catalytic activity (10% of the native form) and a mononuclear site containing predominantly iron (as shown by the visible absorption). It therefore appears precipitation requires that the protein be in an almost fully active form with a binuclear center predominantly occupied by iron. Since precipitation is not expected to occur inside the cell, these data may provide indirect evidence that Rr *exists in*

vivo as a heteromeric multiprotein complex and such a possibility is currently under investigation.

Acknowledgements

This research was supported by grants from the National Institutes of Health (GM 60329 and GM 62407). We thank William B. Whitman for advice about phylogeny and guide tree construction.

REFERENCES

1. **Adams, M. W. W., F. E. Jenney, M. D. Clay, and M. K. Johnson.** 2002. Superoxide reductase: fact or fiction? J. Biol. Inorg. Chem. **7:**647-652.

2. **Alban, P. S., and N. R. Krieg.** 1998. A hydrogen peroxide resistant mutant of *Spirillum volutans* has NADH peroxidase activity but no increased oxygen tolerance. Can. J. Microbiol. **44:**87-91.

3. **Alban, P. S., D. L. Popham, K. E. Rippere, and N. R. Krieg.** 1998. Identification of a gene for a rubrerythrin/nigerythrin-like protein in *Spirillum volutans* by using amino acid sequence data from mass spectrometry and NH2-terminal sequencing. J. Appl. Microbiol. **85:**875-882.

4. **Bonomi, F., D. M. Kurtz, and X. Y. Cui.** 1996. Ferroxidase activity of recombinant *Desulfovibrio vulgaris* rubrerythrin. J. Biol. Inorg. Chem. **1:**67-72.

5. **Brown-Peterson, N. J., and M. L. Salin.** 1993. Purification of a catalase-peroxidase from *Halobacterium halobium*: Characterization of some unique properties of the halophilic enzyme. J. Bacteriol. **175:**4197-4202.

6. **Bryant, F. O., and M. W. W. Adams.** 1989. Characterization of hydrogenase from the hyperthermophilic archaebacterium, *Pyrococcus furiosus*. J. Biol. Chem. **264:**5070-5079.

7. **Coulter, E. D., and D. M. Kurtz.** 2001. A role for rubredoxin in oxidative stress protection in *Desulfovibrio vulgaris*: Catalytic electron transfer to rubrerythrin and two-iron superoxide reductase. Arch. Biochem. Biophys. **394:**76-86.

8. **Coulter, E. D., N. V. Shenvi, Z. M. Beharry, J. J. Smith, B. C. Prickril, and D. M. Kurtz.** 2000. Rubrerythrin-catalyzed substrate oxidation by dioxygen and hydrogen peroxide. Inorg. Chim. Acta. **297:**231-241.

9. **Coulter, E. D., N. V. Shenvi, and D. M. Kurtz.** 1999. NADH peroxidase activity of rubrerythrin. Biochem. Biophys. Res. Commun. **255:**317-323.

10. **Das, A., E. D. Coulter, D. M. Kurtz, and L. G. Ljungdahl.** 2001. Five-gene cluster in *Clostridium thermoaceticum* consisting of two divergent operons encoding rubredoxin oxidoreductase-rubredoxin and rubrerythrin-type A flavoprotein-high-molecular-weight rubredoxin. J. Bacteriol. **183:**1560-1567.

11. **Dawson, R. M. C., D. C. Elliot, W. H. Elliot, and K. M. Jones.** 1986. Data for Biochemical Research, 3rd ed, vol. 1. Clarendon Press, Oxford.

12. **deMare, F., D. M. Kurtz, and P. Nordlund.** 1996. The structure of *Desulfovibrio vulgaris* rubrerythrin reveals a unique combination of rubredoxin-like FeS4 and ferritin-like diiron domains. Nat. Struct. Biol. **3:**539-546.

13. **Eidsness, M., S. O'Dell, D. Kurtz, Jr, R. Robson, and R. Scott.** 1992. Expression of a synthetic gene coding for the amino acid sequence of *Clostridium pasteurianum* rubredoxin. Prot. Eng. **5:**367-371.

14. **Fiala, G., and K. O. Stetter.** 1986. *Pyrococcus furiosus* sp-nov represents a novel genus of marine heterotrophic archaebacteria growing optimally at 100 ^{o}C. Arch. Microbiol. **145:**56-61.

15. **Geissmann, T. A., M. Teuber, and L. Meile.** 1999. Transcriptional analysis of the rubrerythrin and superoxide dismutase genes of *Clostridium perfringens*. J. Bacteriol. **181:**7136-7139.

16. **Gudelj, M., G. O. Fruhwirth, A. Paar, F. Lottspeich, K. H. Robra, A. Cavaco-Paulo, and G. M. Gubitz.** 2001. A catalase-peroxidase from a newly isolated thermoalkaliphilic

Bacillus sp. with potential for the treatment of textile bleaching effluents. Extremophiles **5:**423-429.

17. **Gupta, N., F. Bonomi, D. M. Kurtz, N. Ravi, D. L. Wang, and B. H. Huynh.** 1995. Recombinant *Desulfovibrio vulgaris* rubrerythrin - isolation and characterization of the diiron domain. Biochemistry. **34:**3310-3318.

18. **Heinonen, J. K., and R. J. Lahti.** 1981. A new and convenient colorimetric determination of inorganic ortho-phosphate and its application to the assay of inorganic pyrophosphatase. Anal. Biochem. **113:**313-317.

19. **http://www.secsg.org.**

20. **http://www.tigr.org.**

21. **Jenney, F. E., and M. W. W. Adams.** 2001. Rubredoxin from *Pyrococcus furiosus*. Method Enzymol. **334:**45-55.

22. **Jenney, F. E., M. F. J. M. Verhagen, and M. W. W. Adams.** 1999. Neelaredoxin from *Pyrococcus furiosus* is a novel type of superoxide dismutase. J. Inorg. Biochem. **74:**181-181.

23. **Jenney, F. E., M. F. J. M. Verhagen, X. Y. Cui, and M. W. W. Adams.** 1999. Anaerobic microbes: Oxygen detoxification without superoxide dismutase. Science. **286:**306-309.

24. **Kengen, S. W., F. J. Bikker, W. R. Hagen, W. M. de Vos, and J. Van Der Oost.** 2001. Characterization of a catalase-peroxidase from the hyperthermophilic archaeon *Archaeoglobus fulgidus*. Extremophiles. **5:**323-332.

25. **Kumar, S., K. Tamura, and M. Nei.** 2004. MEGA3: Integrated software for molecular evolutionary genetics analysis and sequence alignment. Briefings in Bioinformatics **(In press)**.

26. **Legall, J., B. C. Prickril, I. Moura, A. V. Xavier, J. J. G. Moura, and B. H. Huynh.** 1988. Isolation and characterization of rubrerythrin, a non-heme iron protein from *Desulfovibrio vulgaris* that contains rubredoxin centers and a hemerythrin-like binuclear iron cluster. Biochemistry. **27:**1636-1642.

27. **Lehmann, Y., L. Meile, and M. Teuber.** 1996. Rubrerythrin from *Clostridium perfringens*: Cloning of the gene, purification of the protein, and characterization of its superoxide dismutase function. J. Bacteriol. **178:**7152-7158.

28. **Li, M., M. Y. Liu, J. Le Gall, L. L. Gui, J. Liao, T. Jiang, J. Zhang, D. Liang, and W. Chang.** 2003. Crystal structure studies on rubrerythrin: Enzymatic activity in relation to the zinc movement. J. Biol. Inorg. Chem. **8:**149-155.

29. **Liu, M. Y., and J. Legall.** 1990. Purification and characterization of two proteins with inorganic pyrophosphatase activity from *Desulfovibrio vulgaris* - rubrerythrin and a new, highly-active, enzyme. Bioch. Biophys. Res. Commun. **171:**313-318.

30. **Lovenberg, W., J. C. Rabinowitz, and B. B. Buchanan.** 1963. Studies on chemical nature of *Clostridial* ferredoxin. J. Biol. Chem. **238:**3899-3913.

31. **Ma, K., and M. W. W. Adams.** 1999. A hyperactive NAD(P)H : rubredoxin oxidoreductase from the hyperthermophilic archaeon *Pyrococcus furiosus*. J. Bacteriol. **181:**5530-5533.

32. **Mccord, J. M., and I. Fridovic.** 1969. Superoxide dismutase-an enzymic function for erythrocuprein. J. Biol. Chem. **244:**6049-6055.

33. **Pierik, A. J., R. B. G. Wolbert, G. L. Portier, M. F. J. M. Verhagen, and W. R. Hagen.** 1993. Nigerythrin and rubrerythrin from *Desulfovibrio vulgaris* each contain two mononuclear iron centers and two dinuclear iron clusters. Eur. J. Biochem. **212:**237-245.

34. **Ravi, N., B. C. Prickril, D. M. Kurtz, and B. H. Huynh.** 1993. Spectroscopic characterization of Fe-57-reconstituted rubrerythrin, a nonheme iron protein with structural analogies to ribonucleotide reductase. Biochemistry. **32:**8487-8491.

35. **Robb, F. T., D. L. Maeder, J. R. Brown, J. DiRuggiero, M. D. Stump, R. K. Yeh, R. B. Weiss, and D. M. Dunn.** 2001. Genomic sequence of hyperthermophile, *Pyrococcus furiosus*: Implications for physiology and enzymology. Methods Enzymol. **330:**134-157.

36. **Rzhetsky, A., and M. Nei.** 1993. Theoretical foundation of the minimum-evolution method of phylogenetic inference. Molecular Biology and Evolution **10:**1073-1095.

37. **Saitou, N., and M. Nei.** 1987. The Neighbor-Joining Method - a New Method for Reconstructing Phylogenetic Trees. Mol. Biol. Evol. **4:**406-425.

38. **Sambrook, J., and D. Russell.** 2001. Molecular Cloning: A Laboratory Manual, 3rd ed. Cold Spring Harbor Laboratory Press, Cold Spring Harbor, NY.

39. **Schut, G. J., S. D. Brehm, S. Datta, and M. W. W. Adams.** 2003. Whole-genome DNA microarray analysis of a hyperthermophile and an archaeon: *Pyrococcus furiosus* grown on carbohydrates or peptides. J. Bacteriol. **185:**3935-47.

40. **Sieker, L. C., M. Holmes, I. Le Trong, S. Turley, M. Y. Liu, J. LeGall, and R. E. Stenkamp.** 2000. The 1.9 angstrom crystal structure of the "as isolated" rubrerythrin from *Desulfovibrio vulgaris*: some surprising results. J. Biol. Inorg. Chem. **5:**505-513.

41. **Sieker, L. C., M. Holmes, I. Le Trong, S. Turley, B. D. Santarsiero, M. Y. Liu, J. LeGall, and R. E. Stenkamp.** 1999. Alternative metal-binding sites in rubrerythrin. Nat. Struct. Biol. **6:**308-309.

42. **Sztukowska, M., M. Bugno, J. Potempa, J. Travis, and D. M. Kurtz.** 2002. Role of rubrerythrin in the oxidative stress response of *Porphyromonas gingivalis*. Mol. Microbiol. **44:**479-488.

43. **Tempel, W., Z. J. Liu, F. D. Schubot, M. V. Weinberg, F. E. Jenney, Jr, M. W. W. Adams, J. P. Rose, and B. C. Wang.** 2004. Structural genomics of *Pyrococcus furiosus*: X-Ray crystallography reveals 3D domain swapping in rubrerythrin. Proteins Struct. Funct. Genet. **In Press**.

44. **Thompson, V. S., K. D. Schaller, and W. A. Apel.** 2003. Purification and characterization of a novel thermo-alkali-stable catalase from *Thermus brockianus*. Biotechnol. Prog. **19:**1292-1299.

45. **Van Beeumen, J. J., G. Van Driessche, M. Y. Liu, and J. LeGall.** 1991. The primary structure of rubrerythrin, a protein with inorganic pyrophosphatase activity from *Desulfovibrio vulgaris* - Comparison with hemerythrin and rubredoxin. J. Biol. Chem. **266:**20645-20653.

46. **Wakagi, T.** 2003. Sulerythrin, the smallest member of the rubrerythrin family, from the strictly aerobic and thermoacidophilic archaeon, *Sulfolobus tokodaii* strain 7. FEMS Microbiol. Lett. **222:**33-37.

CHAPTER 4

COLD SHOCK OF A HYPERTHERMOPHILIC ARCHAEON: *PYROCOCCUS FURIOSUS* EXHIBITS MULTIPLE RESPONSES TO A SUB-OPTIMAL GROWTH TEMPERATURE WITH A KEY ROLE FOR MEMBRANE-BOUND GLYCOPROTEINS[1]

[1] Weinberg, M.V., G.J. Schut, S. Brehm, S. Datta and M.W.W. Adams. Accepted by *Journal of Bacteriology*. Reprinted here with permission from the publisher, 09/20/04.

ABSTRACT

The hyperthermophilic archaeon, *Pyrococcus furiosus,* was grown on maltose near its optimal growth temperature, 95°C, and at the lower end of the temperature range for significant growth, 72°C. In addition, cultures were shocked by rapidly dropping the temperature from 95 to 72°C. This resulted in a 5 hour lag phase, during which time little growth occurred. Transcriptional analyses using whole genome DNA microarrays representing 2,065 open reading frames (ORFs) in the *P. furiosus* genome showed that cells undergo three very different responses at 72°C; an early shock (1-2 hr), a late shock (5 hr), and an adapted response (occurring after many generations at 72°C). Each response involved the up-regulation in the expression of more than thirty ORFs unique to that response. These included proteins involved in translation, solute transport, amino acid biosynthesis, and tungsten and intermediary carbon metabolism, as well as numerous conserved/hypothetical and/or membrane-associated proteins. Two major membrane proteins were evident after 1D SDS-gel analysis of cold-adapted cells and staining revealed them to be glycoproteins. Their cold-induced expression, evident from the DNA microarray analysis, was confirmed by quantitative PCR. Termed CipA (PF0190) and CipB (PF1408), both appear to be solute-binding proteins. While the archaea do not contain members of the bacterial cold shock protein (Csp) family, they all contain homologs of CipA and CipB. These proteins are also related phylogenetically to some cold-responsive genes recently identified in certain bacteria. The Cip proteins may represent a general prokaryotic-type cold response mechanism that is present even in hyperthermophilic archaea**.**

INTRODUCTION

How bacteria respond to temperatures significantly below optimal for growth has been well characterized (9). A decrease in temperature results in a temporary halt in protein synthesis, but a small subset of so-called cold shock proteins are induced during an acclimation phase (27). After a lag phase of several hours, general protein synthesis and cell growth resumes at a much slower rate, and production of most of the cold shock proteins decrease to a basal level. The first major cold shock protein to be characterized was CspA of *Escherichia coli* (24). This organism contains eight CspA homologs (CspB-I) although only four (CspA, B, G and I) are cold inducible (57). They are thought to function as mRNA chaperones that prevent the formation of inhibitory secondary structures, which are stabilized at the lower temperatures. Other cold-inducible proteins in *E. coli* include initiation factor 2 [IF2: (7, 13)], ribosomal binding factor A [RbfA: (25)], and DEAD-box RNA helicase (4, 26, 40), all of which associate with the ribosome and are believed to play a role in protein synthesis. Ribosomal function therefore appears to be compromised at lower temperatures and several new proteins are required to allow protein synthesis to resume. Homologs of the CspA family, IF2 and RbfA are found in a wide range of gram positive (*Bacillus subtilis, Lactococcus monocytogenes*) and gram negative (*Micrococcus luteus*, *Yersinia pestis*) bacteria, as well as psychrophilic (*Pseudomonas fragi*, *Arthrobacter globiformis*), thermophilic (*B. caldolyticus*) and even hyperthermophilic (*Thermotoga maritima*, *Aquifex aeolicus*) species (19).

In contrast to bacteria, little is known about how members of the archaeal domain respond to sub-optimal growth temperatures. The genome of the psychrotrophic methanogen *Methanococcoides burtonii* contains a gene (*deaD*) encoding for a DEAD-box RNA helicase and this was shown to be cold-inducible (34). However, this is the only evidence for a link between

the archaeal and bacterial cold shock responses. Homologs of the canonical cold shock proteins CspA and RbfA are not present in any of the sixteen genome sequences available for mesophilic and thermophilic members of the archaea (19). Therefore, if these organisms possess a cold shock response, it is novel and distinct from the previously characterized cold shock response of bacteria. Of particular interest is the cold-shock response of hyperthermophilic archaea. These are defined as organisms with an optimal growth temperature of at least 80°C (54). So far only one protein implicated in such a response has been studied. Prolyl isomerase was induced when a culture of *Thermococcus* sp. KS-1 growing at its optimal growth temperature of 85°C (14) was shifted to 60°C (20, 21). The enzyme has been proposed to function in the archaea by interacting with the hydrophobic regions of newly synthesized proteins to aid in folding, analogous to the "trigger factor" in *E. coli* which has also been implicated in the bacterial cold shock response (21).

A genome wide approach to studying the response of hyperthermophilic archaea to sub-optimal growth temperatures has not yet been reported. Herein we describe the results of such a study using DNA microarrays to measure transcription profiles in response to cold stress of all 2,065 ORFs that have been annotated in the genome of *Pyrococcus furiosus* (45), an anaerobic heterotroph that grows optimally at 100°C (11). This organism utilizes complex carbohydrates and peptides as carbon and energy sources and produces hydrogen gas, acetate and organic acids as metabolic end products. It was first isolated from a shallow marine hydrothermal vent in 1986 (11). In this niche, the vent fluids are expelled into oxygenated seawater at ambient temperature (20°C), conditions under which *P. furiosus* can survive (29). Growth resumes when the organism is subsequently exposed to temperatures above 70°C under anaerobic conditions. It would therefore seem likely that *P. furiosus* has mechanisms to help it survive temporary

exposure to both oxygen and lower temperatures, as proposed earlier (23). The results presented here show that the organism has three very different cellular responses to the sub-optimal growth temperature of 72°C. An early shock response occurs immediately upon a decrease in temperature, and this is followed by a late shock response. A different suite of proteins is induced in each phase, and they are not the same as those that are up-regulated in cells adapted to the sub-optimal temperature.

MATERIALS AND METHODS

Growth conditions and RNA extraction. *P. furiosus* (DSM 3638) was routinely grown with maltose as the primary carbon source in a 20-liter custom fermentor (1). The medium was the same as that previously reported (1) except that the yeast extract concentration was 0.2% (w/v). There were two types of growth experiments utilized in this study, termed shock and adapted growth. For the adapted growth experiments, cultures were grown at 95 and 72°C. The two cell types used for RNA isolation were grown at their respective temperature after at least three successive transfers using batch cultures grown at that temperature. In the shock experiments, cultures growing at 95°C were rapidly cooled to 72°C when they reached a cell density of ~ 3 x 10^7 cells/ml by pumping them through a glass cooling coil maintained at 20°C. The complete culture (15 L) was cooled from 95 to 72°C within 15 minutes. To prepare cell extracts from adapted cultures, cells were harvested in late log phase (~ 2 x 10^8 cells/ml) and fractionated as previously described (51). For shocked cultures, cells were harvest 2 or 5 hrs after the shock was introduced and fractionated as in the adapted cultures. To obtain RNA for the microarray analyses, samples (2 l) were rapidly removed from the fermentor and cooled to 4°C. Total RNA was extracted using acid-phenol (51) and stored at -80°C until needed.

DNA microarray analyses. The design and construction of DNA microarrays containing all of the 2,065 ORFs in the annotated genome of *P. furiosus* (17), preparation of cDNA from the RNA samples, and hybridization experiments, were all performed as previously described (51). Fluorescently-labeled cDNA was prepared using the ARES DNA labeling kit (Molecular Probes, Eugene, OR). The resulting amine-modified cDNA was purified using a QIAquick PCR Purification Kit (Qiagen, Valencia, CA) according to the manufacturer's instructions except that the wash buffer was replaced with 75% (v/v) ethanol and the cDNA was eluted with 45 µl of distilled water and dried under vacuum. The amine-modified cDNA was labeled with Alexa dye 488, 546, 594 or 647 (Molecular Probes) according to the manufacturer's instructions. The labeled cDNA was purified using the Qiagen kit and dried under vacuum. Differentially-labeled cDNA derived from *P. furiosus* cells grown at different growth temperatures (95 and 72°C) or cold shocked cells harvested at specific times (0, 1, 2 or 5 hrs after a culture was shifted to 72°C) was pooled, hybridized to the DNA microarray, and the fluorescence intensities for the Alexa dyes were measured as described previously (51). For the adapted experiments, each $\log_2$ value represents an average of four hybridization experiments performed in duplicate using cDNA derived from 4 different cultures of *P. furiosus* (two grown at 95°C, two grown at 72°C). Each $\log_2$ value from the shock experiments represent an average of two hybridization experiments performed in duplicate using cDNA derived from two different cultures of *P. furiosus*. Standard deviations for the adapted and shock data sets are included. Individual *t*-test procedures were conducted to identify the significantly expressed ORFs and Holm's step-down *P* value adjustment procedure was performed (16) to give modified *P* values.

Quantitative Real Time PCR. RNA was isolated as described above and further purified using the Absolutely RNA clean up kit (Stratagene, La Jolla, CA). cDNA was then prepared as described previously (51) with the exception that aminoallyl dUTP was replaced by the TTP derivative. The regulated genes PF0190 and PF1408 were selected for study and the non-regulated gene PF0018, which encodes a subunit of DNA polymerase, was selected as a control. Primers for the genes were designed using the program Array Designer v.1.16 (Premier Biosoft International, Palo Alto, CA). All qPCR experiments were carried out using an Mx3000P instrument (Stratagene) using the SYBR-Green assay as a reporter dye. Each experiment used RNA isolated from the four *P. furiosus* adapted cultures used for the microarray experiments (two grown at 95°C and two grown at 72°C) and each was repeated three times. The comparative cycle threshold (C_T) method was used to analyze the resulting data as described by the manufacturer (Applied Biosystems, Bulletin #2).

Enzyme assays. All assays were carried out at 85°C using cell-free extracts that were prepared as described previously (1). Acetolactate synthase activity was measured by the formation of acetoin (58). Aminoacyl-releasing enzyme (AARE) activity was measured by the release of *p*-nitroaniline from a tripeptide substrate (22). The activities of 2-ketoglutarate ferredoxin (Fd) oxidoreductase (KGOR) and pyruvate Fd oxidoreductase (POR) were measured as described previously (50)**.**

Other methods. Sodium dodecyl sulfate (SDS)-PAGE electrophoresis was performed on the cytosolic and membrane fractions using 15% polyacrylamide by the method of Laemmli (33). Protein concentrations were determined by the Bradford method (6) using bovine serum albumin

as the standard. Invitrogen (Carlsbad, CA) Benchmark protein ladder, ranging from 10-220 kDa was used for molecular weight estimation. Unless otherwise specified, gels were stained with Coomassie Brilliant Blue R-250 (Fisher Biotech, Fair Lawn, NJ). To identify proteins, bands were cut out of the SDS-PAGE gel and subjected to in-gel trypsin digestion as described previously (52). The resulting sample was subjected to MALDI-MS using an Applied Biosystems 4700 Proteomics Analyzer at the University of Georgia Proteomics Resource Facility (Athens, GA). Glycoproteins were identified by staining with Pro-Q Emerald 300 (Molecular Probes) after separating them using a 15% SDS-PAGE gel. The total glycoprotein content of the extract was also determined using a Glycoprotein Carbohydrate Estimation Kit (Pierce, Rockford, IL). The detection of potential signal sequences and the number of transmembrane domains in *P. furiosus* ORFs was calculated as described previously (15). Operons are defined as adjacent ORFs (on the same strand) in the *P. furiosus* genome that are less than 16 nucleotides apart and are potentially co-regulated and co-transcribed as described (19). Amino acid sequences were aligned using Vector NTI AlignX software (Suite 9.0.0, Invitrogen). Phylogenetic trees were constructed using MEGA3 software (32) employing the Neighbor Joining (NJ) technique (48). The p-distance substitution model was used to estimate distance values and bootstrap values (10) were determined using 1,000 replicates of the data.

RESULTS AND DISCUSSION

Effect of temperature on growth. *P. furiosus* growing with maltose as the primary carbon source has a generation time of 1 hr at 95°C (11), but this increases to about 5 hrs at 72°C, which is near the minimum growth temperature (Fig. 4.1). In addition, *P. furiosus* exhibits a cold shock response when the temperature of a growing culture is shifted from 95 to 72°C. This results in a

Figure 4.1.

Growth of *P. furiosus* at 95 and 72 °C. Cells were grown at 95°C (closed squares), at 72°C (closed triangles), or at 95°C for 3.5 hr (cell density of ~ 3 x 10^7 cells/ml) and then shocked (indicated by the arrow) by rapidly decreasing the temperature to 72°C (closed circles).

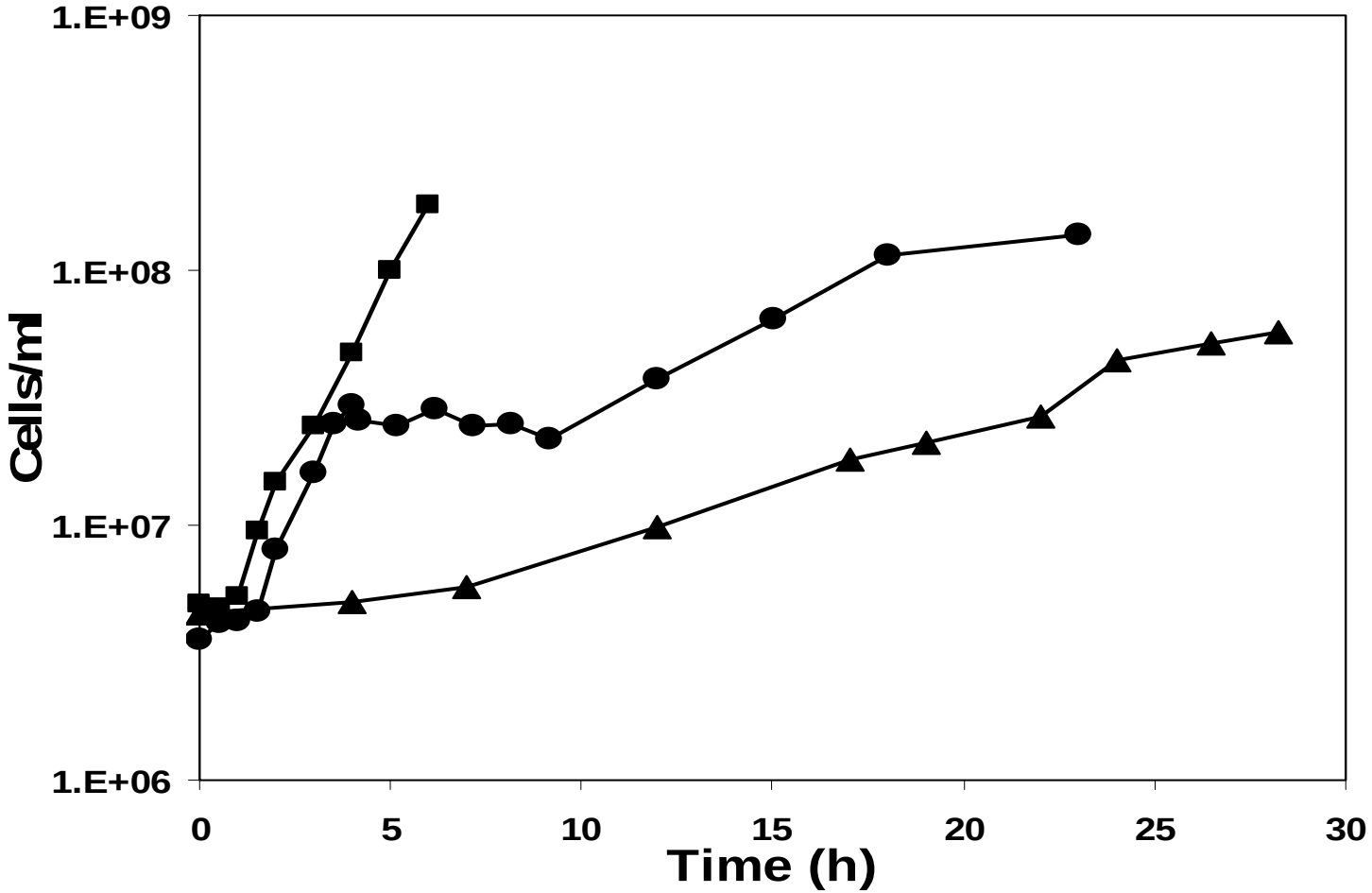
1.E+09
1.E+08
1.E+07
1.E+06
Cells/ml
0
5
10
15
20
25
30
Time (h)

lag phase of about 5 hr during which time there is little if any growth, reminiscent of that seen in bacteria after cold shock (Fig. 4.1). After this acclimation phase, growth of *P. furiosus* resumes at a rate similar to that seen in cultures grown continuously at 72°C (Fig. 4.1). The organism therefore exhibits two cellular responses when exposed to temperatures that support a minimal growth rate. The "cold shock response" occurs when the temperature of a culture is suddenly shifted to the lower growth temperature with no associated growth, while the "cold-adapted response" is exhibited by cultures that are actively growing at the lower temperature. The goals of the present study were, therefore, to determine to what extent these two cell types, cold-shocked and cold-adapted, differed from cells grown at 95°C under standard conditions. This was initially assessed at the transcriptional level using DNA microarrays that represented all 2,065 ORFs annotated (45) in the *P. furiosus* genome.

Genome wide responses to a sub-optimal growth temperature. In the cold shock experiment, the temperature of a log phase culture was rapidly decreased from 95 to 72°C, and cells were removed at different times (1, 2 and 5 hrs post shock) from the same culture to prepare RNA samples for transcriptional profiling, and these were compared with an RNA sample prepared from cells harvested just prior to the temperature change (time zero). The four RNA samples were then differentially-labeled and hybridized to the same DNA microarray. This experimental approach minimizes both biological and experimental variation. In the cold-adapted experiment, RNA expression profiles were compared in two cultures of *P. furiosus* grown independently at the two temperatures (95 and 72°C).

The results of a control experiment using RNA samples prepared from two different cultures of *P. furiosus* grown under identical conditions at 95°C are shown in Figure 4.2A. The

Figure 4.2.

Relative fluorescence intensities of DNA microarrays. A) cDNA vs cDNA derived from two independent cultures of cells grown at 95°C. B) cDNA vs cDNA derived from two independent cultures of cells grown at 95°C and at 72°C. The upper and lower diagonal line indicate 2.5-fold changes in the signal intensities. See text for details.

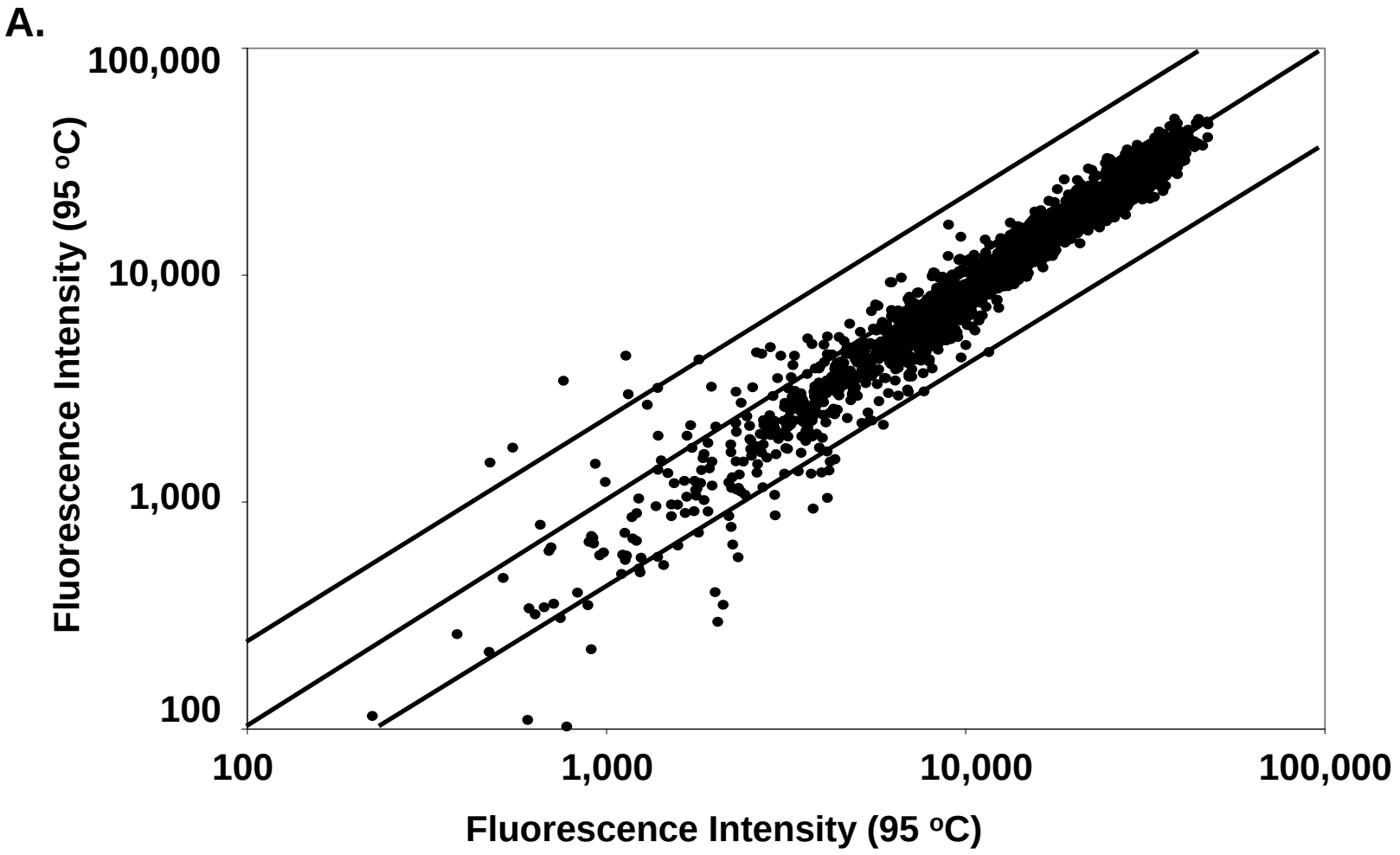
A.
100,000
10,000
1,000
100
Fluorescence Intensity (95 °C)
100
1,000
10,000
100,000
Fluorescence Intensity (95 °C)

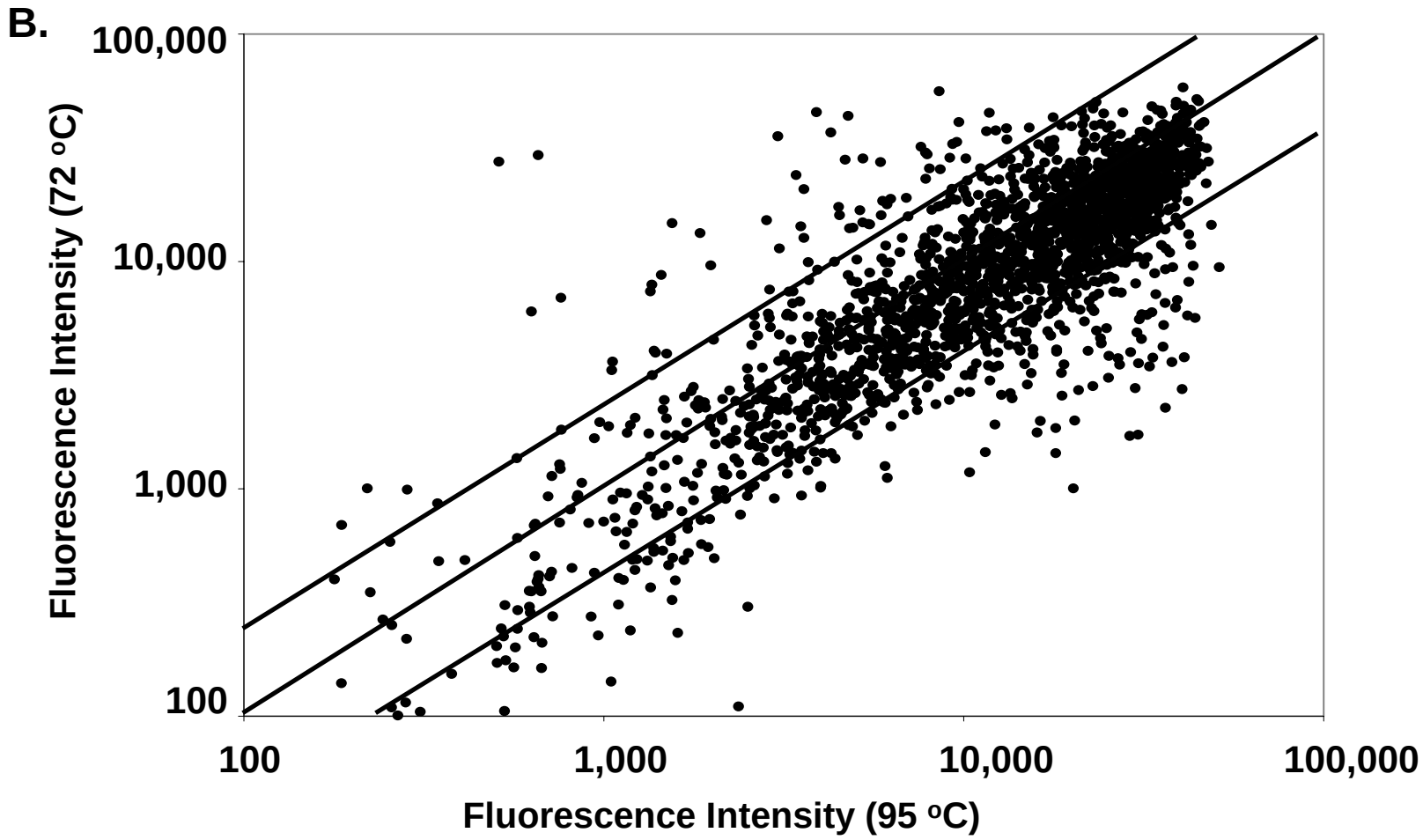
B.
100,000
10,000
1,000
100
Fluorescence Intensity (72 °C)
100
1,000
10,000
100,000
Fluorescence Intensity (95 °C)

fluorescence signal intensities vary over more than a 10^3 range and ORFs with intensities less than 2,000 arbitrary units (or twice the detection limit) are considered not to be expressed at a significant level. As expected, the low-intensity signals show a high standard deviation due to background fluorescence while the more highly expressed ORFs lie close to the diagonal. As shown in Fig. 4.2B, the results of a cold-adapted experiment comparing RNA samples from cells that were grown at 95 and at 72°C reveals a dramatic change in gene expression on a genome-wide basis. Of the 2,065 ORFs analyzed, 245 exhibited statistically-significant up- or down-regulation with *P* values < 0.01 and at least a 2.5-fold change in expression. Most of them (189 of 245) were down-regulated at the lower growth temperature. Similar microarray analyses were performed using RNA samples obtained 1, 2 and 5 hr after switching a culture from 95 to 72°C, and the shock response also resulted in a significant down-regulation of gene expression (after 1, 2 and 5 hr, there were 171, 69 and 152 ORFs, respectively, down-regulated by > 2.5-fold, $P < 0.01$). Hence, compared to growth at 95°C, much less mRNA was present for certain cellular processes at 72°C. Remarkably, on the other hand, there are a number of ORFs whose expression is significantly up-regulated in response to the temperature decrease, and these are the focus of the present work. The products of these ORFs are assumed to be involved in the processes by which the cells become acclimatized to 72°C. After 1, 2 and 5 hr of shock at 72°C, and in cells adapted to 72°C, there were 49, 35, 30 and 59 ORFs, respectively, that were significantly up-regulated (≥ 2.5-fold, $P < 0.01$). Some properties of these ORFs are listed in Tables 4.1 and 4.2 and are depicted diagrammatically in Figure 4.3. Complete genome-wide data sets for all growth conditions are available as supplementary information (http://adams.bmb.uga.edu/pubs/sup252.pdf).

Table 4.1. ORFs whose expression is up-regulated 1, 2 and 5 hr after changing the temperature from 95 to 72 °C.

ORF Number	Description[a]	TMDs[b]	1 hr[c]	2 hr[c]	5 hr[c]
[Threonine biosynthesis]					
PF0029	[Hypothetical protein]	0	2.2± 0.6 (4.6)	1.8± 0.8 (3.5)	1.4± 0.6 (2.7)
PF0030	[Conserved hypothetical protein]	0	2.3± 0.7 (4.8)		1.9± 0.6 (3.7)
PF0031	[Threonine synthase]	0	2.3± 0.7 (4.9)		
PF0085	[DNA helicase]	0			1.6± 0.5 (3.1)
PF0094	Protein disulfide oxidoreductase (3)	0	1.9± 0.6 (3.8)		
PF0101	[Conserved hypothetical protein]	0	2.3± 0.7 (4.9)		
PF0115	[ATP-dependent 26S protease, regulatory]	0	1.5± 0.3 (2.7)		
PF0190	[Conserved hypothetical protein]	2			1.7± 0.7 (3.2)
[Glutamate biosynthesis]					
PF0204	[Glutamine amidotransferase]	0	1.6± 0.5 (3.1)	2.0± 0.5 (4.0)	
PF0205	[Glutamate synthase, alpha]	0	1.4± 0.5 (2.6)		
PF0262	[MFS transporter]	11	1.3± 0.4 (2.6)		
PF0264	[Histidyl-tRNA synthetase]	0	1.6± 0.4 (3.0)		
PF0276	[oxidoreductase]	0	2.0± 0.4 (4.0)	1.6± 0.5 (3.0)	1.4± 0.5 (2.7)
PF0295	[N-type ATP pyrophosphatase]	0			1.4± 0.5 (2.7)
PF0312	ADP-dependent glucokinase (30)	0			1.4± 0.5 (2.6)

PF0318	[Acylaminoacyl releasing enzyme]	0	2.0± 0.4 (4.0)	2.2± 0.4 (4.5)	1.9± 0.7 (3.8)
[Unknown]					
PF0324	[Conserved hypothetical protein]	1		2.4± 0.9 (5.2)	4.6± 2.4 (23.8)[d]
PF0325	[Conserved hypothetical protein]	1		2.3± 0.6 (4.8)	4.4± 1.1 (21.3)
PF0326	[Conserved hypothetical protein]	3			2.3± 0.9 (4.9)
PF0481	[Translation initiation factor eIF-2, beta]	0	1.3± 0.4 (2.5)		
PF0651	[Conserved hypothetical protein]	1	3.1± 0.6 (8.3)	2.9± 0.9 (7.2)	
PF0718	[Conserved hypothetical protein]	5		2.0± 0.4 (4.1)	
PF0721	[Conserved hypothetical protein]	0	1.4± 0.3 (2.7)		1.6± 0.5 (3.0)
PF0822	[Conserved hypothetical protein]	0	1.3± 0.2 (2.5)		
PF0859	[MttC/ TatD homolog]	0	1.8± 0.4 (3.4)	1.4± 0.5 (2.6)	
PF0929	[Conserved hypothetical protein]	0	1.8± 0.5 (3.5)	1.6± 0.4 (3.1)	
[Branched chain amino acid biosynthesis]					
PF0934	[Conserved hypothetical protein]	0			2.5± 0.5 (5.6)
PF0935	[Acetolactate synthase]	0			2.5± 1.0 (5.6)
PF0939	[3-Isopropylmalate dehydratase, small]	0			1.8± 0.7 (3.4)
PF0940	[3-Isopropylmalate dehydrogenase]	0			2.5± 1.0 (5.7)
PF1026	[Malic enzyme]	0	1.3± 0.4 (2.5)		
[Serine/Threonine biosynthesis]					
PF1053	[aspartokinase II, alpha]	0	1.4± 0.4 (2.6)	1.6± 0.5 (3.1)	
PF1054	[Homoserine kinase]	0		1.7± 0.6 (3.2)	2.3± 0.7 (5.0)

PF1055	[Threonine synthase]	0		1.1± 0.3 (2.2)	
PF1056	[Aspartate-semialdehyde dehydrogenase]	1		1.4± 0.4 (2.6)	1.7± 0.4 (3.3)
PF1062	[Nuclease repair enzyme]	0	2.9± 0.9 (7.7)		
PF1104	[Homoserine dehydrogenase]	0	1.3± 0.2 (2.5)		
PF1137	[Translation initiation factor IF-2]	0	1.6± 0.5 (3.0)	1.5± 0.5 (2.8)	
[Methionine biosynthesis]					
PF1266	[Cystathionine gamma-lyase]	0			1.3± 0.5 (2.5)
PF1267	[Conserved hypothetical protein]	0			1.8± 0.5 (2.3)
PF1268	[Conserved hypothetical protein]	0			1.8± 0.7 (3.4)
PF1270	[Conserved hypothetical protein]	0			1.9± 0.9 (3.8)[d]
PF1344	[Maleate cis-trans isomerase]	0			1.4± 0.4 (2.6)
PF1348	[Hypothetical protein]	0			2.9± 1.1 (7.4)
PF1408	[Dipeptide-binding protein]	1			1.7± 0.7 (3.2)
[Unknown]					
PF1454	[Conserved hypothetical protein]	0	1.5± 0.6 (2.7)		
PF1455	[Hypothetical protein]	0	1.9± 0.3 (3.7)		
[Tungstoenzyme-5]					
PF1479	[Oxidoreductase, Fe-S subunit]	0	2.3± 0.8 (4.9)	2.5± 0.5 (5.6)	
PF1480	[Formaldehyde:Fd oxidoreductase, WOR5]	0	2.3± 0.4 (5.0)	2.4± 0.4 (5.1)	2.1± 0.7 (4.2)
[Carbohydrate metabolism]					
PF1535	[Alpha-glucan phosphorylase]	0	1.2± 0.1 (2.3)	1.2± 0.4 (2.3)	

PF1536	[Short chain dehydrogenase]	0	1.0± 0.2 (2.0)	1.1± 0.4 (2.1)	
PF1537	[Conserved hypothetical protein]	5	1.2± 0.4 (2.3)	1.5± 0.3 (2.8)	
PF1538	[Amidohydrolase]	0	1.4± 0.4 (2.7)	1.8± 0.3 (3.5)	
PF1654	[ABC transporter, ATP-binding]	6	1.9± 0.1 (3.7)	1.9± 0.5 (3.8)	
2-Keto acid ferredoxin oxidoreductases					
PF1767	2-Ketoglutarate:Fd oxidoreductase, delta (50)	0	2.3± 0.4 (4.9)	2.5± 0.5 (5.6)	
PF1768	2-Ketoglutarate:Fd oxidoreductase, alpha (50)	0	2.3± 0.5 (4.9)	2.4± 0.5 (5.2)	
PF1769	2-Ketoglutarate:Fd oxidoreductase, beta (50)	0	1.9± 0.6 (3.7)	2.2± 0.5 (4.7)	
PF1770	2-Ketoglutarate:Fd oxidoreductase, gamma (50)	0	1.9± 0.7 (3.7)	2.1± 0.4 (4.3)	
PF1771	[2-Keto acid:Fd oxidoreductase, alpha]	0	2.0± 0.5 (4.0)	2.1± 0.4 (4.4)	
PF1772	[2-Keto acid:Fd oxidoreductase, beta]	0	1.9± 0.6 (3.6)	1.9± 0.5 (3.8)	
PF1773	[2-Keto acid:Fd oxidoreductase, gamma]	0	1.8± 0.6 (3.6)	2.1± 0.5 (4.3)	
[Unknown]					
PF1907	[Conserved hypothetical protein]	1	1.2± 0.3 (2.3)	1.6± 0.3 (3.1)	1.2± 0.3 (2.3)
PF1908	[Conserved hypothetical protein]	1	1.2± 0.4 (2.2)		1.1± 0.3 (2.2)
PF1956	Fructose-1,6-biphosphate aldolase (53)	0	2.2± 0.3 (4.5)	1.8± 0.3 (3.5)	
[Sugar metabolism]					
PF1959	Phosphoglycerate mutase (55)	0	1.1± 0.2 (2.2)		
PF1960	[Aldose reductase]	0	2.4± 0.8 (5.2)	2.4± 0.6 (5.3)	
[DNA Synthesis]					
PF1971	Anaerobic ribonucleotide reductase (44)	0	1.3± 0.6 (2.5)[d]	1.3± 0.7 (2.4)[d]	

PF1972	[Radical SAM enzyme]	0	2.0± 0.6 (3.9)	1.6± 0.4 (3.0)	
PF1973	[Conserved hypothetical protein]	1	2.1± 0.6 (4.3)	2.5± 0.4 (5.5)	1.8± 0.7 (3.4)
PF1975	[Conserved hypothetical protein]	1			1.5± 0.6 (2.8)
[Metal ion transport]					
PF2036	[Magnesium and cobalt transporter]	2	1.3± 0.3 (2.4)		
PF2037	[Hypothetical protein]	0	1.5± 0.6 (2.8)		

[a]The ORF description is derived either from the annotation [(17): given within brackets], from the indicated reference where there is experimental data to support the ORF assignment specifically in *P. furiosus* (given without brackets), or where a particular ORF is discussed in the text. Potential operons are boxed where the intergenic distances are less than 16 nucleotides.

[b]TMDs refers to the number of predicted transmembrane domains in the protein encoded by that ORF.

[c]The fluorescence intensity ratio (72°C/95°C) for each ORF after the indicated time period (1, 2 or 5 hr), is expressed as a $\log_2$± SD value so that the standard deviation can be given. The fold change in intensity is given in parenthesis. The regulation is statistically significant ($P < 0.01$) for all ORFs unless indicated otherwise.

[d]The statistics for the 5 hr value for PF0324 ($P = 0.061$), the 5 hr value for PF1270 ($P = 0.017$), and the 1 and 2 hr values for PF1971 ($P = 0.025$ and 0.067, respectively) are indicated.

Table 4.2. ORFs whose expression is up-regulated in cells adapted to 72 °C compared to cells adapted to 95 °C.

ORF Number	Description	TMDs	5 hr[a]	Adapted[a]
PF0094	Protein disulfide oxidoreductase (3)	0		1.4± 0.7 (2.7)
PF0101	[Conserved hypothetical protein]	0		2.5± 1.3 (5.5)
PF0190	[Conserved hypothetical protein]	2	1.7± 0.7 (3.2)	2.9± 0.6 (7.4)
PF0286	[Conserved hypothetical protein]	0		1.8± 0.6 (3.5)
PF0296	[Cobalamin biosynthesis protein]	4		1.4± 0.8 (2.7)
PF0297	[Conserved hypothetical protein]	0		1.9± 1.0 (3.6)
PF0298	[Conserved hypothetical protein]	0		1.1± 0.4 (2.2)
PF0318	[Acylaminoacyl releasing enzyme]	0	1.9± 0.7 (3.8)	1.6± 0.6 (3.1)
PF0323	[Conserved hypothetical protein]	1		2.4± 1.3 (5.3)
[Unknown]				
PF0324	[Conserved hypothetical protein]	1	4.6± 2.4 (23.8)[b]	5.8± 2.1 (57.4)
PF0325	[Conserved hypothetical protein]	1	4.4± 1.1 (21.3)	5.3± 2.1 (39.0)
PF0327	[Conserved hypothetical protein]	1		2.4± 1.9 (5.3)
PF0371	[Conserved hypothetical protein]	12		1.4± 0.9 (2.6)
PF0428	[alanyl-tRNA, C-terminus]	0		1.4± 0.7 (2.7)
PF0429	[Putative proline permease]	13		3.9± 0.9 (14.6)
PF0516	[Conserved hypothetical protein]	1		1.6± 0.6 (3.1)
PF0665	[Conserved hypothetical protein]	4		1.6± 0.6 (2.9)
PF0708	[Conserved hypothetical protein]	11		1.5± 0.3 (2.9)
PF0709	[Hypothetical protein]	0		1.9± 0.7 (3.7)
PF0718	[Conserved hypothetical protein]	5		2.0± 0.7 (3.9)
PF0719	[Hypothetical protein]	0		2.5± 1.4 (5.5)
PF0727	[Hypothetical protein]	0		2.1± 0.6 (4.4)

PF0934	[Conserved hypothetical protein]	0	2.5± 0.5 (5.6)	2.8± 0.8 (6.9)
[Branched chain amino acid biosynthesis]				
PF0935	[Acetolactate synthase]	0	2.5± 1.0 (5.6)	3.3± 2.2 (9.9)
PF0936	[Ketol-acid reductoisomerase]	0		2.2± 1.4 (4.5)
PF0943	[Conserved hypothetical protein]	0		2.0± 1.3 (3.9)
PF1025	[Conserved hypothetical protein]	0		2.1± 0.5 (4.2)
PF1062	[Conserved hypothetical protein]	0		2.6± 1.0 (6.2)
[Unknown]				
PF1072	[Conserved hypothetical protein]	0		3.7± 0.6 (12.7)
PF1073	[Conserved hypothetical protein]	4		3.3± 0.8 (9.8)
PF1074	[Conserved hypothetical protein]	0	1.5± 0.6 (2.8)	3.5± 0.8 (11.3)
[Gyrase Modulator]				
PF1076	[tldD protein homolog]	0		2.0± 0.4 (4.1)
PF1077	[Protein interaction modulator]	0		2.4± 0.5 (5.3)
PF1100	[Conserved hypothetical protein]	1		1.8± 0.8 (3.5)
PF1247	[Conserved hypothetical protein]	6		1.5± 0.4 (2.8)
PF1270	[Conserved hypothetical protein]	0	1.9± 0.9 (3.8)[b]	1.9± 0.7 (3.8)
[Unknown]				
PF1344	[maleate *cis-trans* isomerase]	0	1.4± 0.4 (2.6)	1.5± 0.4 (2.8)
PF1345	[Arylsulfatase]	0		1.6± 0.3 (3.0)
PF1346	[Pheromone shutdown protein]	0		1.9± 0.6 (3.7)
PF1347	[Hypothetical protein]	0		1.3± 0.6 (2.5)
PF1408	[Probable dipeptide-binding protein]	1	1.7± 0.7 (3.2)	2.2± 0.5 (4.7)
PF1418	[Conserved hypothetical protein]	0		1.6± 0.7 (2.9)
PF1460	[Conserved hypothetical protein]	0		2.1± 1.2 (4.4)
[Vitamin biosynthesis]				
PF1528	[Imidazoleglycerol Pi synthase]	0		2.4± 1.6 (5.2)
PF1529	[Ethylene-inducible protein homolog]	0		1.8± 0.6 (3.5)
PF1670	[Alkaline serine protease]	1		1.4± 0.9 (2.6)
PF1677	[Conserved hypothetical protein]	6		2.8± 1.4 (6.8)

[Branched chain amino acid biosynthesis]				
PF1678	[2-Isopropylmalate synthase]	0		3.2± 1.1 (9.4)
PF1679	[3-Isopropyl malate dehydratase I]	1		3.1± 1.4 (8.8)
[Aromatic amino acid biosynthesis]				
PF1701	[Chorismate mutase]	0		3.9± 2.3 (14.5)
PF1702	[Aspartate aminotransferase]	0		2.8± 0.9 (7.1)
PF1703	[Prephenate dehydrogenase]	0		3.1± 0.8 (8.5)
PF1711	[Indole-3-glycerol phosphate synthase]	0		1.6± 0.8 (3.0)
PF1767	2-ketoglutarate:Fd oxidoreductase, delta (50)	0	1.8± 0.8 (3.4)	1.5± 0.8 (2.8)
PF1944	[Conserved hypothetical protein]	0		1.9± 0.6 (3.8)
[Tungstoenzyme-4]				
PF1960	[aldehyde/aldose reductase]	0		1.8± 0.8 (3.6)
PF1961	WOR4, W-oxidoreductase (47)	0		1.9± 0.5 (3.8)
PF1973	[Conserved hypothetical protein]	1	1.8± 0.7 (3.4)	1.8± 0.7 (3.6)
PF2032	[Conserved hypothetical protein]	11		1.5± 0.7 (2.9)

[a]See Table 1 and the text for details.

[b]The statistics for the 5 hr values for PF0324 ($P = 0.061$) and PF 1270 ($P = 0.017$) are indicated. For all other ORFs. the P values are < 0.010.

From even a cursory look at Figure 4.3 it is clear that *P. furiosus* has, in fact, three different responses to living at 72°C. Virtually all of the 49 ORFs up-regulated 1 hr post-shock are also among the 35 ORFs up-regulated after 2 hr, but very few of these are included with the 30 ORFs up-regulated at 5 hr post-shock (Figure 4.3A, Table 4.1). Similarly, and most surprisingly, virtually none of the 59 ORFs that are up-regulated in the cold-adapted cells (grown at 72°C) are up-regulated after 1, 2 or even 5 hrs after the temperature is decreased from 95 to 72°C (Figure 4.3B, Table 4.2). It therefore appears that there are both early (1-2 hr) and late cold shock (5 hr) responses, in addition to the cold adaptation response, and that these three cellular responses involve very different proteins. However, these proteins do have some properties in common. As indicated in Figure 4.3, a significant number are of unknown function (the conserved/hypothetical), and/or are adjacent to each other on the *P. furiosus* genome and appear to be encoded by operons (19). For example, of the 59 ORFs that were up-regulated in the cold-adapted experiment, 28 of them are part of 12 potential operons, and of the 72 ORFs up-regulated during both the early and late shock responses, 43 ORFs are part of 14 potential operons. Such apparent co-regulation of adjacent genes tends to support the notion that they have related functions. Moreover, of the 22 total putative cold-responsive operons identified, 9 contain exclusively or predominantly conserved/hypothetical proteins. This is not surprising as the genome sequences of hyperthermophilic archaea available lack homologs to cold shock proteins previously identified in bacteria.

The Early Shock Response. The early cold shock response seen within 1 to 2 hr of shifting to 72°C is characterized by the up-regulation of a large number of conserved/hypothetical proteins (17 of 55) and of ORFs whose products appear to be involved in the translation process, in amino

Figure 4.3.

Summary of ORFs whose expression is up-regulated by A) cold shock and B) by cold adaptation. Panel A is a representation of Table 1 and shows the pattern of ORFs that are up-regulated 1, 2 or 5 hr after cold shock. ORFs that are annotated as conserved/hypothetical proteins are given in blue, and those that are part of potential operons are boxed. Those ORFs up-regulated after 1, 2 or 5 hr after cold shock are in red, where light, medium or dark intensity indicates a more than 2.5-, 3.0- or 4.0-fold increase in expression. Panel B is a representation of Table 2 and shows the pattern of ORFs up-regulated by 5 hr cold shock and by cold adaptation. "Adapt" represents all ORFs up-regulated in cells grown at 72°C, and it is indicated whether the same ORF was also up-regulated after 5 hr after cold shock. ORFs that are annotated as conserved/hypothetical proteins are given in blue. The intensity of the red color represents the same as it does in panel A. The data used for panels A and B are taken directly from Tables 1 and 2, respectively.

A.

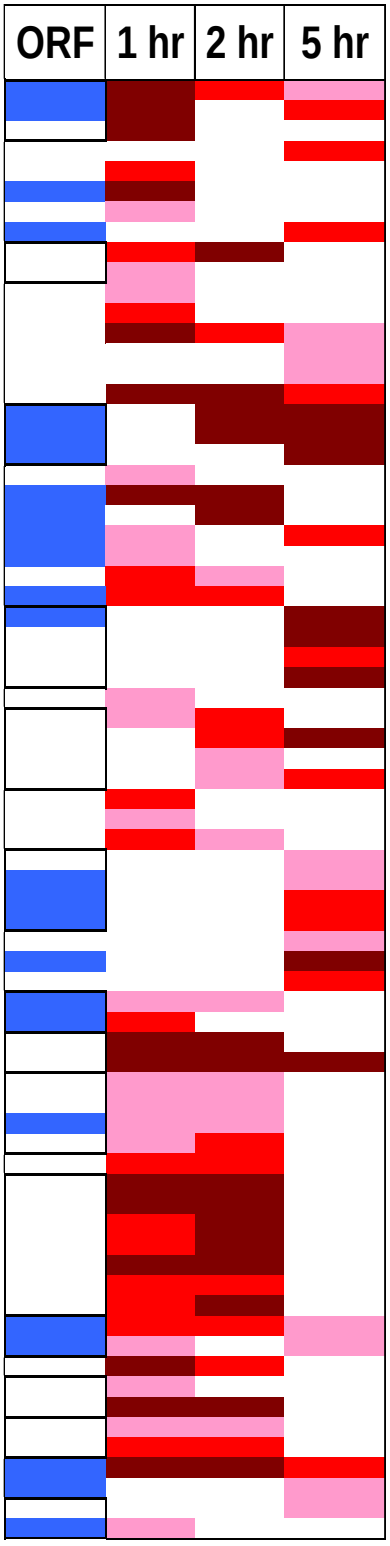

B.

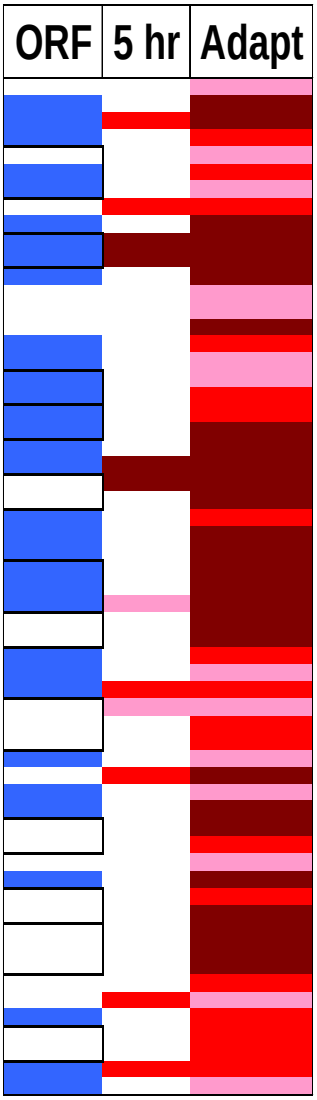

acid and primary carbohydrate metabolism, in oxidoreductase-type reactons, and in solute transport (Table 4.1). Those involved in translation include a histidinyl tRNA synthetase (PF0264), an initiation factor (e-IF2-β, PF0481) and what appears to be an unusual version of an initiation/elongation factor (EF-2-like, PF1137). The *P. furiosus* genome contains homologs of the latter two proteins (PF1349 and PF2012) and these are not affected by the temperature change. *P. furiosus* may therefore possess initiation and elongation factors that are specifically required for and presumably enhance translation at sub-optimal temperatures. There is also tantalizing evidence that DNA biosynthesis may be affected by the temperature decrease. PF1971 encodes anaerobic ribonucleotide reductase and this is up-regulated (2.5 fold) in the early shock response (at 1 and 2 hr). This appears to be coordinately regulated with the adjacent ORF, PF1972, which shows similarity to radical S-adenosylmethionine (SAM) proteins and is up-regulated almost 4-fold. *P. furiosus* also contains a conventional adenosyl-cobalamin-dependent ribonucleotide reductase [PF0440: (44)], the expression of which is downregulated in the adapted cells (by 9.1-fold) although not in cold-shocked cells. Potentially there is a switch to the anaerobic enzyme for DNA synthesis in response to a drop in temperature.

The early response to cold shock also involves modulation of primary carbon metabolism. The two glycolytic enzymes, fructose-1,6-bisphosphate aldolase (PF1956, 4.5-fold, 1 h), and phosphoglycerate mutase (PF1959, 2.2-fold, 1 hr), are both up-regulated (as is a third, glucokinase, PF0312, after 5 hr). What is surprising is that these are not the primary points of regulation in the glycolytic pathway in *P. furiosus* (56), as these are glucose-6-phosphate isomerase (PF0196), phosphofructokinase (PF1784) and glyceraldehyde-3-phosphate oxidoreductase (GAPOR, PF0464). Expression of the latter genes do not change during the shock response, but presumably the cold response requires additional phosphorylated

intermediates and the up-regulated enzymes (PF1956 and PF1959) would otherwise be rate-limiting at 72°C.

Perhaps the most dramatic response in the early phase of the shock response is the up-regulation (≥ 4-fold) of an operon containing seven ORFs (PF1767-1773) that encode two 2-ketoacid, Fd-dependent, oxidoreductases. One is termed 2-ketoglutarate Fd oxidoreductase (KGOR). This preferentially oxidizes 2-ketoglutarate to succinyl CoA and is encoded by four ORFs (PF1767-1770) (38). The remaining three ORFs (PF1771-1773) are proposed to encode an as yet characterized enzyme of this type, XOR, which presumably converts another type of 2-keto-acid to its CoA-derivative. Like the succinyl CoA produced by KGOR, this is presumably utilized for biosynthetic purposes. In support of this notion, KGOR is also up-regulated in peptide-grown cells (49). As shown in Table 4.3, the specific activity of KGOR in cell-free extracts of *P. furiosus* was about 2-fold higher in cells after 2 hr at 72°C, compared to cells grown at 95°C. In contrast, the specific activity of the related enzyme pyruvate Fd oxidoreductase [POR: (31)] was unaffected by the cold response, in accord with the microarray results for its ORFs (data not shown).

The early cold shock response phase is also characterized by an increase in protein degradation, with an up-regulation of the proteosome (PF0115), and an acylaminoacyl-releasing enzyme (AARE; PF0318). Using the assay developed for AARE in a related *Pyrococcus* species (22, 42), the specific activity of AARE increased approximately 3-fold in cell-extracts of cold-shocked *P. furiosus* cells, in agreement with the microarray data (Table 4.3). These proteases could be degrading non-essential proteins or mis-folded essential proteins in the cell upon cold shock to rapidly provide amino acids for protein synthesis. Additional links between carbon and nitrogen metabolism come from the up-regulation of two four-ORF operons, one (PF1535-1538)

Table 4.3. Activities of several key cold-responsive enzymes.

ORF number	Enzyme[a]	Specific Activity[b] (units/mg)			
		95°C (Adapted)	2 hr at 72°C (Shock)	5 hr at 72°C (Shock)	72°C (Adapted)
PF0318	[Aminoacyl releasing enzyme]	0.09± 0.02	0.26± 0.03	0.28± 0.02	0.42± 0.07
PF0935	[Acetolactate synthase]	0.002± 0.001	0.004± 0.001	0.010± 0.001	0.016± 0.003
PF0965-0967, 0971	POR (50)	4.52± 0.40	4.51± 0.04	3.78± 0.39	5.06± 0.42
PF1767-1770	KGOR (50)	0.15± 0.01	0.28± 0.01	0.12± 0.00	0.13± 0.03

[a]Abbreviations: POR, pyruvate Fd oxidoreductase; KGOR, 2-ketoglutarate Fd oxidoreductase.

[b]Units are defined as μmole product formed per min per mg of protein in cell-free extracts of *P. furiosus* cells grown under the indicated conditions. Assays were conducted as described in the Methods section.

encoding a sugar phosphorylase and an amidotransferase, and one (PF0204-0205) encoding a Fd-dependent glutamate synthase. A three-ORF operon (PF0029-0031) encoding a putative threonine synthase is also up-regulated within 1 hr (Table 4.1), although its function is unclear as the canonical threonine/serine biosynthetic pathway (PF1053-1056) is subsequently up-regulated in the 2 – 5 hr time frame.

Other ORFs up-regulated in the early shock response fall into the categories of membrane transporters (PF0262, PF1654 and PF2036) and oxidoreductase-type proteins (PF0094, PF0276, PF1480 and PF1960). PF2036 is a CorA homolog and likely transports magnesium ions, but the solutes bound by the other proteins are not known. The oxidoreductase-type proteins include protein disulfide oxidoreductase [PF0094: (43)] which may facilitate protein folding at the lower temperature, and PF1480, which is proposed to encode the fifth and only uncharacterized member of the so-called AOR family of tungsten-containing, Fd-dependent oxidoreductases found in *P. furiosus* (46). The other members of the family are the glycolytic enzyme GAPOR [PF0464: (41)], aldehyde Fd oxidoreductase [AOR, PF0346; (8)], formaldehyde Fd oxidoreductase [FOR, PF1203; (47)], and aldehyde Fd oxidoreductase-4 [WOR-4, PF1961; (46)], none of which are regulated by the cold (data not shown). This fifth member, aldehyde Fd oxidoreductase-5 (WOR-5, PF1480) appears to be involved in the early cold shock response. Moreover, for the first time, a partner protein is implicated for a member of the AOR family. The adjacent, co-regulated ORF, PF1479, encodes a protein that contains 16 cysteine residues, many as motifs that could bind multiple iron-sulfur clusters. This suggests a role in electron transfer, although the biochemical function of the cold-induced WOR-5 system is obviously unknown.

The Late Shock Response. The expression of virtually all of the annotated ORFs discussed above return to near their pre-shock levels at the end of the acclimation phase, or by 5 hr after the switch to 72°C. The notable exceptions are the putative tungstoprotein WOR5 (PF1480) and AARE (PF0318), as well as several ORFs encoding conserved hypothetical proteins (PF0029, PF0030, PF0721, PF1907, PF1908, PF1973). In contrast, the late cold shock response (5 hr) is characterized by the up-regulation of multiple ORFs involved in the biosynthesis of branched chain amino acids (PF0934-PF940) and methionine (PF1266-PF1270), none of which are up-regulated even after 2 hr, and of the operon involved in serine/threonine biosynthesis (PF1053-1056; partially up-regulated after 2 hr). The up-regulation of one of the ORFs involved in the biosynthesis of branched chain amino acids, PF0935, which encodes acetolactate synthase, was investigated using an enzymatic assay. As shown in Table 4.3, the specific activity increased 5-fold after 5 hr post-shock, in agreement with the microarray data. Other ORFs up-regulated after 5 hr (but not 2 hr) are annotated to encode DNA helicase (PF0085), pyrophosphatase (PF0295), and a dipeptide-binding protein (PF1408), although a precise role of each is not clear. Several conserved hypothetical proteins (PF0190, PF1348) are also up-regulated only after 5 hr. Indeed, an operon (PF0324-PF0326) encoding three conserved/hypothetical proteins is the most dramatically up-regulated of all ORFs involved in the late cold shock response (Table 4.1). The main response at 5 hr after the cold shock therefore seems to be an increase in the biosynthesis of certain amino acids that utilize the activated C-3 and C-4 intermediates generated in the first two hours from the primary carbon source maltose, as well as the up-regulation of a number of proteins of unknown function.

The Cold Growth or Adapted Response. As shown in Table 4.2 and Figure 4.3B, very few of the ORFs that are up-regulated during the late cold-shock response (after 5 hr) remain so once the cells are fully adapted to the growth at the lower temperature (after many generation times) when grown continuously at 72°C. Thus, the complete switch to the expression levels of the adapted state must take place much later than what appears to be the end of the acclimation phase as judged by the growth curve (Figure 4.1). Additional experiments will be required to ascertain when the acclimation phase is complete at the transcriptional level. The few annotated ORFs that are up-regulated in both late shock (5 hrs) and in the adapted cells include those encoding AARE (PF0318) and acetolactate synthase (PF0935). As shown in Table 4.3, the specific activities of both enzymes are at least 5-fold higher in the adapted cells, while the value for KGOR is not affected by adaptation to 72°C, results that are consistent with the array data. On the other hand, there are a number of ORFs encoding conserved/hypothetical proteins that are up-regulated in the late-shock phase that either remain at a similar level in the adapted cells (PF0934, PF1270, PF1973) or increase even further (PF0190, PF1074). The latter include two adjacent ORFs (PF0324, PF0325) up-regulated by > 20-fold after 5 hr and by > 39-fold in the adapted cells. Indeed, the response of the adapted cells is dominated by conserved/hypothetical proteins with 34 of 59 up-regulated ORFs falling in this category. There are also a significant number of ORFs encoding proteins predicted to contain transmembrane domains (21/59, see Table 4.2). It should be noted that while no conclusions can be drawn about the function of conserved/hypothetical proteins, several of the annotated ORFs are only given general, non-descriptive names (Table 4.2). For example, the 3-ORF operon (PF1344-PF1346) that is up-regulated encodes a putative Asp/Glu racemase, a lactamase-type esterase and a regulatory protein, but these descriptions shed no light on its biological role in *P. furiosus*.

On the other hand, some function can be assigned to many of the up-regulated ORFs that are annotated. In fact, the adaptation to growth at 72°C seems to involve many of the same processes as the early and late shock responses, but different proteins are involved. This includes ORFs involved in aromatic amino acid biosynthesis (PF1701-PF1703), carbohydrate metabolism (aldose reductase, PF1960), proteolysis (serine protease, PF1670), transport (PF0371, PF0429, PF1408), and protein synthesis (amino acyl tRNA synthetase; PF0428). One of the most interesting examples of the same theme but different proteins concerns tungsten. The dramatic up-regulation of aldehyde Fd oxidoreductase-5 (WOR-5, PF1480) seen in the shock response is not seen in the adapted response. Rather, aldehyde Fd oxidoreductase-4 (WOR-4, PF1961) is up-regulated in the adapted response. WOR-4 is known to be expressed at a significant level in cells grown at 95°C (46) and why it should be up-regulated in cold-adapted cells (perhaps replacing WOR-5), is not at all clear.

There are also ORFs encoding new processes that are up-regulated in adapted cells. These include proteins involved in vitamin biosynthesis (pyridoxine (B6), PF1528-1529; and cobalamin, PF0296), and in regulating DNA gyrase activity [PF1076, PF1077: (2, 39)]. The latter is particularly intriguing as an enzyme known as reverse gyrase is the only enzyme unique to hyperthermophiles (both archaea and bacteria). It is the only topoisomerase that positively supercoils DNA and is thought to be essential to life at extreme temperatures (12). The notion that "less supercoiling" is needed at sub-optimal growth temperatures and a specific inhibitor of the gyrase is required would support that idea. In support of this, studies in other hyperthermophilic archaea have shown that there was a change in DNA topology in response to sub-optimal growth temperatures, with an increase in negative supercoiling (35-37).

Changes in the proteome content of membranes. In order to assess changes in the proteome, rather than the transcriptome, cytoplasmic and membrane fractions were prepared from *P. furiosus* cells obtained in the early and late shock responses, as well as in the adapted response, and these were analyzed by SDS-PAGE. Although no consistent changes were observed in the protein profiles of the cytoplasmic extracts (data not shown), two major cold-induced proteins were readily evident in the membrane fractions of cold-shocked cells. Moreover, both appeared to increase in concentration throughout the shock phase and to accumulate to high concentrations in the adapted cells (Fig 4.4). These two proteins were given the names CipA and CipB (for Cold Induced Protein) and using MALDI-TOF MS analysis of the bands after in-gel trypsin digestion, were identified as PF0190 (a conserved hypothetical protein) and PF1408 (annotated as a probable dipeptide-binding protein), respectively. As shown in Table 4.2, PF0190 is up-regulated by 3.2- and 7.4-fold, and PF1408 is up-regulated 3.2- and 4.7-fold, after 5 hr post-shock and in the adapted cells, respectively, which is generally consistent with the amount of protein seen on the SDS-gels. In order to validate the results from the DNA microarray data, quantitative real-time PCR (qPCR) was used to assess the expression of PF0190 and PF1408. The RNA preparations examined were the same as those used for the arrays. The qPCR analyses showed that PF0190 and PF1408 were up-regulated in 72°C-adapted cells, relative to those grown at 95°C, by factors of 26.0± 9.3 and 5.8± 1.8, respectively. These data compare well with the values from the arrays (Table 4.2).

Cytoplasmic and membrane fractions from cells grown at either 95 or 72°C were also subjected after initial separation by SDS-PAGE to a glycoprotein stain, which detects carbohydrate groups that can be oxidized by periodate. With the cytosolic fractions, there was no clear staining of any bands, and there were no differences between the two cell types,

Figure 4.4.

SDS-PAGE analysis of membrane fractions of cold-shocked and cold-adapted cells. SDS-PAGE analysis (15%) of the salt-washed (4.0 M NaCl) membrane fractions of *P. furiosus* cells grown at various temperatures: 1, 95°C; 2 – 4, 72°C (from three different cultures grown independently); 5, grown at 95°C and then shocked at 72°C for 2 hr; 6, grown at 95°C and then shocked at 72°C for 5 hr; 7, 95°C; M are molecular weight markers. Lanes 1-7 each contained 7 μg of protein. The positions of the bands representing CipA and CipB are indicated.

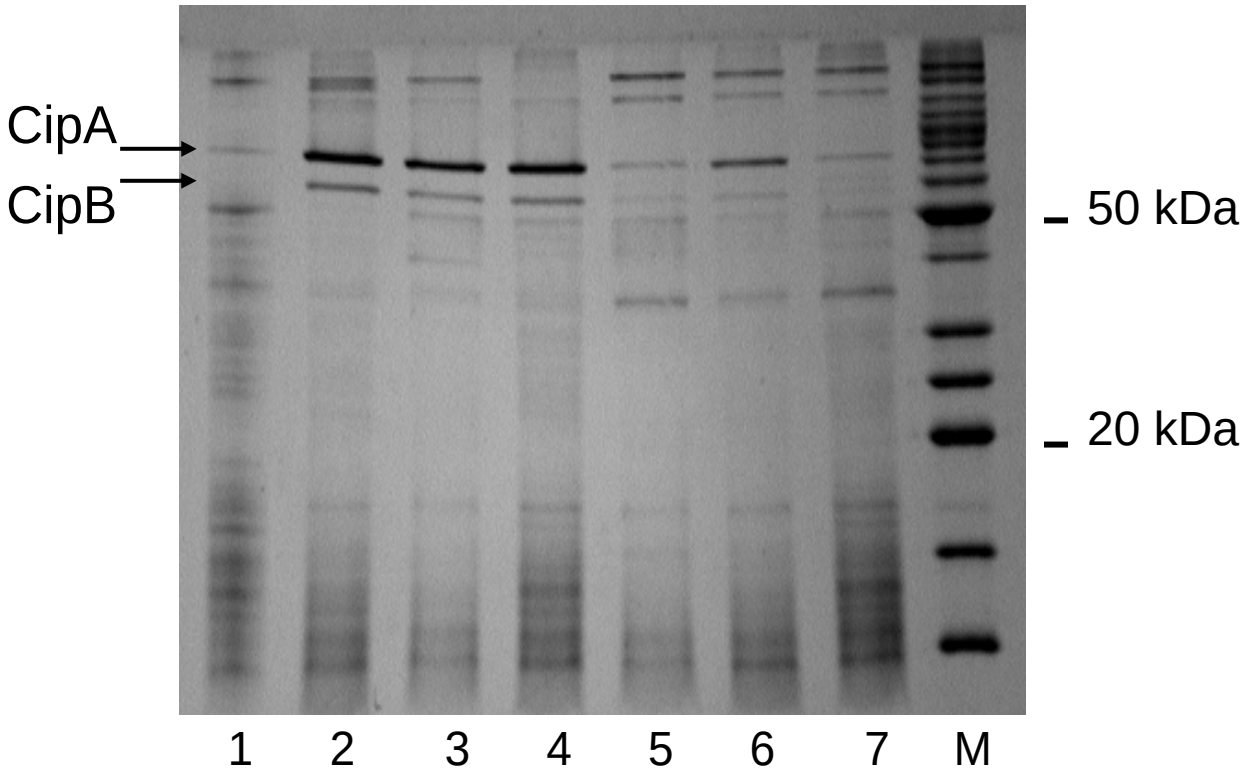
CipA
CipB
50 kDa
20 kDa
1
2
3
4
5
6
7
M

indicating that there are few if any glycoproteins in the cytosol of *P. furiosus* grown at either temperature. However, the membrane fractions gave dramatically different results. First, as shown in Fig. 4.5B, the membrane fraction from cells grown at 95°C showed five major glycoproteins with apparent masses of 18, 35, 52, 75 and 100 kDa. Second, in the cold-adapted cells, the lower molecular weight proteins (18, 35 and 52 kDa) decreased in intensity, the 100 kDa band remained the same, while the band at 75 kDa dramatically increased in intensity and a new band appeared near 65 kDa. The bands near 65 and 75 kDa were cut out of the gel, subjected to in gel trypsin digestion, analyzed by MALDI-TOF MS, and were identified as CipA (PF0190) and CipB (PF1408), respectively. Thus, the two major proteins induced by cold shock and adaptation in the membranes of *P. furiosus* are glycoproteins. Attempts to identify the 14, 40, 50 and 100 kDa glycoproteins by tryptic/MS analyses have so far been unsuccessful**.** Despite the apparent increase in glycoprotein content according to SDS-PAGE, the overall glycoprotein content of the membrane fractions of cells grown at 95 and 72°C remains virtually the same by the periodate-detection method.

CipA (PF0190) and CipB (PF1408) are large proteins (94.7 and 79.3 kDa, respectively) and both are predicted to be membrane-associated with transmembrane domains and signal sequences, consistent with biochemical data. CipB (PF1408) is annotated as a dipeptide binding protein and by the InterPro (18) analysis belongs to the solute-binding protein family (IPR000914). Although CipA is annotated as a conserved hypothetical protein and is 'null' by the InterPro analysis, by BLAST analysis it is also appears to be a member of the same solute-binding protein family, showing 10% identity (22% similarity) to CipB. Interestingly, CipA and CipB are each upstream of a cluster of four ORFs (PF0191-PF0194 for CipA, and PF1409-

Figure 4.5.

SDS-PAGE analysis of membrane fractions of cold-adapted cells stained for carbohydrates. SDS-PAGE analysis (15%) of the salt-washed (4.0 M NaCl) membrane fractions of *P. furiosus* cells grown at the indicated temperature (72 or 95°C, where M is marker proteins). The gel were stained for protein (with Coomassie Brilliant Blue, *left*) or for carbohydrate (with Emerald 300 Q glycoprotein stain, *right*). The arrows indicate the positions of the bands representing CipA (*upper*) and CipB (*lower*).

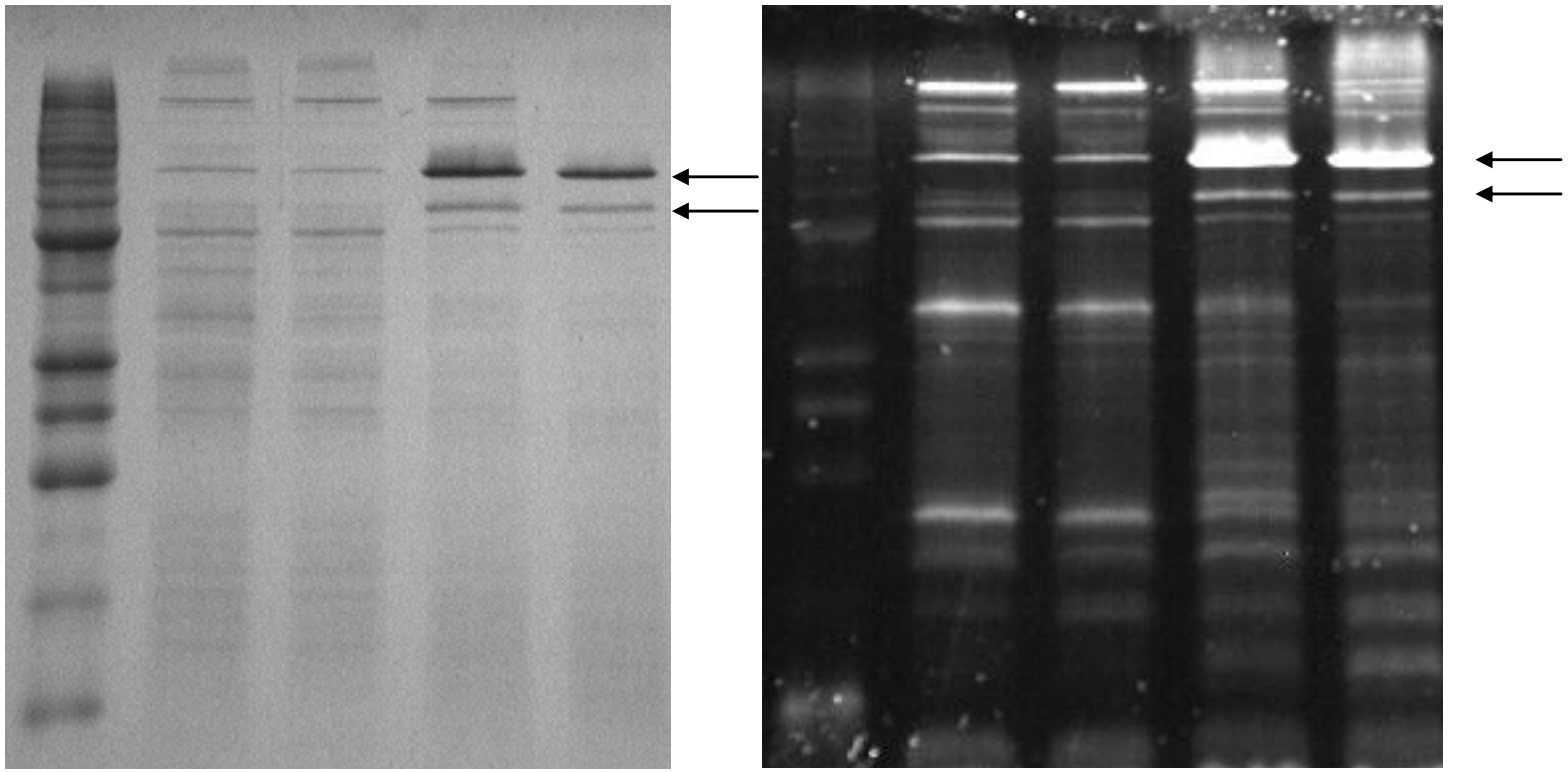
M
95°
95°
72°
72°
M
95°
95°
72°
72°

PF1412 for CipB). The two nearest ORFs in each cluster are annotated as dipeptide transport system permease proteins, while the more distant two ORFs are annotated as dipeptide transport ATP binding proteins (Fig. 4.6). While the Cip ORFs and their adjacent four-ORF clusters clearly encode an ABC-type transporter system, the microarray data indicate that of all 10 ORFs, only CipA and CipB are up-regulated in response to the cold stress. In fact, all of the other ORFs in these clusters are actually down-regulated in response to cold stress (up to 6.7-fold).

The oligopeptide-binding protein OppA of *Listeria monocytogenes* is also included in the same solute-binding family as CipB (12% identity, 23% similarity). Interestingly, OppA was recently shown to be up-regulated in response to cold shock (5). Moreover, it and the two Cip proteins are part of the same gene arrangement, where the solute binding protein (OppA, PF0190 or PF1408) is located far upstream (100-300 nts) of a 4-ORF cluster that encodes two permeases and two ATP-binding proteins (Figure 4.6). The two 4-ORF clusters in *P. furiosus* show much higher sequence similarity to their corresponding partners in *L. monocytogenes* than do CipA and CipB to OppA. For example, for PF0191-PF0194 the sequence similarities range from 33 to 59% (19-44% identity). In addition, not only is OppA required for growth of *L. monocytogenes* at sub-optimal growth temperatures (5°C), it is expressed using its own promoter and is not co-expressed with the rest of the operon (5), as seems to be the case with CipA and CipB of *P. furiosus.* Similar operons are found in *Bacillus subtilis*, *Salmonella typhimurium* and *Streptococcus pyogenes* (Figure 4.6).

Interestingly, expression of the Cip homolog in *B. subtilis* was not affected at 18°C (28), although a lower temperature might be required as up-regulation of the expression of OppA was seen after cold shock at 4°C in *L. monocytogenes.* The cold-responsive relationship between CipA and CipB of *P. furiosus* and OppA of *L. monocytogenes* is extremely significant because it

Figure 4.6.

Genome organization for CipA and CipB gene clusters. The arrangement of CipA and CipB with respect to downstream genes is indicated. The arrangement of analogous gene clusters in *Listeria monocytogenes* (Lmo2196-2192), *Bacillus subtilis* (Bsu1144-1148), *Streptococcus pyogenes* (SPs0221-0225) and *Salmonella typhimurium* (STM1746-1742) are shown for comparison. The ORFs and intergenic distances are drawn approximately to scale (the bar indicates 100 nts). The information on the bacterial genes was modified from ref. 5 and the sequences were taken from ref. 19.

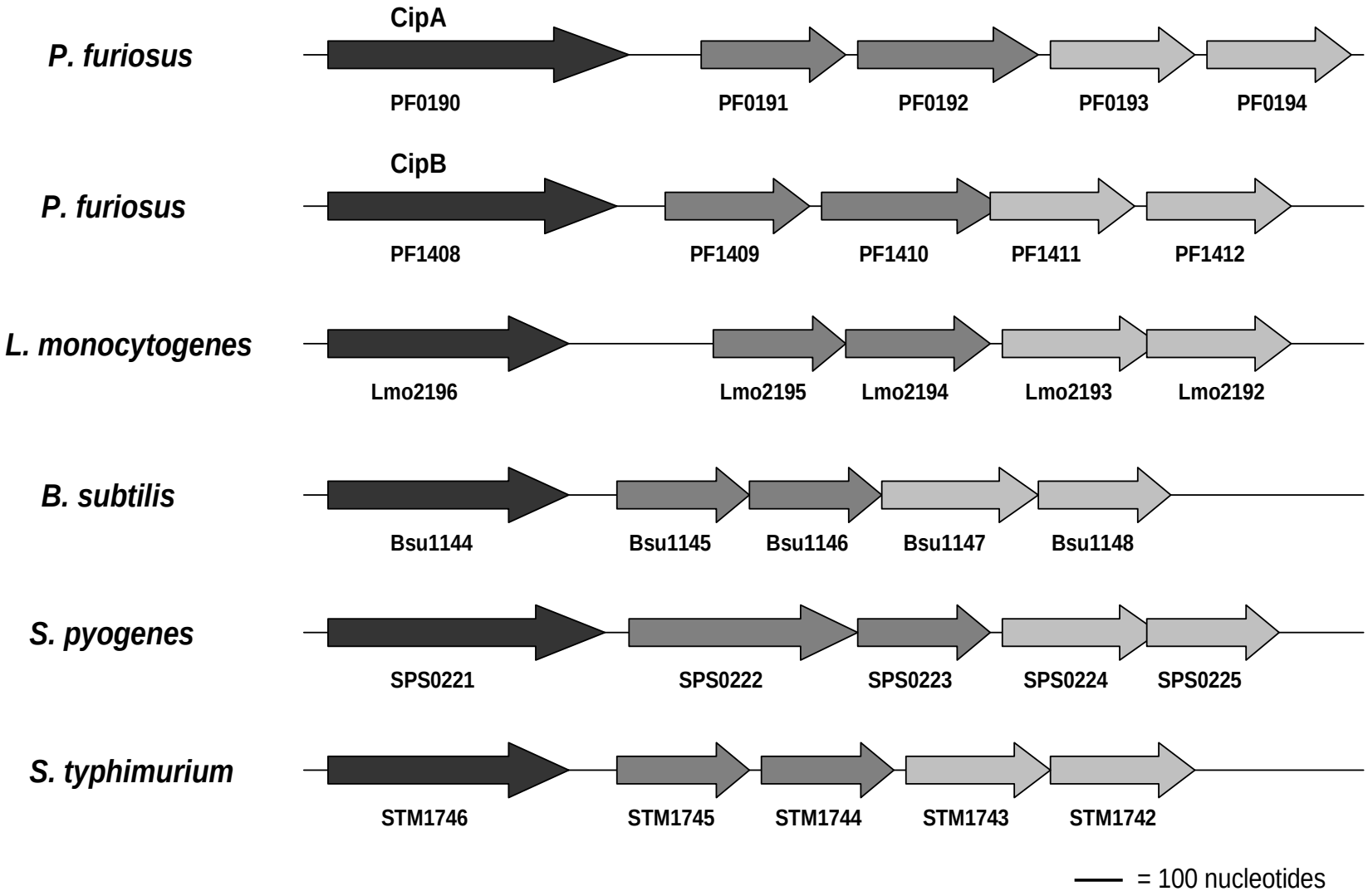
CipA
P. furiosus
PF0190
PF0191
PF0192
PF0193
PF0194
CipB
P. furiosus
PF1408
PF1409
PF1410
PF1411
PF1412
L. monocytogenes
Lmo2196
Lmo2195
Lmo2194
Lmo2193
Lmo2192
B. subtilis
Bsu1144
Bsu1145
Bsu1146
Bsu1147
Bsu1148
S. pyogenes
SPS0221
SPS0222
SPS0223
SPS0224
SPS0225
S. typhimurium
STM1746
STM1745
STM1744
STM1743
STM1742
= 100 nucleotides

Figure 4.7.

Phylogeny of CipA and CipB. CipA (PF0190) and CipB (PF1408) are shown in boxes. Genes from bacterial sources are underlined while all others are from archaea. Genes that are homologs of CipA (bold type), CipB (plain) and OppA (underlined) are so indicated. The bar indicates a branch length equivalent of 0.1 changes per amino acid and bootstrap values greater than 50% are indicated at the appropriate branch points. The abbreviations are: AF, *Archaeoglobus fulgidus*; APE, *Aeropyrum pernix*; Bsu, *Bacillus subtilis*; DVU, *Desulfovibrio vulgaris*; lmo, *Listeria monocytogenes*; MA, *Methanosarcina acetivorans*; MM, *Methanosarcina mazei*; PAB, *Pyrococcus abysii*; PAE, *Pyrobaculum aerophylum*; PH, *Pyroccous horikoshii*; PF, *Pyrococcus furiosus*; PM, *Pasteurella multocida;* SAG, *Streptococcus agalactiae;* SPs, *Streptococcus pyogenes*; SSO, *Sulfolobus solfataricus*; ST, *Sulfolobus tokodaii*; STM, *Salmonella typhimurium*; and TM, *Thermotoga maritima.*

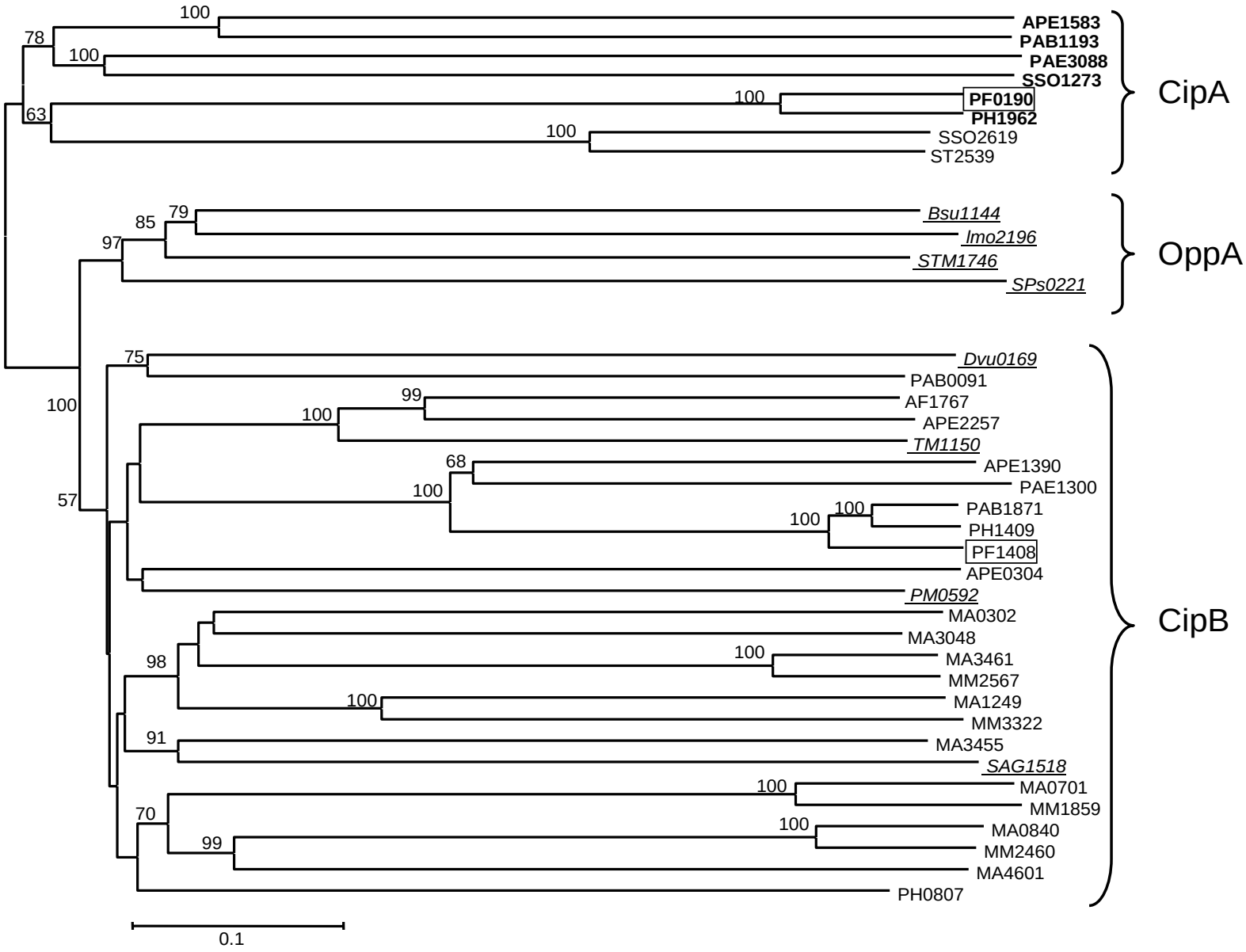
APE1583
PAB1193
PAE3088
SSO1273
PF0190
PH1962
SSO2619
ST2539
CipA
Bsu1144
lmo2196
STM1746
SPs0221
OppA
Dvu0169
PAB0091
AF1767
APE2257
TM1150
APE1390
PAE1300
PAB1871
PH1409
PF1408
APE0304
PM0592
MA0302
MA3048
MA3461
MM2567
MA1249
MM3322
MA3455
SAG1518
MA0701
MM1859
MA0840
MM2460
MA4601
PH0807
CipB
0.1

is the first definitive overlap between the hyperthermophilic archaeal and bacterial cold shock response. None of the previously defined bacterial cold shock proteins, such as the CspA family, CsdA, or RbfA, are present in the genomes of any sequenced hyperthermophilic archaea. The phylogenetic relationship between CipA, CipB and OppA are shown in Figure 4.7. Close homologs CipA and CipB are present throughout the archaea, although CipB seems to be absent from methanogens and the CipB homologs in *Sulfolobus* species seem to be more closely related to their CipA homologs. On the other hand, the OppA protein family is found only in the bacterial domain and they encompass well over a hundred sequences in the database (only a representative sample is shown in Figure 4.7). However, four of these are more closely related to the CipB proteins than they are to OppA, including that of the hyperthermophilic bacterium, *Thermotoga maritima* (Figure 4.7).

The hyperthermophilic archaea therefore appear to utilize, at least in part, the same types of proteins to respond to a drop in temperature from 95 to 72°C that bacteria, at least represented by *L. monocytogenes,* use when the growth temperature drops from 30 to 5°C. Other than these solute-binding proteins, however, the archaeal response, or responses in the case of *P. furiosus*, is clearly very different from that previously seen in any bacterium. Although the present work does not provide insight into specific mechanisms of how the organism deals with cold stress, the results do establish that there are three distinct responses, and for each provides a framework for future studies. These are currently directed towards the characterization of the novel cold-responsive glycoproteins and of key proteins involved in the other responses, in particular those involving carbohydrate and amino acid metabolism, translation and replication, and the intriguing role of tungsten.

Acknowledgements

This research was funded by grants from the National Institutes of Health (GM 60329), the National Science Foundation (MCB 0129841 and BES-0317911) and the Department of Energy (FG05-95ER20175). We thank Frank E. Jenney, Jr. for many helpful discussions and Farris Poole for bioinformatic analyses.

REFERENCES

1. **Adams, M. W. W., J. F. Holden, A. L. Menon, G. J. Schut, A. M. Grunden, C. Hou, A. M. Hutchins, F. E. Jenney, C. Kim, K. S. Ma, G. L. Pan, R. Roy, R. Sapra, S. V. Story, and M. F. J. M. Verhagen.** 2001. Key role for sulfur in peptide metabolism and in regulation of three hydrogenases in the hyperthermophilic archaeon *Pyrococcus furiosus*. J. Bacteriol. **183:**716-724.

2. **Allali, N., H. Afif, M. Couturier, and L. Van Melderen.** 2002. The highly conserved TldD and TldE proteins of *Escherichia coli* are involved in microcin B17 processing and in CcdA degradation. J. Bacteriol. **184:**3224-3231.

3. **Bartolucci, S., D. De Pascale, and M. Rossi.** 2001. Protein disulfide oxidoreductase from *Pyrococcus furiosus*: Biochemical properties. Methods Enzymol **334:**62-73.

4. **Beran, R. K., and R. W. Simons.** 2001. Cold-temperature induction of *Escherichia coli* polynucleotide phosphorylase occurs by reversal of its autoregulation. Mol. Microbiol. **39:**112-125.

5. **Borezee, E., E. Pellegrini, and P. Berche.** 2000. OppA of *Listeria monocytogenes*, an oligopeptide-binding protein required for bacterial growth at low temperature and involved in intracellular survival. Infect. Immun. **68:**7069-7077.

6. **Bradford, M. M.** 1976. Rapid and sensitive method for quantitation of microgram quantities of protein utilizing principle of protein-dye binding. Anal. Biochem. **72:**248-254.

7. **Caldas, T., S. Laalami, and G. Richarme.** 2000. Chaperone properties of bacterial elongation factor EF-G and initiation factor IF2. J. Biol. Chem. **275:**855-860.

8. **Chan, M. K., S. Mukund, A. Kletzin, M. W. W. Adams, and D. C. Rees.** 1995. Structure of a Hyperthermophilic Tungstopterin Enzyme, Aldehyde Ferredoxin Oxidoreductase. Science **267:**1463-1469.

9. **Ermolenko DN, M. G.** 2002. Bacterial cold-shock proteins. Cell Mol Life Sci **59:**1902-13.

10. **Felsenstein, J.** 1996. Inferring phylogenies from protein sequences by parsimony, distance and likelihood methods. Methods Enzymol. **266:**418-427.

11. **Fiala, G., and K. O. Stetter.** 1986. *Pyrococcus furiosus* sp-nov represents a novel genus of marine heterotrophic archaebacteria growing optimally at 100 ^{o}C. Arch. Microbiol. **145:**56-61.

12. **Forterre, P.** 2002. A hot story from comparative genomics: reverse gyrase is the only hyperthermophile-specific protein. Trends Genet. **18:**236-238.

13. **Gualerzi, C. O., A. Maria Giuliodori, and C. L. Pon.** 2003. Transcriptional and posttranscriptional control of cold shock genes. J. Mol. Biol. **331:**527-39.

14. **Hoaki, T., M. Nishijima, M. Kato, K. Adachi, S. Mizobuchi, N. Hanzawa, and T. Maruyama.** 1994. Growth Requirements of Hyperthermophilic Sulfur-Dependent Heterotrophic Archaea Isolated from a Shallow Submarine Geothermal System with Reference to Their Essential Amino-Acids. Appl. Environ. Microbiol. **60:**2898-2904.

15. **Holden, J. F., F. L. Poole, S. L. Tollaksen, C. S. Giometti, H. Lim, J. R. Yates, and M. W. W. Adams.** 2001. Identification of membrane proteins in the hyperthermophilic archaeon *Pyrococcus furiosus* using proteomics and prediction programs. Comp. Funct. Genom. **2:**275-288.

16. **Holm, S.** 1979. A simple sequentially rejective multiple test procedure. Scand. J. Statist. **6:**65-70.

17. **http://comb5-156.umbi.umd.edu/genemate/:.**

18. **http://www.ebi.ac.uk/interpro/.**

19. **http://www.tigr.org.**

20. **Ideno, A., and T. Maruyama.** 2002. Expression of long- and short-type FK506 binding proteins in hyperthermophilic archaea. Gene **292:**57-63.

21. **Ideno, A., T. Yoshida, T. Iida, M. Furutani, and T. Maruyama.** 2001. FK506-binding protein of the hyperthermophilic archaeum, *Thermococcus* sp. KS-1, a cold-shock-inducible peptidyl-prolyl cis-trans isomerase with activities to trap and refold denatured proteins. Biochem. J. **357 (Pt 2):**465-471.

22. **Ishikawa, K., H. Ishida, Y. Koyama, Y. Kawarabayasi, J. Kawahara, E. Matsui, and I. Matsui.** 1998. Acylamino acid-releasing enzyme from the thermophilic archaeon *Pyrococcus horikoshii*. J. Biol. Chem. **273:**17726-17731.

23. **Jenney, F. E., M. F. J. M. Verhagen, X. Y. Cui, and M. W. W. Adams.** 1999. Anaerobic microbes: Oxygen detoxification without superoxide dismutase. Science. **286:**306-309.

24. **Jiang, W. N., Y. Hou, and M. Inouye.** 1997. CspA, the major cold-shock protein of *Escherichia coli*, is an RNA chaperone. J. Biol. Chem. **272:**196-202.

25. **Jones, P. G., and M. Inouye.** 1996. RbfA, a 30S ribosomal binding factor, is a cold-shock protein whose absence triggers the cold-shock response. Mol. Microbiol. **21:**1207-1218.

26. **Jones, P. G., M. Mitta, Y. Kim, W. Jiang, and M. Inouye.** 1996. Cold shock induces a major ribosomal-associated protein that unwinds double-stranded RNA in *Escherichia coli.* Proc. Natl. Acad. Sci. USA. **93:**76-80.

27. **Jones, P. G., R. A. Vanbogelen, and F. C. Neidhardt.** 1987. Induction of proteins in response to low temperature in *Escherichia coli*. J. Bacteriol. **169:**2092-2095.

28. **Kaan, T., G. Homuth, U. Mader, J. Bandow, and T. Schweder.** 2002. Genome-wide transcriptional prfiling of the *Bacillus subtilis* cold-shock response. Microbiology **148:**3441-3455.

29. **Kelly, R. M., and M. W. W. Adams.** 1994. Metabolism in Hyperthermophilic Microorganisms. Antonie Van Leeuwenhoek **66:**247-270.

30. **Kengen, S. W. M., J. E. Tuininga, F. A. M. deBok, A. J. M. Stams, and W. M. deVos.** 1995. Purification and characterization of a novel ADP-dependent glucokinase from the hyperthermophilic Archaeon *Pyrococcus furiosus*. J. Biol. Chem. **270:**30453-30457.

31. **Kletzin, A., and M. W. W. Adams.** 1996. Molecular and phylogenetic characterization of pyruvate and 2-ketoisovalerate ferredoxin oxidoreductases from Pyrococcus furiosus and pyruvate ferredoxin oxidoreductase from Thermotoga maritima. J. Bacteriol. **178:**248-257.

32. **Kumar, S., K. Tamura, and M. Nei.** 2004. MEGA3: Integrated software for molecular evolutionary genetics analysis and sequence alignment. Briefings in Bioinformatics **(In press)**.

33. **Laemmli, U. K.** 1970. Cleavage of structural proteins during assembly of head of bacteriophage-T4. Nature. **227:**680-&.

34. **Lim, J., T. Thomas, and R. Cavicchioli.** 2000. Low temperature regulated DEAD-box RNA helicase from the Antarctic archaeon, *Methanococcoides burtonii*. J. Mol. Biol. **297:**553-567.

35. **Lopez-Garcia, P., and P. Forterre.** 1999. Control of DNA topology during thermal stress in hyperthermophilic archaea: DNA topoisomerase levels, activities and induced thermotolerance during heat and cold shock in *Sulfolobus*. Mol. Microbiol. **33:**766-777.

36. **Lopez-Garcia, P., and P. Forterre.** 2000. DNA topology and the thermal stress response, a tale from mesophiles and hyperthermophiles. Bioessays. **22:**738-746.

37. **Lopez-Garcia, P., and P. Forterre.** 1997. DNA topology in hyperthermophilic archaea: reference states and their variation with growth phase, growth temperature, and temperature stresses. Mol. Microbiol **23:**1267-1269.

38. **Mai, X. H., and M. W. W. Adams.** 1996. Characterization of a fourth type of 2-keto acid-oxidizing enzyme from a hyperthermophilic archaeon: 2-ketoglutarate ferredoxin oxidoreductase from *Thermococcus litoralis*. J. Bacteriol. **178:**5890-5896.

39. **Maruyama, T., and M. Furutani.** 2000. Archaeal peptidyl prolyl cis-trans isomerases (PPIases). Front. Biosci. **5:**D821-836.

40. **Moll, I., S. Grill, A. Grundling, and U. Blasi.** 2002. Effects of ribosomal proteins S1, S2 and the DeaD/CsdA DEAD-box helicase on translation of leaderless and canonical mRNAs in *Escherichia coli*. Mol. Microbiol. **44:**1387-1396.

41. **Mukund, S., and M. W. W. Adams.** 1995. Glyceraldehyde-3-phosphate ferredoxin oxidoreductase, a novel tungsten-containing enzyme with a potential glycolytic role in the hyperthermophilic archaeon *Pyrococcus furiosus*. J. Biol. Chem. **270:**8389-8392.

42. **Onoe, S., S. Ando, M. Ataka, and K. Ishikawa.** 2002. Active site of deblocking aminopeptidase from *Pyrococcus horikoshii*. Biochem. Biophys. Res. Comm. **290:**994-997.

43. **Ren, B., G. Tibbelin, D. de Pascale, M. Rossi, S. Bartolucci, and R. Ladenstein.** 1998. A protein disulfide oxidoreductase from the archaeon Pyrococcus furiosus contains two thioredoxin fold units. Nat. Struct. Biol. **5:**602-611.

44. **Riera, J., F. T. Robb, R. Weiss, and M. Fontecave.** 1997. Ribonucleotide reductase in the archaeon *Pyrococcus furiosus*: a critical enzyme in the evolution of DNA genomes? Proc. Natl. Acad. Sci. U S A **94:**475-8.

45. **Robb, F. T., D. L. Maeder, J. R. Brown, J. DiRuggiero, M. D. Stump, R. K. Yeh, R. B. Weiss, and D. M. Dunn.** 2001. Genomic sequence of hyperthermophile, *Pyrococcus furiosus*: Implications for physiology and enzymology. Methods Enzymol. **330:**134-157.

46. **Roy, R., and M. W. W. Adams.** 2002. Characterization of a fourth tungsten-containing enzyme from the hyperthermophilic archaeon Pyrococcus furiosus. J. Bacteriol. **184:**6952-6956.

47. **Roy, R., S. Mukund, G. J. Schut, D. M. Dunn, R. Weiss, and M. W. W. Adams.** 1999. Purification and molecular characterization of the tungsten-containing formaldehyde ferredoxin oxidoreductase from the hyperthermophilic archaean *Pyrococcus furiosus*: The third of a putative five-member tungstoenzyme family. J. Bacteriol. **181:**1171-1180.

48. **Saitou, N., and M. Nei.** 1987. The Neighbor-Joining Method - a New Method for Reconstructing Phylogenetic Trees. Mol. Biol. Evol. **4:**406-425.

49. **Schut, G. J., S. D. Brehm, S. Datta, and M. W. W. Adams.** 2003. Whole-genome DNA microarray analysis of a hyperthermophile and an archaeon: *Pyrococcus furiosus* grown on carbohydrates or peptides. J. Bacteriol. **185:**3935-47.

50. **Schut, G. J., A. L. Menon, and M. W. W. Adams.** 2001. 2-keto acid oxidoreductases from *Pyrococcus furiosus* and *Thermococcus litoralis*. Methods Enzymol. **331:**144-158.

51. **Schut, G. J., J. Z. Zhou, and M. W. W. Adams.** 2001. DNA microarray analysis of the hyperthermophilic archaeon *Pyrococcus furiosus*: Evidence for a new type of sulfur-reducing enzyme complex. J. Bacteriol. **183:**7027-7036.

52. **Shevchenko, A., M. Wilm, O. Vorm, and M. Mann.** 1996. Mass spectrometric sequencing of proteins from silver stained polyacrylamide gels. Anal. Chem. **68:**850-858.

53. **Siebers, B., H. Brinkmann, C. Dorr, B. Tjaden, H. Lilie, J. van der Oost, and C. H. Verhees.** 2001. Archaeal fructose-1,6-bisphosphate aldolases constitute a new family of archaeal type class I aldolase. J. Biol. Chem. **276:**28710-28718.

54. **Stetter, K.** 1996. Hyperthermophilic prokaryotes. FEMS Microbiol. Rev. **18:**149-158.

55. **Van Der Oost, J., M. Huynen, and C. Verhees.** 2002. Molecular characterization of phosphoglycerate mutase in archaea. FEMS Microbiol. Lett. **212:**111-120.

56. **Verhees, C. H., S. W. M. Kengen, J. E. Tuininga, G. J. Schut, M. W. W. Adams, W. M. De Vos, and J. Van der Oost.** 2003. The unique features of glycolytic pathways in Archaea. Biochem. J. **375:**231-246.

57. **Wang, N., K. Yamanaka, and M. Inouye.** 1999. CspI, the ninth member of the CspA family of *Escherichia coli*, is induced upon cold shock. J. Bacteriol. **181:**1603-1609.

58. **Xing, R. Y., and W. B. Whitman.** 1987. Sulfometuron methyl-sensitive and methyl-resistant acetolactate synthases of the archaebacteria *Methanococcus* Spp. J. Bacteriol. **169:**4486-4492.

CHAPTER 5

SUMMARY AND DISCUSSION

Response to environmental stress (ie heat, cold, ROS, starvation) has been studied to varying degrees (111). While many questions have been answered in reference to bacterial stress responses, archaea, specifically hyperthermophilic archaea, have yet to be studied as extensively. While the bacterial heat shock response is one of the most widely known and studied mechanisms of biology (116)**,** the study of the archaeal heat shock response is in its infancy (122, 134). In addition, while oxidative stress in aerobic microbes have been studied extensively (127), the anaerobic oxidative stress response has only recently been identified (62), with *Pyrococcus furiosus* being one of the model organisms. The cold shock response is yet another rapidly growing research topic, though the vast majority of work has been performed on bacteria such as *Escherichia coli* and *Bacillus subtilis* (46). More recent publications have branched out to other organisms, however (23, 30). This is in opposition to archaea, where the most recent review discusses mostly the cold adaptation of psychrophiles to make up for the lack of knowledge about an actual stress response (18). The goal of this research project, therefore, was to study poorly understood aspects of environmental stress responses in hyperthermophilic archaea, namely 1) the biochemical pathway employed by anaerobes in response to reactive oxygen species (ROS) and 2) the hyperthermophilic archaeal cold shock response. A biochemical characterization of the none-heme iron protein rubrerythrin (Rr) functionally places it in the ROS detoxification pathway of *P. furiosus* and a new reconstitution protocol allows for the recombinant production of another enzyme involved in anaerobic oxidative stress,

NADPH:rubredoxin oxidoreductase (NROR). A second aspect was to identify cold inducible elements in the hyperthermophilic archaeon *P. furiosus*, as well as to identify other aspects of the cellular response to the stress. This was accomplished by employing whole genome microarray analyses as well as proteomic techniques, enzyme assays and quantitative real time PCR to confirm these cold induced targets. This body of work successfully accomplishes these goals, making significant contributions to the fields of oxidative stress in anaerobic and microaerophilic microbes as well as cold stress in hyperthermophilic archaea.

An active, recombinant form of NROR was produced from the work in chapter 2. This recombinant form is just as active as the native form (~500 U/mg) and a study of its kinetic parameters showed its K_m and V_{max} towards several substrates is no more than two-fold different from the native enzyme (Table 2.3). Thermostability studies also indicated the recombinant protein was just as stable at elevated temperatures (80 and 95 ^oC). The emerging study of oxidative stress in anaerobic and microaerophilic microbes necessitates the study of NROR and how it relates to the other enzymes of the response, namely superoxide reductase (SOR), rubredoxin (Rd) and Rr. This point is highlighted by the study of Rr in chapter 3, which will be discussed further below. Prior to this work, the only way to obtain NROR was by purifying the native form from *P. furiosus* cells. Both cell growth and purification was time consuming, resulting in poor yields (~ 10 mg from 400 g wet weight cells) (96). Previous attempts at recombinant expression were unsuccessful, hypothesized to be due to interference of the recombinant protein with redox chemistry of the host, resulting in cell death. It appears that the addition of a His-Tag on the recombinant protein affects its expression to the point that FAD (a necessary cofactor for activity) is not readily inserted into the recombinant protein, which reduces activity by a significant margin (40-fold less than the native). This allows for the

expression of inactive NROR in the host cell. Reconstitution of the purified recombinant protein with FAD returns the enzyme to native-level activity.

The significance of obtaining recombinant NROR is that the previously time consuming steps of large scale (500 L) *P. furiosus* fermentor growth and native anaerobic protein purification are replaced with much smaller scale *E. coli* growth (1 L) and recombinant affinity chromatography, resulting in more protein purified with similar properties in less time. As the study of anaerobic oxidative stress continues, the need for NROR will increase. NROR has already been shown to function in providing a reduced pool of Rd in the cell for the SOR reaction (62). Future study of SOR and how it relates to the oxidative stress response as a whole will require NROR. Further, as chapter 3 shows, *P. furiosus* employs a pathway in which NADH eventually reduced H_2O_2 to water using NROR, Rd and Rr as electron carrier intermediates. The recombinant production of active NROR would facilitate experiments such as these.

In addition, there is interest in solving the X-ray crystal structure of the active form of NROR. This could give insight as to how the protein interacts with its substrates Rd and NADPH, as well as if and/or how it interacts with other proteins in the detoxification pathway, such as SOR and Rr. The recombinant active NROR undoubtedly makes this effort much easier and less time consuming.

As stated above, there is a relationship between the enzymes NROR and Rr that has yet to be fully established. Much like NROR, the enzyme Rr has been implicated in the ROS stress response of anaerobic and microaerophilic microbes. To date, the most data on Rr has been accumulated from the anaerobic bacteria *Desulfovibrio vulgaris*, characterizing its spectroscopic, biochemical and structural properties extensively (12, 19-22, 24, 26, 47, 48, 63, 77, 78, 80, 84,

87, 89, 94, 95, 108-110, 123, 124, 132). Despite the vast library of work in this and other organisms, its true function and role have been elusive. Phosphatase (132), ferroxidase (12), NADH peroxidase (22) and Rd peroxidase (19) activity have all been attributed to Rr, with the Rd peroxidase activity being the latest and most convincing (19). Until recently its function has only been able to be indirectly implicated as a peroxidase in the oxidative stress response of various anaerobic organisms (4, 5, 19, 20, 85, 129). As a result, the study of the ROS response has been at somewhat of a standstill for some time. The major question to be addressed is, what happens to the H_2O_2 produced from the SOR reaction? There must be some way the cell acts on this deleterious ROS to render it inactive. The results of research conducted in chapter 3 further establishes the Rd peroxidase activity as the likely physiological role for Rr, as well as identifies a physiologically relevant electron donor for this system as NAD(P)H via NROR.

As a result of the data reported herein, a number of characteristics of the *P. furiosus* and *D. vulgaris* proteins can now be compared. Not surprisingly, many properties between these two proteins are very similar (Table 5.1), including subunit size and amino acid sequence. The Rd peroxidase activity for the *P. furiosus* enzyme compared favorably with that shown previously in *D. vulgaris* Rr (19). This further establishes Rr as a peroxidase and its close proximity to Rd and SOR in the *P. furiosus* genome suggests a relationship between them. It was therefore proposed that Rr reduces H_2O_2 resulting from the SOR reaction, resulting in the full reduction and detoxification of O_2^- to H_2O. The affinity of Rr for Rd and H_2O_2, the proposed substrates of the enzyme, was certainly within a respectable range for enzyme activity (70 and 35 uM, respectively).

In contrast to native *P. furiosus* Rr, which contains 3 Fe/monomer, the recombinant forms of *P. furiosus* Rr had one or two iron atoms replaced with zinc, depending on the growth medium

of the host cell. This change in metal content of the protein resulted in a decrease in Rd peroxidase activity. While the native protein had a specific activity of ~36 U/mg, the activities of the 2-iron and 1-iron forms of Rr were 10 (~ 3 U/mg) and 100 fold less (~ 0.3 U/mg). This indicates a requirement for 3 iron atoms for Rr activity. The metal content dependency on activity could also explain why *D. vulgaris* had so many biochemical activities attributed to it (12, 20, 22, 89), since this Rr had several metal contents reported for it, depending on its growth and purification procedures.

As alluded to earlier, studies to investigate how NROR, SOR, Rd and Rr interact are already under way. Chapter 3 shows how NROR, Rd and Rr are intermediates in the reduction pathway of H_2O_2 to water using NADH as the electron donor. Further studies need to be performed to determine how SOR functions in this pathway. It would be interesting to see how SOR and Rr compete with one another for Rd, the electron donor in each reaction. It would also be interesting to see how all of these enzymes interact with each other structurally. For example, do they form a ternary complex, and one that could be trapped by chemical cross-linking? These questions are starting to be addressed, as structural studies have played a major role in the research of Rr. The X-ray crystal structure of the *D. vulgaris* proteins have been reported (87, 123). It is a homodimeric protein where each subunit is composed of 2 domains: an N-terminal 4 helix bundle that has no structural homology to any protein and a C-terminal Rd-like domain. In addition to the *D. vulgaris* Rr, a crystal structure for a Rr-like protein from *Sulfolobus tokodaii* has also been solved (34). The major difference between the *S. tokodaii* protein and other Rr's is the lack of Rd-like domain at the C-terminus of the protein, resulting in the absence of the Cys motifs required for one of the metal binding sites (135). What remains is only the N-terminal 4 helix bundle, which resembles the Rr overall structure but has one significant difference, an

Table 5.1. Purified native homologs of rubrerythrin

	P. furiosus	***D. vulgaris***
Subunit Mol. Wt. (kDa)	19.4	21.9 kDa
# Amino Acids	170	191
Subunit Composition	Homodimer	Homodimer
Metal Content	3 Fe/monomer (native) 2 Fe,1 Zn/monomer (rec) 1 Fe, 2 Zn/monomer (rec)	3 Fe/monomer (native) 2 Fe,1 Zn/monomer (rec)
Ferroxidase Activity?	No	Yes
NADH Peroxidase Activity?	No	No
Rd peroxidase activity?	Yes	Yes
UV-visible spectrum (oxidized)	280, 373, 490	280, 365, 492 nm
Thermostability (absorbance @ 490 nm at 80 ^{o}C)	< 10% decrease overnight	> 95% decrease in 5 minutes

extremely rare case of domain swapping (90). Instead of each 4 helix bundle being made from each subunit, in this case two helices come from one subunit, the other two come from the other subunit, hence a "swapping" of domains (34). This hyperthermophilic archaeon is strictly aerobic, which may or may not indicate that aerobes do not require the Rd-like site of Rr for activity. The Rr-like protein also did not show pyrophosphatase or SOD activity, two enzyme activities previously detected for the *D. vulgaris* enzyme (but not for *P. furiosus* Rr). Further, since *P. furiosus* Rr only exhibits Rd peroxidase activity (whereas *D. vulgaris* Rr showed various other activities, including Rd peroxidase activity), it would be interesting to see if this activity could be detected in the *S. tokodaii* protein.

The *P. furiosus* Rr crystal structure has also been recently resolved (130). Amazingly, the same domain swapping scenario is seen in the *P. furiosus* structure as well. Each 4 helix bundle is comprised of two helices from each subunit. How this relates to the *S. tokodaii* protein remains to be seen, but it appears the hyperthermophilic nature of both of these organisms has something to do with the domain swapping. A comparison of the primary structures of these three proteins does not reveal an answer as to why or how this would happen (Fig 5.1). Regardless, this is an exciting development for the study of Rr and bears further research that may or may not explain some of the differences between the three different forms.

A feature specific to native Rr that has not been fully explained by this study is its precipitation upon exposure to aerobic conditions. None of the recombinant proteins show this property, so this issue appears to be the result of the metal content of the protein. It is reasonable to hypothesize that the native protein is encountering hydrogen peroxide or other oxidizing substrates, resulting in the oxidation of the iron present in the protein and thus making the protein insoluble. There is another possibility that there is a partner protein that protects or acts

on concert with Rr in the cell under oxidizing conditions, acting as a makeshift chaperone that is obviously not present once Rr is purified. Obvious candidates are SOR and Rd, but their effects on the stability of Rr have not been analyzed.

At the outset of this research project, the stress response of hyperthermophilic archaea was largely unknown. In particular, there was very little known about the cold shock response of hyperthermophilic archaea, with the microarray data described in chapter 4 one of the first reports on the topic. Previous cold shock response studies on hyperthermophilic archaea were performed on *Sulfolobus*, *Thermococcus*, and *Methanococcus*. In contrast to chapter 4, however, the two topics these studies highlight are the cold inducibility of specific proteins (a chaperonin and a FK506 binding protein, see Introduction for details) involved in protein folding in these organisms, as well as how DNA topology is affected by growth temperature in these organisms (91-93). The DNA topology issue is particularly interesting, as the *P. furiosus* cold shock study revealed the up-regulation of two putative DNA gyrase regulators (PF1076 and 1077), which would presumably affect DNA coiling in response to cold shock. There is currently no reference to date defining a whole genome analysis of the response of hyperthermophilic archaeon's response to cold shock or cold stress other than chapter 4.

The study involving the cold induction of the chaperonin (also called rosettasome) from the hyperthermoacidophilic archaeon *Sulfolobus shibatae* indicates some overlap between the cold shock and heat shock response (69). This rosettasome is composed of three different subunits (alpha, beta and gamma) whose expression changed depending on the growth temperature of the organism. Alpha and beta expression increased due to heat shock (86 ^{o}C for 30 minutes) while being decreased due to cold shock conditions (60 ^{o}C for 30 minutes). On the other hand, expression of the gamma subunit was not detectable under heat shock and normal

growth conditions (75 ^{o}C), but was induced upon cold shock. Due to this change in expression the subunit ratios changed as well. At 75 ^{o}C, the rosettasome had a ratio of 1α:1β:0.1γ, a ratio of 1:3:1 at 60 ^{o}C and 2:3:0 at 86 ^{o}C. This data indicates that in some hyperthermophilic archaea, protein folding machinery changes as a function of growth temperature. However, some hyperthermophilic archaea, such as *P. furiosus*, only have one identified chaperonin subunit in their genome, indicating this temperature dependent response is not widespread in all archaea.

The only other information on the archaeal cold shock response was performed on a FK506 binding protein (FKBP) from *Methanococcus jannaschii* and *Thermococcus* sp. (57, 58). This is a peptidyl-prolyl *cis-trans* isomerase (PPIase) which, like the chaperonin, helps in protein folding. Long (26-33 kDa) and short (16-18 kDa) types have been identified in archaea. In both organisms studied, expression of only the short type has been shown to increase when exposed to cold shock conditions (in both cases, 60 ^{o}C). Just as significant is the investigation of *Pyrococcus horikoshii*, which only has the long type of FKBP. Cold shock response studies of this protein in this organism showed there was no temperature dependent change in expression. Much like the chaperonin study, this fact eliminates a wide spread use of this mechanism among hyperthermophilic archaea to combat cold shock stress.

The lack of knowledge about cold stress in hyperthermophilic archaea is extremely obvious in the most recent review on the topic (18). In addition, the fact that the most recent review is four years old indicates that little progress has been made in the time since its publication. The authors readily admit this scarcity of data, dubbing the first section of the introduction “A lack of knowledge”. As they point out, although hyperthermophiles dominate the overall knowledge of archaea, much more is known about cold stress in psychrophilic archaea.

Figure 5.1.

Comparison of the amino acid sequence of *P. furiosus* rubrerythrin with those of *D. vulgaris* rubrerythrin and *S. tokodaii* sulerythrin. All three of these proteins have been crystallized. The black boxes indicate identical residues whereas shaded boxes indicate similar residues. The amino acid residues comprising the binuclear metal binding domain are indicated with an arrow (^), the residues comprising the Rd-like metal binding domain are indicated with a star (*).

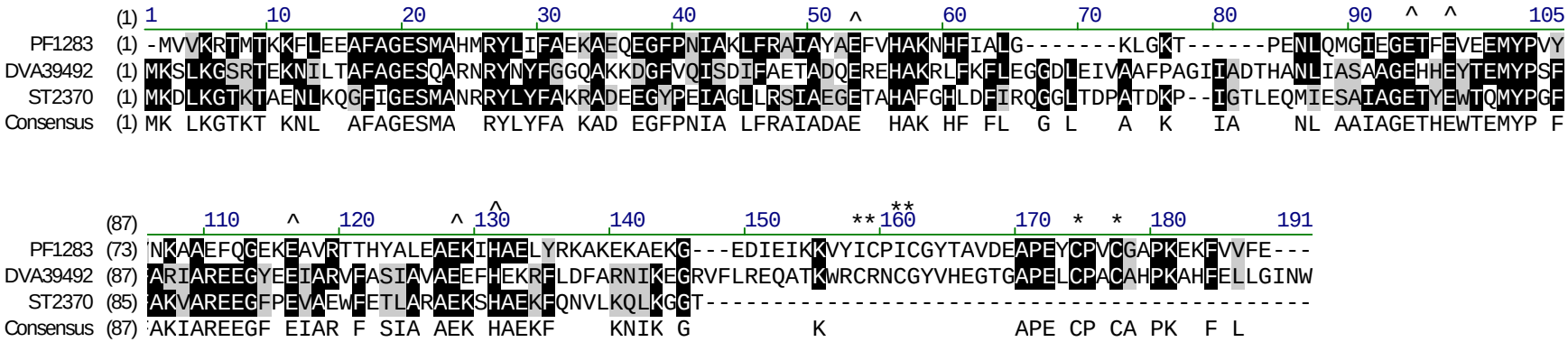
(1) 1 10 20 30 40 50 60 70 80 90 105
PF1283 (1) -MVVKRIMTKKFLEEAFAGESMAHMRYLIFAEKAEQEGFPNIAKLFRAIAYAEFVHAKNHFIALG-------KLGKT------PENLQMGIEGETFEVEEMYPVY
DVA39492 (1) MKSLKGSRTEKNILTAFAGESQARNRYNYFGGQAKKDGFVQISDIFAETADQEREHAKRLFKFLEGGDLEIVAAFPAGIIADTHANLIASAAGEHHEYTEMYPSF
ST2370 (1) MKDLKGTKTAENLKQGFIGESMANRRYLYFAKRADEEGYPEIAGLLRSIAEGETAHAFGHLDFIRQGGLTDPATDKP--IGTLEQMIESAIAGETYEWTQMYPGF
Consensus (1) MK LKGTKT KNL AFAGESMA RYLYFA KAD EGFPNIA LFRAIADAE HAK HF FL G L A K IA NL AAIAGETHEWTEMYP F
(87) 110 120 130 140 150 160 170 180 191
PF1283 (73) NKAAEFQGEKEAVRTTHYALEAEKIHAELYRKAKEKAEKG---EDIEIKKVYICPICGYTAVDEAPEYCPVCGAPKEKFVVFE---
DVA39492 (87) ARIAREEGYEEIARVFASIAVAEEFHEKRFLDFARNIKEGRVFLREQATKWRCRNCGYVHEGTGAPELCPACAHPKAHFELLGINW
ST2370 (85) AKVAREEGFPEVAEWFETLARAEKSHAEKFQNVLKQLKGGT----------
Consensus (87) AKIAREEGF EIAR F SIA AEK HAEKF KNIK G K APE CP CA PK F L

Thus, it is important to gain insight into the regulatory mechanisms, determine a cellular response to the stress and identify cold inducible elements in these hyperthermophilic organisms.

Chapter 4 shows cold inducible elements of *P. furiosus*, which can presumably, at least on a preliminary basis, be a model for all hyperthermophilic archaea. The microarray data in fact revealed three different responses, an early shock response (1-2 hours post shock), a late shock response (5 hrs post shock) and a cold growth response (where the culture temperature is 72 ^{o}C over the entire growth). From these three responses, several trends emerged. Although there was an overall down-regulation of transcription, genes encoding proteins involved in amino acid metabolism, ABC transporters and protein degradation enzymes, in addition to a large number of conserved hypothetical proteins all appear to be up-regulated. The working hypothesis is that these up-regulated proteins results in a pool of amino acids needed to rapidly produce a subset of proteins (specifically, but not limited to, the conserved hypothetical proteins that are up-regulated) needed for growth to resume at this lower than optimal temperature. The real strength of the microarray data is that it identifies target genes for further study using a variety of other methods, depending on the type of protein involved. However, no genetic system has been developed for *P. furiosus*, so while determining the functions of these conserved hypothetical proteins is no small task, it certainly is of interest.

Proteomics was one of the methods used to confirm some of the microarray data. Two cold inducible proteins in the membrane fraction of cell extracts were identified by MALDI-MS as PF0190 and PF1408, both if which were up-regulated according to microarray data. Further studies examining extracts from control and cold shocked cells using such methods as 2-dimensional difference gel electrophoresis (2-D DIGE) and mass spectrometry could provide further evidence that some of the genes up-regulated indicated by the microarray data results in

higher levels of the corresponding protein. Since many of the up-regulated genes encode for conserved hypothetical proteins for which there is no enzyme assay, this is an extremely important aspect of this research. Quantitative PCR as well as enzymatic assays were also employed in order to confirm genes identified as cold up-regulated. Since PF0190 and PF1408 were identified by proteomic procedures, they were also subjected to quantitative PCR analysis. The up-regulation of both these ORFs was confirmed, as PF0190 and PF1408 were up-regulated 26.0 and 5.8 fold, respectively (Chapter 4). Some of the microarray data were enzymatic assays. Although many up-regulated ORFs are annotated as (conserved) hypothetical, there were several genes encoding assayable enzymes, including KGOR, AARE and acetolactate synthase (Table 4.3).

One of the major aspects of the cold shock response of *P. furiosus* is the up-regulation of encoding proteins in several amino acid biosynthetic pathways, as well as those encoding 2-keto acid oxidoreductases, which potentially generate activated intermediates (CoA derivatives) for amino acid biosynthesis (120). Many of these genes have already been shown to be up-regulated when comparing peptide grown cells to those grown on maltose (119, 121). Based on these findings, it would interesting to see how peptide grown *P. furiosus* that is cold shocked differs from the maltose grown cold shocked cells.

The regulation of various stress responses in a range of microorganisms has been widely studied (18, 106). Regulation of the heat shock response, as well as the cold shock response in bacteria, has been investigated extensively once the response itself was discovered (46, 111). How the response is regulated is just as important as what the response accomplishes once it is turned on. Elucidating the regulatory mechanisms in most hyperthermophilic archaea is made much more difficult by the fact no genetic system has been developed to easily knockout genes

and/or manipulate promoter sequences to determine the effect on transcription. Nevertheless, the microarray data reveal several possible candidates for cold shock regulatory elements. As shown in Table 5.2, all of these have predicted pI's that are very basic, they contain a zinc finger or leucine zipper domain and are only slightly up-regulated upon cold shock, which are all characteristic of regulatory elements.

Chapters 2 and 3 provided advances in the field of anaerobic oxidative stress response. A recombinant, active form of NROR was produced, which should facilitate further study of this stress response. Rr was also studied from a biochemical standpoint and and further evidence for its function as a Rd peroxidase was established. This provided a mechanism by which H_2O_2 produced from SOR is reduced to H_2O and rendered non-reactive to cellular material such as iron sulfur clusters in proteins and membranes. Chapter 4 laid the groundwork for many studies in the field of cold shock response in hyperthermophilic archaea. Targets for study were identified by microarray analysis and some of these were confirmed using proteomic, RT-PCR and enzymatic measurements. Studies to investigate the regulation of the response, confirming more of these targets by proteomics, how the conserved hypothetical proteins play into the response and how similar this response is to that of bacteria are all possible ways to continue with the cold shock response of hyperthermophilic archaea. A similarity in ABC transporters being up-regulated in *Listeria monocytogenes* that is similar to PF0190 and Pf1408 has already been identified as a result of this study (13).

Table 5.2 Possible cold shock regulatory elements in *P. furiosus* identified by microarray data.

Genemate ORF number	Regulation Fold[a]				Molecular Weight(kDa)	Predicted pI	Domain[b] (Leu zip/Zn finger)
	1 hr	2 hr	5 hr	Batch			
PF0095	1.9	**2.3**	**2.1**	1.2	27	5.3	ArsR, HTH
PF0286	1.3	1.7	1.7	**3.1**	32	9.2	HTH
PF0297	1.0	1.2	1.4	**2.7**	16	9.8	HTH
PF0481	**2.5**	**2.1**	1.5	1.9	16	8.3	Translation factor IF2β, Zn finger?
PF0709	1.5	1.7	**2.1**	**3.2**	7.0	9.4	MarR, HTH (for AB resistance)
PF0710	1.4	1.7	1.3	**5.4**	9.3	8.0	HTH
PF1060	**2.1**	1.2	1.1	1.4	24	5.1	Zn finger, Zpr1
PF1072	3.5*	2.9*	1.2	**11.7**	16	6.3	ArsR HTH
PF1137	**3.0**	**2.8**	**3.0**	1.1	11	6.0	Transl. IF2, GTP binding, intein
PF1284	**2.1**	**2.6**	1.5	2.1	7.0	9.1	Histone fold, TATA BP?,Transc.Factor?
PF1302	**2.4**	1.8	1.2	1.9	16	4.7	AbrB transr. Reg
PF1560	1.2	1.4	**2.5**	1.9*	16	9.5	Transcr. Term/antiterm, nusA, KH-RNA binding
PF1926	**2.1**	**2.7**	1.4	1.4*	38	6.2	HhH-DNA binding w/ enz act
PF1927	**2.1**	1.3	1.0	2.0*	23	7.0	tIF-5 w/ Zn finger

[a]Data obtained from studies performed in chapter 4. Genes up-regulated >2-fold are indicated in bold. Except when indicated with a *, all numbers indicate up-regulation fold.
[b]Domains identified from sequences searchers using Interpro Software (54). HTH indicates a helix turn helix domain, and Zn finger indicates the Zinc finger domain. Both are characteristic of DNA binding proteins that serve a regulatory function in gene expression.

REFERENCES

1. **Adams, M. W. W. 1999.** The biochemical diversity of life near and above 100 ^{o}C in marine environments. J. Appl. Microbiol. Symp. Suppl. **85**:108S-117S.
2. **Adams, M. W. W., J. F. Holden, A. L. Menon, G. J. Schut, A. M. Grunden, C. Hou, A. M. Hutchins, F. E. Jenney, C. Kim, K. S. Ma, G. L. Pan, R. Roy, R. Sapra, S. V. Story, and M. F. J. M. Verhagen.** 2001. Key role for sulfur in peptide metabolism and in regulation of three hydrogenases in the hyperthermophilic archaeon *Pyrococcus furiosus*. J. Bacteriol. **183**:716-724.
3. **Adams, M. W. W., and A. Kletzin.** 1996. Oxidoreductase-type enzymes and redox proteins involved in fermentative metabolisms of hyperthermophilic archaea. Adv. Protein Chem. **48**:101-180.
4. **Alban, P. S., and N. R. Krieg.** 1998. A hydrogen peroxide resistant mutant of *Spirillum volutans* has NADH peroxidase activity but no increased oxygen tolerance. Can. J. Microbiol. **44**:87-91.
5. **Alban, P. S., D. L. Popham, K. E. Rippere, and N. R. Krieg.** 1998. Identification of a gene for a rubrerythrin/nigerythrin-like protein in *Spirillum volutans* by using amino acid sequence data from mass spectrometry and NH2-terminal sequencing. J. Appl. Microbiol. **85**:875-882.
6. **Atlung, T., and F. G. Hansen.** 1999. Low-temperature-induced DnaA protein synthesis does not change initiation mass in *Escherichia coli* K-12. J. Bacteriol. **181**:5557-5562.

7. **Bae, W., B. Xia, M. Inouye, and K. Severinov.** 2000. *Escherichia coli* CspA-family RNA chaperones are transcription antiterminators. Proc. Natl. Acad. Sci. USA **97**:7784-7789.

8. **Bauer, M. W., S. B. Halio, and R. M. Kelly.** 1996. Proteases and glycosyl hydrolases from hyperthermophilic microorganisms. Adv. Protein Chem. **48**:271-310.

9. **Beran, R. K., and R. W. Simons.** 2001. Cold-temperature induction of *Escherichia coli* polynucleotide phosphorylase occurs by reversal of its autoregulation. Mol. Microbiol. **39**:112-125.

10. **Blochl, E., S. Burggraf, G. Fiala, G. Laurerer, G. Huber, R. Huber, R. Rachel, A. Segerer, K. O. Stetter, and P. Volkl.** 1995. Isolation, taxonomy and phylogeny of hyperthermophilic microorganisms. World J. Microb. Biot. **11**:9-16.

11. **Blochl, E., R. Rachel, S. Burggraf, D. Hafenbradl, H. W. Jannasch, and K. O. Stetter.** 1997. *Pyrolobus fumarii,* gen. and sp. nov., represents a novel group of archaea, extending the upper temperature limit for life to 113 ^{o}C. Extremophiles **1**:14-21.

12. **Bonomi, F., D. M. Kurtz, and X. Y. Cui.** 1996. Ferroxidase activity of recombinant *Desulfovibrio vulgaris* rubrerythrin. J. Biol. Inorg. Chem. **1**:67-72.

13. **Borezee, E., E. Pellegrini, and P. Berche.** 2000. OppA of *Listeria monocytogenes,* an oligopeptide-binding protein required for bacterial growth at low temperature and involved in intracellular survival. Infect. Immun. **68**:7069-7077.

14. **Brandi, A., P. Pietroni, C. O. Gualerzi, and C. L. Pon.** 1996. Post-transcriptional regulation of CspA expression in *Escherichia coli*. Mol. Microbiol. **19**:231-240.

15. **Brandi, A., C. L. Pon, and C. O. Gualerzi.** 1994. Interaction of the main cold shock protein CS7.4 (CspA) of *Escherichia coli* with the promoter region of *hns*. Biochimie **76**:1090-1098.

16. **Briolat, V., and G. Reysset.** 2002. Identification of the *Clostridium perfringens* genes involved in the adaptive response to oxidative stress. J. Bacteriol. **184**:2333-2343.

17. **Carlson, B. W., L. L. Miller, P. Neta, and J. Grodowski.** 1984. Oxidation of NADH involving rate-limiting one electron transfer. J. Am. Chem. Soc. **106**:7233-7239.

18. **Cavicchioli, R., T. Thomas, and P. M. G. Curmi.** 2000. Cold stress response in archaea. Extremophiles **4**:321-331.

19. **Coulter, E. D., and D. M. Kurtz.** 2001. A role for rubredoxin in oxidative stress protection in *Desulfovibrio vulgaris*: Catalytic electron transfer to rubrerythrin and two-iron superoxide reductase. Arch. Biochem. Biophys. **394**:76-86.

20. **Coulter, E. D., N. V. Shenvi, Z. M. Beharry, J. J. Smith, B. C. Prickril, and D. M. Kurtz.** 2000. Rubrerythrin-catalyzed substrate oxidation by dioxygen and hydrogen peroxide. Inorg. Chim. Acta. **297**:231-241.

21. **Coulter, E. D., N. V. Shenvi, and D. M. Kurtz.** 1999. *In vitro* and *in vivo* activities of rubrerythrin. J. Inorg. Biochem. **74**:197-197.

22. **Coulter, E. D., N. V. Shenvi, and D. M. Kurtz.** 1999. NADH peroxidase activity of rubrerythrin. Biochem. Biophys. Res. Commun. **255**:317-323.

23. **Datta, P. P., and R. K. Bhadra.** 2003. Cold shock response and major cold shock proteins of *Vibrio cholerae*. Appl. Environ. Microbiol. **69**:6361-6369.

24. **Dave, B. C., R. S. Czernuszewicz, B. C. Prickril, and D. M. Kurtz.** 1994. Resonance raman spectroscopic evidence for the FeS_4 and Fe-O-Fe sites in rubrerythrin from *Desulfovibrio vulgaris*. Biochemistry **33**:3572-3576.

25. **de Smit, M. H., and J. van Duin.** 1990. Control of prokaryotic translational initiation by mRNA secondary structure. Prog. Nucleic Acid Res. Mol. Biol. **38**:1-35.

26. **deMare, F., D. M. Kurtz, and P. Nordlund.** 1996. The structure of *Desulfovibrio vulgaris* rubrerythrin reveals a unique combination of rubredoxin-like FeS4 and ferritin-like diiron domains. Nat. Struct. Biol. **3**:539-546.

27. **Ding, H., E. Hidalgo, and B. Demple.** 1996. The redox state of the [2Fe-2S] clusters in SoxR protein regulates its activity as a transcription factor. J. Biol. Chem. **271**:33173-33175.

28. **Fang, L., W. Jiang, W. Bae, and M. Inouye.** 1997. Promoter-independent cold-shock induction of *cspA* and its derepression at 37 ^{o}C by mRNA stabilization. Mol. Microbiol. **23**:355-364.

29. **Farewell, A., and F. C. Neidhardt.** 1998. Effect of temperature on *in vivo* protein synthetic capacity in *Escherichia coli*. J. Bacteriol. **180**:4704-4710.

30. **Favaro, R., and G. Deho.** 2003. Polynucleotide phosphorylase-deficient mutants of *Pseudomonas putida*. J. Bacteriol. **185**:5279-5286.

31. **Fiala, G., and K. O. Stetter.** 1986. *Pyrococcus furiosus* sp-nov represents a novel genus of marine heterotrophic archaebacteria growing optimally at 100 ^{o}C. Arch. Microbiol. **145**:56-61.

32. **Flint, D., J. Tuminello, and M. Emptage.** 1993. The inactivation of Fe-S cluster containing hydro-lyases by superoxide. J. Biol. Chem. **268**:22369-22376.

33. **Forterre, P., C. Brochier, and H. Philippe.** 2002. Evolution of the Archaea. Theor. Popul. Biol. **61**:409-22.

34. **Fushinobu, S., H. Shoun, and T. Wakagi.** 2003. Crystal structure of sulerythrin, a rubrerythrin-like protein from a strictly aerobic archaeon, *Sulfolobus tokodaii* strain 7, shows unexpected domain swapping. Biochemistry **42**:11707-11715.

35. **Garwin, J. L., and J. E. Cronan, Jr.** 1980. Thermal modulation of fatty acid synthesis in *Escherichia coli* does not involve de novo enzyme synthesis. J. Bacteriol. **141**:1457-1459.

36. **Garwin, J. L., A. L. Klages, and J. J E Cronan.** 1980. Beta-ketoacyl-acyl carrier protein synthase II of *Escherichia coli*: Evidence for function in the thermal regulation of fatty acid synthesis. J. Biol. Chem. **255**:3263-3265.

37. **Gaudu, P., and B. Weiss.** 1996. SoxR, a [2Fe-2S] transcription factor, is active only in its oxidized form. Proc. Natl. Acad. Sci. USA **93**:10094-10098.

38. **Geissmann, T. A., M. Teuber, and L. Meile.** 1999. Transcriptional analysis of the rubrerythrin and superoxide dismutase genes of *Clostridium perfringens*. J. Bacteriol. **181**:7136-7139.

39. **Giangrossi, M., A. M. Giuliodori, C. O. Gualerzi, and C. L. Pon.** 2002. Selective expression of the beta-subunit of nucleoid-associated protein HU during cold shock in *Escherichia coli*. Mol. Microbiol. **44**:205-216.

40. **Giangrossi, M., C. O. Gualerzi, and C. L. Pon.** 2000. Mutagenesis of the downstream region of the *Escherichia coli hns* promoter. Biochimie **83**:251-259.

41. **Goldenberg, D., I. Azar, and A. B. Oppenheim.** 1996. Differential mRNA stability of the *cspA* gene in the cold-shock response of *Escherichia coli*. Mol. Microbiol. **19**:241-248.

42. **Goldenberg, D., I. Azar, A. B. Oppenheim, A. Brandi, C. L. Pon, and C. O. Gualerzi**. 1997. Role of *Escherichia coli cspA* promoter sequences and adaptation of translational apparatus in the cold shock response. Mol. Gen. Genet. **256**:282-290.

43. **Goldstein, J., N. S. Pollitt, and M. Inouye.** 1990. Major cold shock protein of *Escherichia coli*. Proc. Natl. Acad. Sci. USA. **87**:283-287.

44. **Gonzalez-Flecha, B., and B. Demple.** 1995. Metabolic sources of hydrogen peroxide in aerobically growing *Escherichia coli*. J. Biol. Chem. **270**:13681-13687.

45. **Gort, A., and J. A. Imlay.** 1998. Balance between endogenous superoxide stress and antioxidant defenses of *Escherichia coli*. J. Bacteriol. **180**:1402-1410.

46. **Gualerzi, C. O., A. Maria Giuliodori, and C. L. Pon.** 2003. Transcriptional and posttranscriptional control of cold shock genes. J. Mol. Biol. **331**:527-39.

47. **Gupta, N., F. Bonomi, D. M. Kurtz, N. Ravi, D. L. Wang, and B. H. Huynh.** 1995. Recombinant *Desulfovibrio vulgaris* rubrerythrin - isolation and characterization of the diiron domain. Biochemistry **34**:3310-3318.

48. **Gupta, N., D. M. Kurtz, N. Ravi, D. L. Wang, and B. H. Huynh.** 1995. Structure and redox properties of the diiron cluster in recombinant rubrerythrin. Abstracts of Papers of the American Chemical Society **209**:214-218.

49. **Hensel, R., K. Matussek, and K. Michalke.** 1997. *Sulphobococcus zilligi* gen. nov., spec. nov. a novel hyperthermophilic archaeon isolated from hot alkaline springs of Iceland. Syst. Appl. Microbiol. **20**:102-110.

50. **Hidalgo, E., J. M. Bollinger, T. M. Bradley, C. T. Walsh, and B. Temple.** 1995. Binuclear [2Fe-2S] clusters in the *Escherichia coli* SoxR protein and role of the metal clusters in transcription. J. Biol. Chem. **270**:20908-20914.

51. **Hidalgo, E., and B. Demple.** 1996. Adaptive responses to oxidative stress: the *soxRS* and *OxyR* regulons. RG Landes Company, Austin.

52. **Hoaki, T., M. Nishijima, M. Kato, K. Adachi, S. Mizobuchi, N. Hanzawa, and T. Maruyama.** 1994. Growth requirements of hyperthermophilic sulfur-dependent heterotrophic archaea isolated from a shallow submarine geothermal system with reference to their essential amino acids. Appl. Environ. Microbiol. **60**:2898-2904.

53. http://comb5-156.umbi.umd.edu/genemate/:.

54. http://www.ebi.ac.uk/interpro/.

55. **Huber, H., M. J. Hohn, R. Rachel, T. Fuchs, V. C. Wimmer, and K. O. Stetter.** 2002. A new phylum of archaea represented by a nanosized hyperthermophilic symbiont. Nature **417**.:63-7.

56. **Huber, R., H. Huber, and K. O. Stetter.** 2000. Towards the ecology of hyperthermophiles: biotopes, new isolation strategies and novel metabolic properties. FEMS Microbiol. Rev. **24**:615-23.

57. **Ideno, A., and T. Maruyama.** 2002. Expression of long- and short-type FK506 binding proteins in hyperthermophilic archaea. Gene **292**:57-63.

58. **Ideno, A., T. Yoshida, T. Iida, M. Furutani, and T. Maruyama.** 2001. FK506-binding protein of the hyperthermophilic archaeum, *Thermococcus* sp. KS-1, a cold-shock-inducible peptidyl-prolyl cis-trans isomerase with activities to trap and refold denatured proteins. Biochem. J. **357** (Pt 2):465-471.

59. **Imlay, J. A.** 2002. How oxygen damages microbes: Oxygen tolerance and obligate anaerobiosis. Adv. Microb. Physiol. **46**:111-153.

60. **Imlay, J. A., and S. Linn.** 1988. Toxic DNA damage by hydrogen peroxide through the Fenton reaction *in vivo* and *in vitro*. Science **240**:640-642.

61. **Jannasch, H. W., and M. J. Mottl.** 1985. Geomicrobiology of deep sea hydrothermal vents. Science **229**:7177-7125.

62. **Jenney, F. E., M. F. J. M. Verhagen, X. Y. Cui, and M. W. W. Adams.** 1999. Anaerobic microbes: Oxygen detoxification without superoxide dismutase. Science **286**:306-309.

63. **Jin, S., Z. J. Liu, J. Rose, B. C. Wang, and D. M. Kurtz. 2001.** Structural and functional studies of rubrerythrin from *Desulfovibrio vulgaris*. J. Inorg. Biochem. **86**:282-282.

64. **Jones, P. G., and M. Inouye.** 1994. The cold-shock response - A hot topic. Mol. Microbiol. **11**:811-818.

65. **Jones, P. G., and M. Inouye.** 1996. RbfA, a 30S ribosomal binding factor, is a cold-shock protein whose absence triggers the cold-shock response. Mol. Microbiol. **21**:1207-1218.

66. **Jones, P. G., R. Krah, S. R. Tafuri, and A. P. Wolffe.** 1992. DNA gyrase, CS7.4, and the cold shock response in *Escherichia coli*. J. Bacteriol. **174**:5798-5802.

67. **Jones, P. G., M. Mitta, Y. Kim, W. Jiang, and M. Inouye.** 1996. Cold shock induces a major ribosomal-associated protein that unwinds double-stranded RNA in *Escherichia coli.* Proc. Natl. Acad. Sci. USA. **93**:76-80.

68. **Jones, P. G., R. A. Vanbogelen, and F. C. Neidhardt.** 1987. Induction of proteins in response to low temperature in *Escherichia coli*. J. Bacteriol. **169**:2092-2095.

69. **Kagawa, H. K., T. Yaoi, L. Brocchieri, R. A. McMillan, T. Alton, and J. D. Trent.** 2003. The composition, structure and stability of a group II chaperonin are temperature regulated in a hyperthermophilic archaeon. Mol. Microbiol. **48**:143-156.

70. **Kandror, O., A. DeLeon, and A. L. Goldberg.** 2002. Trehalose synthesis is induced upon exposure of *Escherichia coli* to cold and is essential for viability at low temperatures. Proc. Natl. Acad. Sci. USA **99**:9727-9732.

71. **Kandror, O., and A. L. Goldberg.** 1997. Trigger factor is induced upon cold shock and enhances viability of *Escherichia coli* at low temperatures. Proc. Natl. Acad. Sci. USA. **94**:4978-4981.

72. K**ashefi, K., J. M. Tor, D. E. Holmes, C. V. Gaw Van Praagh, A. L. Reysenbach, and D. R. Lovley.** 2002. *Geoglobus ahangari* gen. nov., sp. nov., a novel hyperthermophilic archaeon capable of oxidizing organic acids and growing autotrophically on hydrogen with Fe(III) serving as the sole electron acceptor. Int. J. Syst. Evol. Microbiol. **52**:719-28.

73. **Kengen, S. W., F. A. de Bok, N. D. van Loo, C. Dijkema, A. J. Stams, and W. M. de Vos.** 1994. Evidence for the operation of a novel Embden-Meyerhof pathway that involves ADP-dependent kinases during sugar fermentation by *Pyrococcus furiosus.* J. Biol. Chem. **269**:17537-17541.

74. **Kengen, S. W., A. J. M. Stams, and W. M. de Vos.** 1996. Sugar metabolism of hyperthermophiles. FEMS Microbiol. Rev. **18**:119-137.

75. **Keyer, K., and J. A. Imlay.** 1996. Superoxide accelerates DNA damage by elevating free-iron levels. Proc. Natl. Acad. Sci. USA **93**:13635-13640.

76. **Krahe, M., G. Antranikian, and H. Markl.** 1996. Fermentation of extremophilic microorganisms. FEMS Microbiol. Rev. **18**:271-285.

77. **Kurtz, D. M.** 1996. In vitro metal ion incorporation into nonheme diiron proteins: Hemerythrin, myohemerythrin, and rubrerythrin. Adv. Inorg. Biochem.:19-40.

78. **Kurtz, D. M.** 1997. Structural similarity and functional diversity in diiron-oxo proteins. J. Biol. Inorg. Chem. **2**:159-167.

79. **Kurtz, D. M., and E. D. Coulter. 2002.** The mechanism(s) of superoxide reduction by superoxide reductases *in vitro* and *in vivo*. J. Biol. Inorg. Chem. **7**:653-658.

80. **Kurtz, D. M., and B. C. Prickril.** 1991. Intrapeptide sequence homology in rubrerythrin from *Desulfovibrio vulgaris* - Identification of potential ligands to the diiron site. Biochem. Biophys. Res. Commun. **181**:337-341.

81. **La teana, A., A. Brandi, M. Falconi, R. Spurio, C. L. Pon, and C. O. Gualerzi.** 1991. Identification of a cold shock transcriptional enhancer of the *Escherichia coli* gene encoding nucleoid protein H-NS. Proc. Natl. Acad. Sci. USA **88**:10907-10911.

82. **Lang, K., F. X. Schmid, and G. Fischer.** 1987. Catalysis of protein folding by prolyl isomerase. Nature **329**:268-270.

83. **Lee, S. J., A. G. Xie, W. N. Jiang, J. P. Etchegaray, P. G. Jones, and M. Inouye.** 1994. Family of the major cold-shock protein, CspA (CS7.4), of *Escherichia coli*, whose members show a high sequence similarity with the eukaryotic Y-box binding-proteins. Mol. Microbiol. **11**:833-839.

84. **Legall, J., B. C. Prickril, I. Moura, A. V. Xavier, J. J. G. Moura, and B. H. Huynh.** 1988. Isolation and characterization of rubrerythrin, a non-heme iron protein from

Desulfovibrio vulgaris that contains rubredoxin centers and a hemerythrin-like binuclear iron cluster. Biochemistry **27**:1636-1642.

85. **Lehmann, Y., L. Meile, and M. Teuber.** 1996. Rubrerythrin from *Clostridium perfringens*: Cloning of the gene, purification of the protein, and characterization of its superoxide dismutase function. J. Bacteriol. **178**:7152-7158.

86. **Lelivelt, M. J., and T. H. Kawula.** 1995. Hsc66, an Hsp70 homolog in *Escherichia coli*, is induced by cold shock but not by heat shock. J. Bacteriol. **177**:4900-4917.

87. **Li, M., M. Y. Liu, J. Le Gall, L. L. Gui, J. Liao, T. Jiang, J. Zhang, D. Liang, and W. Chang.** 2003. Crystal structure studies on rubrerythrin: Enzymatic activity in relation to the zinc movement. J. Biol. Inorg. Chem. **8**:149-155.

88. **Lim, J., T. Thomas, and R. Cavicchioli.** 2000. Low temperature regulated DEAD-box RNA helicase from the Antarctic archaeon, *Methanococcoides burtonii*. J. Mol. Biol. **297**:553-567.

89. **Liu, M. Y., and J. Legall.** 1990. Purification and characterization of two proteins with inorganic pyrophosphatase activity from *Desulfovibrio vulgaris* - rubrerythrin and a new, highly-active, enzyme. Bioch. Biophys. Res. Commun. **171**:313-318.

90. **Liu, Y., and D. Eisenberg.** 2002. 3D domain swapping: As domains continue to swap. Protein Sci. **11**:1285-1299.

91. **Lopez-Garcia, P., and P. Forterre.** 1999. Control of DNA topology during thermal stress in hyperthermophilic archaea: DNA topoisomerase levels, activities and induced thermotolerance during heat and cold shock in *Sulfolobus*. Mol. Microbiol. **33**:766-777.

92. **Lopez-Garcia, P., and P. Forterre.** 2000. DNA topology and the thermal stress response, a tale from mesophiles and hyperthermophiles. Bioessays **22**:738-746.

93. **Lopez-Garcia, P., and P. Forterre.** 1997. DNA topology in hyperthermophilic archaea: reference states and their variation with growth phase, growth temperature, and temperature stresses. Mol. Microbiol **23**:1267-1269.

94. **Lumppio, H. L., N. V. Shenvi, R. P. Garg, A. O. Summers, and D. M. Kurtz.** 1997. A rubrerythrin operon and nigerythrin gene in *Desulfovibrio vulgaris* (Hildenborough). J. Bacteriol. **179**:4607-4615.

95. **Lumppio, H. L., N. V. Shenvi, A. O. Summers, G. Voordouw, and D. M. Kurtz.** 2001. Rubrerythrin and rubredoxin oxidoreductase in *Desulfovibrio vulgaris*: a novel oxidative stress protection system. J. Bacteriol. **183**:101-108.

96. **Ma, K., and M. W. W. Adams.** 1999. A hyperactive NAD(P)H : rubredoxin oxidoreductase from the hyperthermophilic archaeon *Pyrococcus furiosus*. J. Bacteriol. **181**:5530-5533.

97. **Mai, X., and M. W. W. Adams.** 1996. Purification and characterization of two reversible and ADP-dependent acetyl coenzyme A synthetases from the hyperthermophilic archaeon *Pyrococcus furiosus*. J. Bacteriol. **178**:5897-5903.

98. **Mai, X. H., and M. W. W. Adams.** 1996. Characterization of a fourth type of 2-keto acid-oxidizing enzyme from a hyperthermophilic archaeon: 2-ketoglutarate ferredoxin oxidoreductase from *Thermococcus litoralis*. J. Bacteriol. **178**:5890-5896.

99. **Maruyama, T., and M. Furutani.** 2000. Archaeal peptidyl prolyl cis-trans isomerases (PPIases). Front. Biosci. **5**:D821-836.

100. **Mccord, J. M., and I. Fridovic.** 1969. Superoxide dismutase-an enzymic function for erythrocuprein. J. Biol. Chem. **244**:6049-6055.

101. **Mccord, J. M., B. B. Keele, and I. Fridovich.** 1971. An enzyme-based theory of obligate anaerobiosis: the physiological function of superoxide dismutase. Proc. Natl. Acad. Sci. USA **68**:1024-1027.

102. **Morita, M. T., Y. Tanaka, T. S. Kodama, Y. Kyogoku, H. Yanagi, and T. Yura.** 1999. Translational induction of heat shock transcription factor sigma32: evidence for a built-in RNA thermosensor. Genes Dev. **13**:655-665.

103. **Mukund, S., and M. W. W. Adams.** 1995. Glyceraldehyde-3-phosphate ferredoxin oxidoreductase, a novel tungsten-containing enzyme with a potential glycolytic role in the hyperthermophilic archaeon *Pyrococcus furiosus*. J. Biol. Chem. **270**:8389-8392.

104. **Nakashima, K., K. Kanamaru, T. Mizuno, and K. Horikoshi.** 1996. A novel member of the *cspA* family of genes that is induced by cold shock in *Escherichia coli*. J. Bacteriol. **178**:2994-2997.

105. **Nelson, K. E., R. A. Clayton, S. R. Gill, M. L. Gwinn, R. J. Dodson, D. H. Haft, E. K. Hickey, L. D. Peterson, W. C. Nelson, K. A. Ketchum, L. McDonald, T. R. Utterback, J. A. Malek, K. D. Linher, M. M. Garrett, A. M. Stewart, M. D. Cotton, M. S. Pratt, C. A. Phillips, D. Richardson, J. Heidelberg, G. G. Sutton, R. D. Fleischmann, J. A. Eisen, O. White, S. L. Salzberg, H. O. Smith, J. C. Venter, and C. M. Fraser.** 1999. Evidence for lateral gene transfer between archaea and bacteria from genome sequence of *Thermotoga maritima*. Nature **399**:323-329.

106. **Panoff, J. M., B. Thammavongs, M. Gueguen, and P. Boutibonnes.** 1998. Cold stress responses in mesophilic bacteria. Cryobiology **36**:75-83.

107. **Phadtare, S., J. Alsina, and M. Inouye.** 1999. Cold shock response and cold-shock proteins. Curr.Opin. Microbiol. **2**:175-180.

108. **Pierik, A. J., R. B. G. Wolbert, G. L. Portier, M. F. J. M. Verhagen, and W. R. Hagen.** 1993. Nigerythrin and rubrerythrin from *Desulfovibrio vulgaris* each contain two mononuclear iron centers and two dinuclear iron clusters. Eur. J. Biochem. **212**:237-245.

109. **Prickril, B. C., D. M. Kurtz, B. H. Huynh, and N. Ravi.** 1993. Rubrerythrin - a nonheme iron protein with structural analogies to ribonucleotide reductase and methane monooxygenase. Abstracts of Papers of the American Chemical Society **205**:538.

110. **Prickril, B. C., D. M. Kurtz, J. Legall, and G. Voordouw.** 1991. Cloning and sequencing of the gene for rubrerythrin from *Desulfovibrio vulgaris* (Hildenborough). Biochemistry. **30**:11118-11123.

111. **Ramos, J. L., M. T. Gallegos, S. Marques, M. I. Ramos-Gonzalez, M. Espinosa-Urgel, and A. Segura.** 2001. Responses of Gram-negative bacteria to certain environmental stressors. Curr. Opin. Microbiol. **4**:166-171.

112. **Raven, N. D., and R. J. Sharp.** 1997. Development of defined and minimal media for the growth of the hyperthermophilic archaeon *Pyrococcus furiosus* Vc1. FEMS Microbiol. Rev. **146**:135-141.

113. **Ravi, N., B. C. Prickril, D. M. Kurtz, and B. H. Huynh.** 1993. Spectroscopic characterization of Fe-57-reconstituted rubrerythrin, a nonheme iron protein with structural analogies to ribonucleotide reductase. Biochemistry. **32**:8487-8491.

114. **Rinker, K. D., and R. M. Kelly.** 1996. Growth physiology of the hyperthermophilic archaeon *Thermococcus litoralis*: development of a sulfur-free defined medium, characterization of an exopolysaccharide and evidence of biofilm formation. Appl. Environ. Microbiol. **62**:4478-4485.

115. **Robb, F. T., D. L. Maeder, J. R. Brown, J. DiRuggiero, M. D. Stump, R. K. Yeh, R. B. Weiss, and D. M. Dunn.** 2001. Genomic sequence of hyperthermophile, *Pyrococcus furiosus*: Implications for physiology and enzymology. Methods Enzymol. **330**:134-157.

116. **Rosen, R., and E. Z. Ron.** 2002. Proteome analysis in the study of the bacterial heat-shock response. Mass Spectrom. Rev. **21**:244-265.

117. **Sako, Y., N. Nomura, A. Uchida, Y. Ishida, H. Morii, Y. Koga, T. Hoaki, and T. Maruyama.** 1996. *Aeropyrum pernix* gen. nov., sp. nov., a novel aerobic hyperthermophilic archaeon growing at temperatures up to 100 ^{o}C. Int. J. Syst. Bacteriol. **46**:1070-1077.

118. **Sapra, R., K. Bagramayan, and M. W. W. Adams.** 2004. A simple energy-conserving system: Proton reduction coupled to proton translocation. Proc. Natl. Acad. Sci. USA (in press.)

119. **Schut, G. J., S. D. Brehm, S. Datta, and M. W. W. Adams.** 2003. Whole-genome DNA microarray analysis of a hyperthermophile and an archaeon: *Pyrococcus furiosus* grown on carbohydrates or peptides. J. Bacteriol. **185**:3935-47.

120. **Schut, G. J., A. L. Menon, and M. W. W. Adams.** 2001. 2-keto acid oxidoreductases from *Pyrococcus furiosus* and *Thermococcus litoralis*. Methods Enzymol. **331**:144-158.

121. **Schut, G. J., J. Z. Zhou, and M. W. W. Adams.** 2001. DNA microarray analysis of the hyperthermophilic archaeon *Pyrococcus furiosus*: Evidence for a new type of sulfur-reducing enzyme complex. J. Bacteriol. **183**:7027-7036.

122. **Shockley, K. R., D. E. Ward, S. R. Chhabra, S. B. Conners, C. I. Montero, and R. M. Kelly.** 2003. Heat shock response by the hyperthermophilic archaeon *Pyrococcus furiosus*. Appl. Environ. Microbiol. **69**:2365-71.

123. **Sieker, L. C., M. Holmes, I. Le Trong, S. Turley, M. Y. Liu, J. LeGall, and R. E. Stenkamp.** 2000. The 1.9 angstrom crystal structure of the "as isolated" rubrerythrin from *Desulfovibrio vulgaris*: some surprising results. J. Biol. Inorg. Chem. **5**:505-513.

124. **Sieker, L. C., M. Holmes, I. Le Trong, S. Turley, B. D. Santarsiero, M. Y. Liu, J. LeGall, and R. E. Stenkamp.** 1999. Alternative metal-binding sites in rubrerythrin. Nat. Struct. Biol. **6**:308-309.

125. **Sinensky, M.** 1974. Homeoviscous adaptation--a homeostatic process that regulates the viscosity of membrane lipids in *Escherichia coli*. Proc. Natl. Acad. Sci. USA **71**:522-525.

126. **Stetter, K. O.** 1996. Hyperthermophiles in the history of life. Ciba Found. Symp. **202**:11-8D.

127. **Storz, G., and J. A. Imlay.** 1999. Oxidative stress. Curr. Opin. Microbiol. **2**:188-194.

128. **Sunna, A., M. Moracci, M. Rossi, and G. Antranikian.** 1997. Glycosyl hydrolases from hyperthermophiles. Extremophiles **1**:2-13.

129. **Sztukowska, M., M. Bugno, J. Potempa, J. Travis, and D. M. Kurtz.** 2002. Role of rubrerythrin in the oxidative stress response of *Porphyromonas gingivalis*. Mol. Microbiol. **44**:479-488.

130. **Tempel, W., Z. J. Liu, F. D. Schubot, M. V. Weinberg, F. E. Jenney, Jr, M. W. W. Adams, J. P. Rose, and B. C. Wang.** 2004. Structural genomics of *Pyrococcus furiosus*: X-Ray crystallography reveals 3D domain swapping in rubrerythrin. Proteins Struct. Funct. Genet. **In Press**.

131. **Thieringer, H. A., P. G. Jones, and M. Inouye.** 1998. Cold shock and adaptation. Bioessays **20**:49-57.

132. **Van Beeumen, J. J., G. Van Driessche, M. Y. Liu, and J. LeGall.** 1991. The primary structure of rubrerythrin, a protein with inorganic pyrophosphatase activity from *Desulfovibrio vulgaris* - Comparison with hemerythrin and rubredoxin. J. Biol. Chem. **266**:20645-20653.

133. **Vanbogelen, R. A., and F. C. Neidhardt.** 1990. Ribosomes as sensors of heat and cold shock in *Escherichia coli*. Proc. Natl. Acad. Sci. USA **87**:5589-5593.

134. **Vierke, G., A. Engelmann, C. Hebbeln, and M. Thomm.** 2003. A novel archaeal transcriptional regulator of heat shock response. J. Biol. Chem. **278**:18-26.

135. **Wakagi, T.** 2003. Sulerythrin, the smallest member of the rubrerythrin family, from the strictly aerobic and thermoacidophilic archaeon, *Sulfolobus tokodaii* strain 7. FEMS Microbiol. Lett. **222**:33-37.

136. **Wang, N., K. Yamanaka, and M. Inouye.** 1999. CspI, the ninth member of the CspA family of *Escherichia coli*, is induced upon cold shock. J. Bacteriol. **181**:1603-1609.

137. **Woese, C. R., and G. E. Fox.** 1977. Phylogenetic structure of the prokaryotic domain: the primary kingdoms. Proc. Natl. Acad. Sci. USA **74**:5088-5090.

138. **Wood, P. M.** 1987. The two redox potentials for oxygen reduction to superoxide. Trends Biol. Sci. **12**:250-251.

139. **Xia, B., H. Ke, and M. Inouye.** 2001. Acquirement of cold sensitivity by quadruple deletion of the *cspA* family and its suppression by PNPase S1 domain in *Escherichia coli*. Mol. Microbiol. **40**:179-188.

140. **Yamanaka, K., and M. Inouye.** 1997. Growth phase dependent expression of *cspD*, encoding a member of the CspA family in *Escherichia coli*. J. Bacteriol. **179**:5126-5130.

141. **Yamanaka, K., and M. Inouye.** 2001. Selective mRNA degradation by polynucleotide phosphorylase in cold shock adaptation in *Escherichia coli.* J. Bacteriol. **183**:2808-2816.

142. **Yamanaka, K., T. Mitani, T. Ogura, H. Niki, and S. Hiraga.** 1994. Cloning, sequencing, and characterization of multicopy suppressors of a *mukB* mutation in *Escherichia coli.* Mol. Microbiol. **13**:301-312.

143. **Yura, T., and K. Nakahigashi.** 1999. Regulation of the heat shock response. Curr. Opin. Microbiol. **2**:153-158.

144. **Zangrossi, S., F. Briani, D. Ghisotti, M. E. Regonesi, P. Tortora, and G. Deho.** 2000. Transcriptional and posttranscriptional control of polynucleotide phosphorylase during cold acclimation in *Escherichia coli.* Mol. Microbiol. **36**:1470-1480.

145. **Zheng, M., F. Aslund, and G. Storz.** 1998. Activation of the OxyR transcription factor by reversible disulfide bond formation. Science **279**:1718-1721.